SPIN-ORBIT COUPLING EFFECTS IN DIATOMIC MOLECULES.

Abstract of a Thesis presented for the Degree of Doctor of Philosophy in the University of Oxford.

by

David L. Cooper

Brasenose College

April, 1981

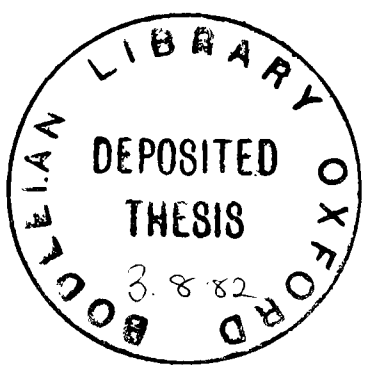

ABSTRACT.

Spin-orbit coupling and the related effects of Λ-doubling and spin-splitting have been well known to spectroscopists for some considerable time. The importance of these phenomena stems from the advent of radioastronomy and the study of the interstellar medium. Identification of the molecules, and the molecular transitions, in the interstellar dust clouds is necessary for an understanding of the cooling process by which these clouds can contract to form new stars.

The building blocks in the various proposed reaction schemes leading to the polyatomic species are small ions and radicals. Many of these are so reactive that their study in the laboratory is rather difficult. Furthermore, it is necessary to extrapolate to the conditions that prevail in the molecular clouds (low temperatures and pressures) and this can lead to large uncertainties. Even the lowest rotational transitions of light species such as OH and CH lie outside the region studied by radioastronomers. These molecules are detected via electric-dipole allowed transitions between Λ-doublet components. There are many other species which should be detectable in this way provided accurate frequency predictions can be made.

Ab initio calculations of Λ-doubling frequencies for CH and for OH have been in remarkable agreement with astrophysical observation. In this work, these calculations are extended to the molecule SiH which is of particular interest since Si is apparently depleted in the molecular clouds relative to solar abundance. The phenomenon known as core polarisation is also considered for this molecule.

Some molecules, such as OH, OD and SH, can be studied in the radiofrequency range using terrestrial molecular beam experiments. There is a need to use higher order Λ-doubling and spin-splitting parameters even for low rotational levels. Calculations are presented of these higher order constants and excellent agreement is found with fitted quantities. The relative importance of the various contributions to these higher order terms is also examined. Accurate data is also available for LiO but there are large uncertainties in the fitting procedure. Ab initio parameters are calculated and excellent agreement is found with experiment; the calculated quantities should be of considerable help in renewed attempts to analyse the experimental data.

Spin-splitting is considered for CaH since calcium is another element which is very heavily depleted in the interstellar medium. The results are in good agreement with terrestrial experiment. Similar methods are used for BH.

which is of interest since there are serious problems in the fitting procedure due to unresolved spin-splitting.

The theoretical expressions for Λ-doubling contain explicit summation over vibrational levels of perturbing states. A method is described which avoids this explicit sum over vibrational levels and which automatically includes all contributions from the bound levels and from the continuum of a given perturbing state. The method is tested for OH, LiO and for a system with an unbound perturbing state. The direct summation over vibrational levels is then used to treat HF^+ which has a weakly bound perturbing state. This molecule is interesting since it has been proposed as a possible interstellar maser. The Λ-doubling in NaAr is also examined using this method and good agreement is found with experiment giving some information on the Na + Ar interaction. The spin-orbit coupling in this system is found to be intermediate between molecular and atomic limits. This possibility is also considered in $HeNe^+$.

Extensions to new problems are discussed: spin-orbit coupling in larger systems such as CCN and CNC is considered and this is found to be very successful; the binding in molecular ions containing He is studied so as to decide whether the He analogues of molecules such as OH and CH might be detectable in the interstellar medium via Λ-doubling transitions; preliminary work on the accidental

predissociation of particular states of Li_2 and CH^* is presented.

SPIN-ORBIT COUPLING EFFECTS IN DIATOMIC MOLECULES.

A Thesis presented for the Degree of Doctor of Philosophy in the University of Oxford.

by

David L. Cooper

Brasenose College

April, 1981

Acnowledgements.

All of the computational work described in this thesis was carried out using the facilities of the Rutherford and Appleton Laboratories (RAL) and was funded by the Science Research Council. I should like to thank all the staff of the Atlas Computing Division at RAL for helping to make this work so enjoyable.

I wish to thank my supervisor, W. Graham Richards, for his guidance and encouragement throughout the course of my research and for providing so many useful opportunities. I should like to acknowledge the collaboration of Jeremy M. Hutson on the work described in chapter 4, of Leif Veseth on the work in chapter 6 and of Stephen Wilson on the study of noble gas molecular ions.

Thanks are due to Hélène Lefèbvre-Brion for hospitality in Paris in the Summer of 1979 (funded by NATO) and to Leif Veseth for a very profitable stay in Oslo in the Summer of 1980 which was made possible by a Senior Hulme Scholarship from Brasenose College.

Production.

With the exception of the mathematical equations, this thesis was produced predominantly on a Diablo 1640 daisy-wheel printer. Layout of the text was effected by the GEROFF program developed at RAL and run under CMS on an IBM 3032. Mathematical equations were mostly drawn on the III FR80 film recorder at RAL using the specially developed SOFTY (Spin-Orbit Fortran TYpesetting) programs which were run on the Central IBM System at RAL and which are described in Appendix A.

Figures 1, 2 and 3 in chapter 2 and figures 2, 3 and 4 in chapter 3 were produced using the Culham GHOST system on the OUCS ICL 1906A. Figures 1, 2 and 3 in chapter 4 were drawn by Jeremy M. Hutson on the OUCS ICL 2980. Figure 1 in chapter 7 was produced using programs run on the GEC 4085 at RAL and was drawn on a Benson 1302 plotter. SOFTY was used to produce the figures in Appendix A.

Spin-orbit coupling effects in diatomic molecules.

Units.

A number of units have been employed in this work which do not conform to the SI standard since there is a considerable advantage to be had by working in atomic units. In this system, the electron has unit charge and unit mass. The atomic unit of length is the bohr and that of energy is the hartree; Planck's constant takes the value $h=2\pi$. Useful conversion factors are

$$
\begin{aligned}
1 \text{ hartree} &= 219474.618 \text{ cm}^{-1} \\
&= 27.2097 \text{ eV} \\
1 \text{ bohr} &= 0.529172 \text{ Å} \\
1 \text{ Å} &= 10^{-10} \text{ m} \\
1 \text{ cm}^{-1} &= 1.986 \times 10^{-23} \text{ J} \\
&= 29979.246 \text{ MHz} \\
1 \text{ eV} &= 8065.7 \text{ cm}^{-1} \\
&= 1.6021 \times 10^{-19} \text{ J}
\end{aligned}
$$

The ångstrom and the wavenumber are "spectroscopic" units which are still very widely used.

CHAPTER ONE

Introduction.

CHAPTER 1 Introduction.

1.1 Spin-orbit coupling.

The spin angular momentum of an electron leads to a magnetic field which can interact with the magnetic field created by the orbital motion of the electron round the nucleus. This causes the lifting of the degeneracy of states which would otherwise be orthogonal. Indeed, the interaction of the spin of one electron with the orbit of another electron is also important. These spin-orbit and spin-other-orbit interactions are collectively known as spin-orbit coupling.

The effects of spin-orbit coupling are particularly easy to observe in atomic spectra. For example, the sodium D lines arise from transitions between the ^2S and ^2P states; the splitting of the ^2P energy level into $^2P_{1/2}$ and $^2P_{3/2}$ sublevels occurs because of spin-orbit coupling. The effect is very roughly proportional to the fourth power of the nuclear charge and so there is a dramatic increase in this splitting as the group of alkali metals is descended.

For an electronic configuration which represents a shell which is less than half-filled then, for a given multiplicity and orbital angular momentum, the level with the lowest value of the total angular momentum J lies lowest in energy. The state with the largest value of J lies lowest if the shell is more than half-full. This reflects the sign

of the spin-orbit coupling constant A which is positive for electronic shells less than half-filled and which is negative for shells more than half-filled (i.e. we may consider holes in the electronic shell). The energy diagram in figure 1 is for a p^2 configuration of an atom for which the Russell-Saunders coupling scheme is valid. The hyperfine spacings between the ^3P sublevels are proportional to J: this is the Landé interval rule.

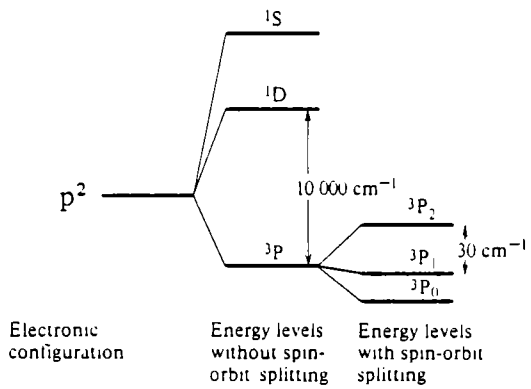

Figure 1

Energy level diagram for the configuration p^2.

Spin-orbit coupling manifests itself in linear molecules in much the same way as it does in atoms except that the axial symmetry causes the sublevels to be equidistant. The multiplet splittings in a regular $^3\Pi$ state (less than half-filled shell) are shown in figure 2 and should be compared with the atomic ^3P case. The values of spin-orbit coupling constants are valuable in the identification of states and in the assignment of electronic configurations. Ab initio calculations are useful for

predicting these molecular parameters and can also give deep insight into the physical origin of these effects.

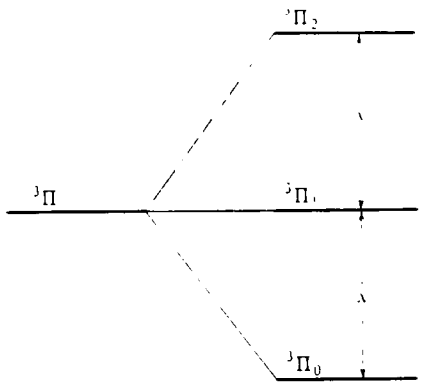

Figure 2

Multiplet splitting in a $^3\Pi$ state.

In addition to these multiplet splittings, various off-diagonal effects due to the mixing of otherwise orthogonal states have been revealed as spectroscopy has moved to higher and higher resolution. These effects include Λ-doubling and spin-splitting.

It is in relation to the molecular clouds in the interstellar medium that the most interesting aspects of spin-orbit coupling effects become especially important and so we shall briefly review the interstellar medium.

1.2 The interstellar medium.

Many of the brightest stars in our Galaxy have a lifetime of the order of a million years. It is clear that

these stars must have been formed in the recent past and that they are almost certainly still forming. Stars are formed from the interstellar medium, age as they use up fuel and then eventually die. If a star is sufficiently massive then it explodes violently as a supernova (such as the one responsible for the Crab Nebula). The material ejected is enriched with the products of the thermonuclear process. Consideration of the abundances of elements heavier than hydrogen in the Solar System suggests that it was made from 're-cycled material'. The interstellar medium plays a crucial rôle in the evolution of the Galaxy.

Gravitational effects give indirect evidence for the existence of interstellar matter but the main evidence is spectroscopic. The interstellar medium has been studied over the entire range of the electromagnetic spectrum but particularly at long wavelengths where extinction by dust grains is less critical. Radiofrequency observations are especially important.

The interstellar gas can be divided into five major components (see Dyson and Williams, 1980)

(1) Radiatively excited regions. These have low densities (about 10^{4} atom m^{-3}) and high temperatures (about 10^{6} K). These regions are highly ionised.

(2) Cool regions of mainly atomic hydrogen. These regions are denser (about 10^{5} atom m^{-3}) and cooler (less than 10^{4} K) and are partially ionised. Much more

material exists in mainly neutral clouds with densities of 10^7 - 10^9 atom m^{-3} and temperatures of 100 K. These clouds are observed by the hydrogen atom 21 cm line but they also contain some simple molecules such as H_2 and CO.

(3) Cool regions of mainly molecular hydrogen. Interstellar molecules are found in these dark, dense clouds (10^9 - 10^{10} molecules m^{-3}) which are among the most massive known objects. Temperatures are usually quite low (about 10 K) but denser, slightly warmer (about 50 K) regions also exist and it is in these 'black clouds' that the more complex molecules are formed.

(4) Inter-cloud gas. This gas contains hot (about 5000 K) neutral hydrogen atoms and fills a substantial fraction of interstellar space.

(5) Coronal gas. This component consists of very hot, very low density, fully ionised hydrogen and is frequently associated with supernovae sites.

Radiofrequency studies of molecules such as CO, H_2CO, NH_3 and H_2O give detailed information concerning prevailing densities and temperatures. Photons emitted from the stars heat the dust which then re-radiates in the infra-red. Thus, IR studies of the centre of the Galaxy give information about energetics. A combination of the two techniques is used to study the molecular clouds.

There are about 5000 giant molecular clouds in a ring around the centre of the Galaxy with masses of the order of 10^5 solar masses. This distribution is a consequence of the spiral structure of the Galaxy. These are also many less massive clouds but these seem to be less important for star formation (as do the non-spiral galaxies).

We can briefly trace the formation of massive stars (greater than a few solar masses) as follows. The hot gas contracts to form clouds in which molecules can form. Cooling then occurs, by way of the molecular transitions, to a cold dense gas. Collapse and fragmentation occur to coccoon stars which burn up their fuel in a few million years. The star dies as a supernova whose shock front prompts the next generation of stars. Formation of smaller stars is rather less violent. Note that although these are more numerous, they are less observable since luminosity is proportional to $(\text{mass})^3$.

It is important to identify the molecular transitions (and thus the molecules) present in the interstellar medium before the cooling process can be fully understood. Furthermore, abundance ratios such as H:D and $^{12}C:^{13}C$ give important clues as to the date of the 'big bang' and masses etc.. Chemical interest is centred on the dark clouds in which more than fifty molecules have been detected. In denser regions, molecules are shielded from UV photodissociation by the interstellar grains; molecules as

complex as HC_8CN have been detected. Many of the important building blocks are small radicals and ions. For the lightest of these, the frequencies of even the lowest rotational transitions lie outside the region studied by radioastronomers. Molecules such as OH and CH are detected by the electric dipole allowed transitions between components of the Λ-doublets in the ground $X^2\Pi$ states.

1.3 Λ-doubling.

Λ-doubling arises because the motions of the nuclei and electrons may not be treated as totally independent; it may be very crudely pictured in terms of 'electron slip' but it must be stressed that this picture must not be taken too seriously. In a rotating molecule, the electrons may lag behind the motion of the nuclear framework: the electrons and nuclear framework thus have slightly different angular momenta. The diagram below (figure 3) shows the effect of rotation on the otherwise degenerate π^* and π orbitals. Whereas the π orbital is scarcely affected, the nuclei in the case of the π^* orbital can come into a region of non-zero electron density (as in σ orbitals). There is a lifting of the degeneracy of orbitals with the same value of $|\Omega|$, a blurring of the distinction between σ and π molecular orbitals, and a removal of the orthogonality of Σ and Π molecular states. It is to be expected from this picture that the Λ-doublet splitting would increase with rate of rotation (and thus with J).

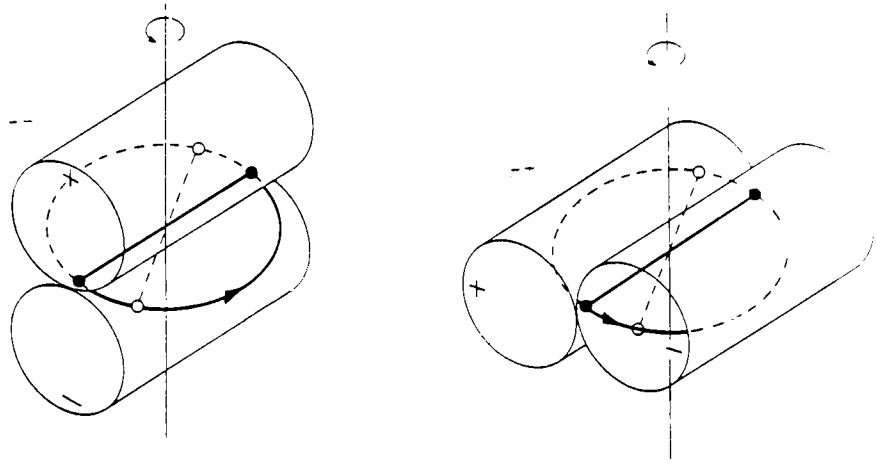

Figure 3

A schematic representation of the mechanism for Λ-doubling in a diatomic molecule. On rotation if the electrons lag slightly, in π^- the nuclei will remain in a nodal plane of the orbital while in π^+ the nuclei will come into a region of non-zero electron density.

Spectroscopists usually fit the Λ-doublet splitting observed in different rotational levels to an expression containing J and two parameters (½p+q) and q. Even very crude calculations of these parameters are of value since they may give some indication of the origins of the magnitudes of measured properties. In particular, the relative signs of p and q may be used to determine whether a state is regular or inverted. More accurate calculations allow estimates of molecular constants in cases where the experimental method is difficult. Electronic spectroscopy

has particular difficulties in the case of very reactive species whose lifetimes may be too short for very high resolution studies. The importance of even more accurate ab initio calculations arises from the radiofrequency, electric-dipole allowed transitions between the components of the Λ-doublets.

Electronic spectroscopy is generally not carried out under the conditions that prevail in the molecular clouds: very low temperatures and densities. Even if high-resolution spectra can be produced, a large amount of work must go into extrapolating quantities relating to excited rotational levels. There are frequently large uncertainties in the fitting procedure arising from the choice of different methods. For some molecules, the microwave spectrum can be measured in the laboratory and ab initio calculations are particularly important for these systems.

There is a long history of successful calculations of fine-structure constants (Richards, 1979; Richards, Trivedi, and Cooper, 1981). In particular, calculations on the CH radical (Hammersley, 1974) predicted the radioastronomical transitions more accurately than did conventional terrestrial experimental spectroscopy. Figure 4 indicates the observed radioastronomical transitions in the lowest rotational level of OH; the epicentres are separated by 1666 MHz and this is the ab initio value obtained by Cooper (1979).

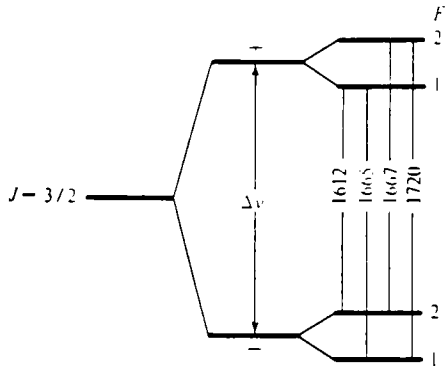

Figure 4

Λ-doubling ($\Delta\nu$) in the lowest rotational level of OH ($^2\Pi_{3/2}$, $J = 3/2$) showing the observed radioastronomical transitions in MHz (not to scale).

The quality of this agreement provides the impetus to extend this type of work to those potentially important interstellar species which are still to be detected.

CHAPTER TWO

Λ-doubling in SiH.

CHAPTER 2 Λ-doubling in SiH.

2.1 Electronic wavefunctions.

The starting point for the calculation of the energy levels of a diatomic molecule is the Born-Oppenheimer approximation which recognises that there is a large difference in mass between nuclei and electrons. It is thus more appropriate to refer the electron motion to a frame which rotates with the nuclei rather than to an external frame. The approximation does not come in the transformation of variables but in the factorisation of the wavefunction as the product of a wavefunction describing electronic motion for fixed nuclei and a wavefunction describing nuclear motion.

Even for the hydrogen molecule-ion, the non-relativistic time-independent Schrödinger equation cannot be solved analytically - so that the Born-Oppenheimer approximation must be used. Further approximations allow separation of the wavefunction for nuclear motion into rotational and vibrational parts. For molecules more complex than the hydrogen molecule-ion, we encounter correlation energy (i.e. inter-electronic repulsion) and even within the Born-Oppenheimer approximation, the Schrödinger equation has no analytic solution. There are two simple methods of overcoming this problem. Valence bond (VB) theory treats a bond in terms of the participating atoms; it often gives chemical insight into bonding and has been extensively used.

VB theory has not been as widely used in fine structure calculations as has molecular orbital (MO) theory. The MO approach treats the system in much the same way as atoms: orbitals extend over the whole molecule. In the self-consistent field (SCF) method developed by Roothaan (1951), the Hartree-Fock equations for open-shell molecules are reduced to single eigenvalue equations by absorbing off-diagonal terms into an effective hamiltonian. Within MO theory, the electronic wavefunction is expressed in terms of Slater determinants of one-electron wavefunctions. Frequently, for open-shell molecules, the wavefunction is actually a linear combination of two or more determinants; this is necessary to ensure that the complete wavefunction is antisymmetric with respect to electron exchange and is also an eigenfunction of $\mathbf{S}^2$ (where $\mathbf{S}$ is the total electron spin). It is usual to expand molecular orbitals as linear combinations of atomic orbitals (LCAO-MO-SCF).

Two types of basis set are in general use. Gaussian-type orbitals (GTOs) are used for calculations on large molecules since integrals involving this type of basis function are frequently quite easy to calculate and the results obtained for energies are usually quite good. Unfortunately, GTOs tend to give a rather poor representation of the part of the molecular orbital close to the nucleus. This is critical for many calculations of molecular properties (particularly fine structure). For work on small systems, such as diatomic molecules, the molecular

orbitals are best expanded in terms of Slater-type orbitals (STOs) :

$$\chi_{nlm} = N_{nlm} Y_{lm}(\theta,\phi) r^{n-1} \exp(-\zeta r)$$

where $Y_{lm}(\theta,\phi)$ is a spherical harmonic, N_{nlm} is a normalisation constant and ζ is an exponent which is usually chosen by an optimisation procedure. Tables of suitable zeta values exist for a very large number of atoms and molecules.

2.2 Λ–doubling in $^2\Pi$ states.

Λ–doubling arises from the mixing of states with different Λ values via off–diagonal matrix elements of the spin–orbit coupling operator, H_{so} , and of operators such as $B(L^+S^- + L^-S^+)$; B is an operator proportional to $1/\mu R^2$ (where μ is the reduced mass and R is the internuclear distance), and L^+ and S^+ are raising operators for orbital and spin angular momenta. The phenomenon may be regarded as a breakdown of the Born-Oppenheimer approximation; the motions of the electrons and nuclei may not be treated as totally independent. Λ–doubling in $^2\Pi$ states is usually dominated by interactions with $^2\Sigma$ states. There are exceptions such as NH^+ where a $^4\Sigma^-$ state is important.

In the conventional theory due to Van Vleck (1929) and Dousmanis, Sanders and Townes (1955) and Kovács (1969), the non-relativistic hamiltonian for a free molecule (in the absence of external fields) is written as:

$$H = H^{(0)} + H^{(1)}$$

where the zeroth-order hamiltonian is purely vibronic and the perturbation contains spin-orbit (H_{so}) and rotational (H_{rot}) parts. For a linear molecule pointing along the z-axis, the rotational part of $H^{(1)}$ may be expanded:

$$\begin{aligned} H_{rot} &= B(J-L-S)^2 \\ &= B(J^2-J_z^2)+B(S^2-S_z^2)+B(L^2-L_z^2) \\ &+B(L^+S^-+L^-S^+)-B(J^+S^-+J^-S^+) \\ &-B(J^+L+J^-L^+) \end{aligned}$$

Note that J^+ (and J^-) refer to a molecule-fixed frame of reference and actually represent a lowering (raising) operator of the total angular momentum. The last term in the above expression resembles the Coriolis energy in the classical case. The operator H_{so} will be discussed in more detail in section 2.4; non-zero off-diagonal matrix elements occur for

$$\Delta J=0,\ \Delta\Omega=0,\ \Delta\Lambda=-\Delta\Sigma=\pm 1$$

An expression for the Λ-doubling may be obtained by considering a perturbation matrix which arises from all the vibrational levels (u,v) of the relevant $^2\Pi$ state and all the vibrational levels (k,l) of all $^2\Sigma$ states. This matrix of infinite order may be reduced, by means of a Van Vleck transformation (Zare et al., 1973), to an effective two-by-two matrix describing the $^2\Pi_{1/2}$ and $^2\Pi_{3/2}$ substates of a particular rotational and vibrational level. There are various systems of nomenclature for the two sets of levels

that arise because of Λ-doubling. The e/f notation is to be preferred since it is then possible to take linear combinations of the eigenfunctions

$$|^2\Lambda_\Omega\ v\rangle = |\Lambda\ S\ \Sigma\ J\ v\rangle \pm |-\Lambda\ \ S\ -\Sigma\ J\ v\rangle$$

so that levels of one parity are e levels whilst levels of the other parity (or sign, in the linear combination) are f levels. Matrix elements between parity eigenfunctions are given in table I.

A Van Vleck transformation to second order yields the Λ-doubling matrix

$$\begin{pmatrix} \pm\ \frac{1}{2}\ (p_v+2q_v)(J+\frac{1}{2}) & \pm\ \frac{1}{2}\ q_v\ X(J+\frac{1}{2}) \\ \pm\ \frac{1}{2}\ q_v X\ (J+\frac{1}{2}) & 0 \end{pmatrix}$$

The upper left element refers to the $^2\Pi_{1/2}$ substate. The meaning of X is

$$X^2 = (J+\tfrac{1}{2})^2 - 1$$

and the parameters p_v and q_v are as defined by Mulliken and Christy (1931):

$$p_v = 4 \sum_{n' v'} \frac{(-1)^t \langle {}^2\Pi\ v|H_{so}|n'v'\rangle\langle n'v'|B(L^+S^- + L^-S^+)|{}^2\Pi\ v\rangle}{E_{\Pi v} - E_{n'v'}}$$

$$q_v = 2 \sum_{n' v'} \frac{(-1)^t |\langle {}^2\Pi\ v|B(L^+S^- + L^-S^+)|n'v'\rangle|^2}{E_{\Pi v} - E_{n'v'}}$$

The denominator in each case is the energy separation between the interacting vibronic levels. The summations

TABLE I

Matrix elements between parity eigenfunctions

$$\langle {}^2\Pi_{1/2}\, v|\, H^{(1)}|\, {}^2\Sigma\, k\rangle = 1/2\, A_{vk} + B_{vk} \pm (-1)^S\, B_{vk}(J+1/2)$$

$$\langle {}^2\Pi_{3/2}\, v|\, H^{(1)}|\, {}^2\Sigma\, k\rangle = B_{vk}\, [(J+1/2)^2 - 1\,]^{1/2}$$

$$\langle {}^2\Pi_{1/2}\, v|\, H^{(1)}|\, {}^2\Pi_{1/2}\, u\rangle = B_{vu}\, (J+1/2)^2 - 1/2\, A_{vu}$$

$$\langle {}^2\Pi_{3/2}\, v|\, H^{(1)}|\, {}^2\Pi_{3/2}\, u\rangle = B_{vu}\, [(J+1/2)^2 - 2] + 1/2\, A_{vu}$$

$$\langle {}^2\Pi_{1/2}\, v|\, H^{(1)}|\, {}^2\Pi_{3/2}\, u\rangle = B_{vu}\, [(J+1/2)^2 - 1]^{1/2}$$

$$\langle {}^2\Sigma\, k\ |\, H^{(1)}|\, {}^2\Sigma\ell\,\rangle = B_{k\ell}\ (J+1/2)^2 \pm (-1)^S\, B_{k\ell}(J+1/2)$$

where

$B_{vu} = \langle {}^2\Pi v\, |B|\, {}^2\Pi\, u\,\rangle$

$A_{vu} = 2\langle\, {}^2\Pi v\, |H_{SO}|\, {}^2\Pi u\,\rangle$

$B_{vk} = \langle {}^2\Pi v\, |BL^+S^-|\, {}^2\Sigma k\,\rangle$

$A_{vk} = 2\langle\, {}^2\Pi v\, |H_{SO}|\, {}^2\Sigma k\,\rangle$

$B_{k\ell} = \langle {}^2\Sigma k\, |B|\, {}^2\Sigma\ell\,\rangle$

$S = 0$ for ${}^2\Sigma^+$ states and $S = 1$ for ${}^2\Sigma^-$ states.

H_{SO} is the spin-orbit coupling operator.

extend over all vibrational levels (v') of all $^2\Sigma$ states (n') and, in principle, over $^4\Sigma$ states and so on. The Λ-doubling splitting may be expressed to second order in terms of the Mulliken and Christy formula:

$$\Delta\nu = -(\tfrac{1}{2}p+q)[1 \pm (2-Y)/X](J+\tfrac{1}{2}) \mp (2q/X)(J+3/2)(J+\tfrac{1}{2})(J-\tfrac{1}{2})$$

In this expression, Y is the ratio of the spin-orbit coupling constant to the rotational constant; the upper sign relates to F_2 sublevels while the lower sign relates to F_1 sublevels;

$$X^2 = Y(Y-4)+4(J+\tfrac{1}{2})^2$$

2.3 Calculation of potential energy curves.

Cade and Huo (1967 b) have optimised a Slater-type orbital basis set in a single configuration calculation on the ground state of SiH. The basis set is given in table II and consists of twelve σ functions on Si, four σ functions on H, six π functions on Si and two π functions on H.

Separate SCF procedures were carried out for each of the $X^2\Pi_r$ $(1\sigma^2 2\sigma^2 3\sigma^2 4\sigma^2 5\sigma^2 1\pi^4 2\pi^1)$, $B^2\Sigma^+$ $(1\sigma^2 2\sigma^2 3\sigma^2 4\sigma^2 5\sigma^1 1\pi^4 2\pi^2)$ and $^2\Sigma^-$ $(1\sigma^2 2\sigma^2 3\sigma^2 4\sigma^2 5\sigma^1 1\pi^4 2\pi^2)$ states of SiH using the ALCHEMY system of programs of Bagus, Lui, McLean and Yoshimine. Configuration interaction (CI) was used to improve all three potential curves. Large sets of configuration state functions (CSFs) were used to obtain the potential curves in tables III, IV and V and figures 1, 2

Table II Basis set used for SiH.

	Si		H	
σ:	1s	16.38055	σ: 1s	1.12639
	2s	4.39476	1s	1.41075
	2s	14.25721	2s	1.74325
	3s	1.21796	2p	1.44092
	3s	1.97032		
	3s	8.20077		
	2p	3.86131		
	2p	6.51564		
	2p	11.49723		
	3p	0.99860		
	3p	1.76017		
	3d	1.66407		
π:	2p	3.84787	π: 2p	1.30197
	2p	6.51310	3d	1.83774
	2p	11.53490		
	3p	1.00488		
	3p	1.73608		
	3d	1.65878		

and 3. The excited CSFs used in the CI were constructed from both the occupied and unoccupied ('virtual') orbitals generated by the SCF procedure. The virtual orbitals are rather poor descriptions of the occupied molecular orbitals; CSFs generated from the virtual orbitals are generally poor representations of the part of the wavefunction not represented by the Hartree-Fock limit. This can lead to slow convergence in SiH where energy convergence in, say, the lowest $^2\Sigma^-$ state is very slow; there is a considerable change in energy when increasing the number of CSFs from 185 to 364.

Values are required for the energy separations between the $X^2\Pi$ and $B^2\Sigma^+$ states and between the $X^2\Pi$ and $^2\Sigma^-$ states. For the $B^2\Sigma^+$ state, an experimental value is available but for the unbound $^2\Sigma^-$ state, a calculated value must be used. Because it is difficult to recover all the correlation energy (inter-electron interactions), ab initio energy differences are not always reliable. However, the calculated value for the separation between $X^2\Pi_r$, v''=0 and $B^2\Sigma^+$, v'=0 agrees favourably with experiment (see table VI) and this gives some encouragement that the calculated value for $^2\Sigma^-$ may be reasonable. The finally adopted value for the energy separation between the $X^2\Pi$, v''=0 level and the asymptote of the lowest $^2\Sigma^-$ state is 25036.5 cm^{-1}.

R/bohr	E(total)/hartree	
	no CI	642 CSFs
1.60	-289.00198	-289.07275
1.80	-289.18881	-289.25936
2.00	-289.30329	-289.37432
2.20	-289.37149	-289.44339
2.40	-289.40990	-289.48291
2.50	-289.42139	-289.49502
2.60	-289.42906	-289.50355
2.70	-289.43368	-289.50864
2.80	-289.43584	-289.51151
2.85	-289.43616	-289.51219
2.87	-289.43616	-289.51236
2.95	-289.43555	-289.51231
3.00	-289.43471	-289.51183
3.10	-289.43213	-289.51002
3.20	-289.42859	-289.50727
3.30	-289.42431	-289.50379
3.40	-289.41945	-289.49976
4.00	-289.38455	-289.47067
4.50	-289.35451	-289.44708
5.00	-289.32680	-289.42782

Table III $X^2\Pi_r$ state of SiH

FIGURE 1

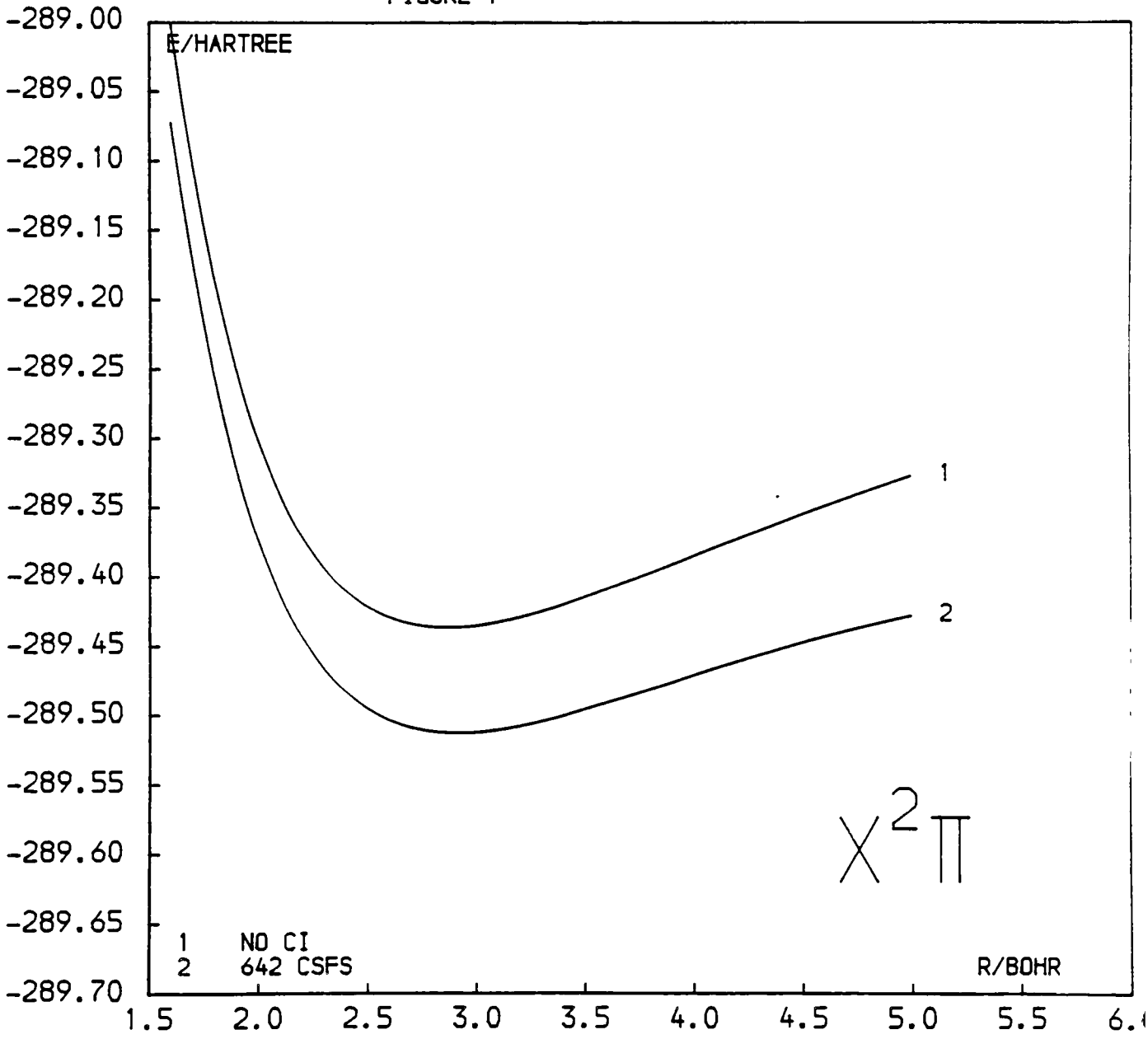
E/HARTREE
-289.00
-289.05
-289.10
-289.15
-289.20
-289.25
-289.30
-289.35
-289.40
-289.45
-289.50
-289.55
-289.60
-289.65
-289.70
1
2
1 NO CI
2 642 CSFS
R/BOHR
1.5
2.0
2.5
3.0
3.5
4.0
4.5
5.0
5.5
6.
X 2Π

R/bohr	E(total)/hartree	
	no CI	407 CSFs
1.60	-288.86743	-288.93848
2.00	-289.15983	-289.23180
2.20	-289.22465	-289.29802
2.40	-289.26007	-289.33529
2.50	-289.27024	-289.34653
2.60	-289.27672	-289.35418
2.70	-289.28032	-289.35902
2.80	-289.28167	-289.36168
2.85	-289.28170	-289.36237
2.95	-289.28077	-289.36275
3.00	-289.27996	-289.36256
3.10	-289.27804	-289.36162
3.20	-289.27640	-289.36019
3.30	-289.27544	-289.35856
3.40	-289.27494	-289.35704
4.00	-289.27476	-289.35803
4.50	-289.27531	-289.36201
5.00	-289.27573	-289.36381

Table IV $B^2\Sigma^+$ state of SiH

FIGURE 2

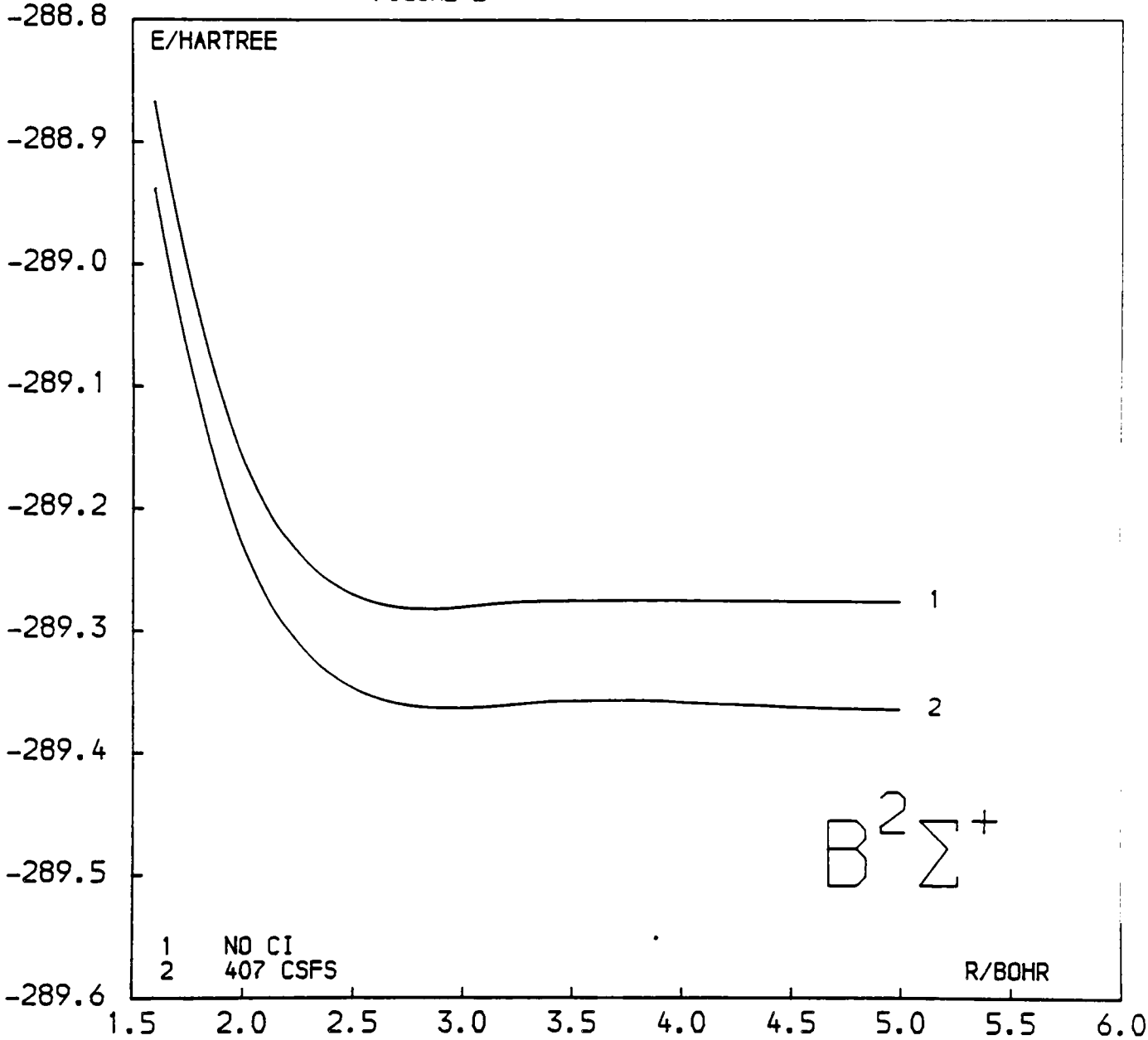
E/HARTREE
-288.8
-288.9
-289.0
-289.1
-289.2
-289.3
-289.4
-289.5
-289.6
1.5
2.0
2.5
3.0
3.5
4.0
4.5
5.0
5.5
6.0
R/BOHR
1
2
$B^2\Sigma^+$
1 NO CI
2 407 CSFS

R/bohr	E(total)/hartree	
	no CI	364 CSFs
1.30	-288.38340	-288.45126
1.40	-288.58813	-288.65491
1.50	-288.75052	-288.81648
1.60	-288.87892	-288.94443
1.70	-288.98011	-289.04558
1.80	-289.05958	-289.12536
1.90	-289.12168	-289.18810
2.00	-289.16989	-289.23723
2.10	-289.20699	-289.27548
2.20	-289.23524	-289.30505
2.30	-289.25646	-289.32773
2.40	-289.27214	-289.34494
2.50	-289.28360	-289.35786
2.60	-289.29204	-289.36741
2.70	-289.29878	-289.37435
2.80	-289.30477	-289.37930
2.90	-289.31015	-289.38280
3.10	-289.31912	-289.38699
3.20	-289.32285	-289.38821
3.40	-289.32909	-289.38980
3.60	-289.33409	-289.39094
4.00	-289.34143	-289.39316
4.30	-289.34525	-289.39490
5.00	-289.35051	-289.39821

Table V $^2\Sigma^-$ state of SiH

FIGURE 3

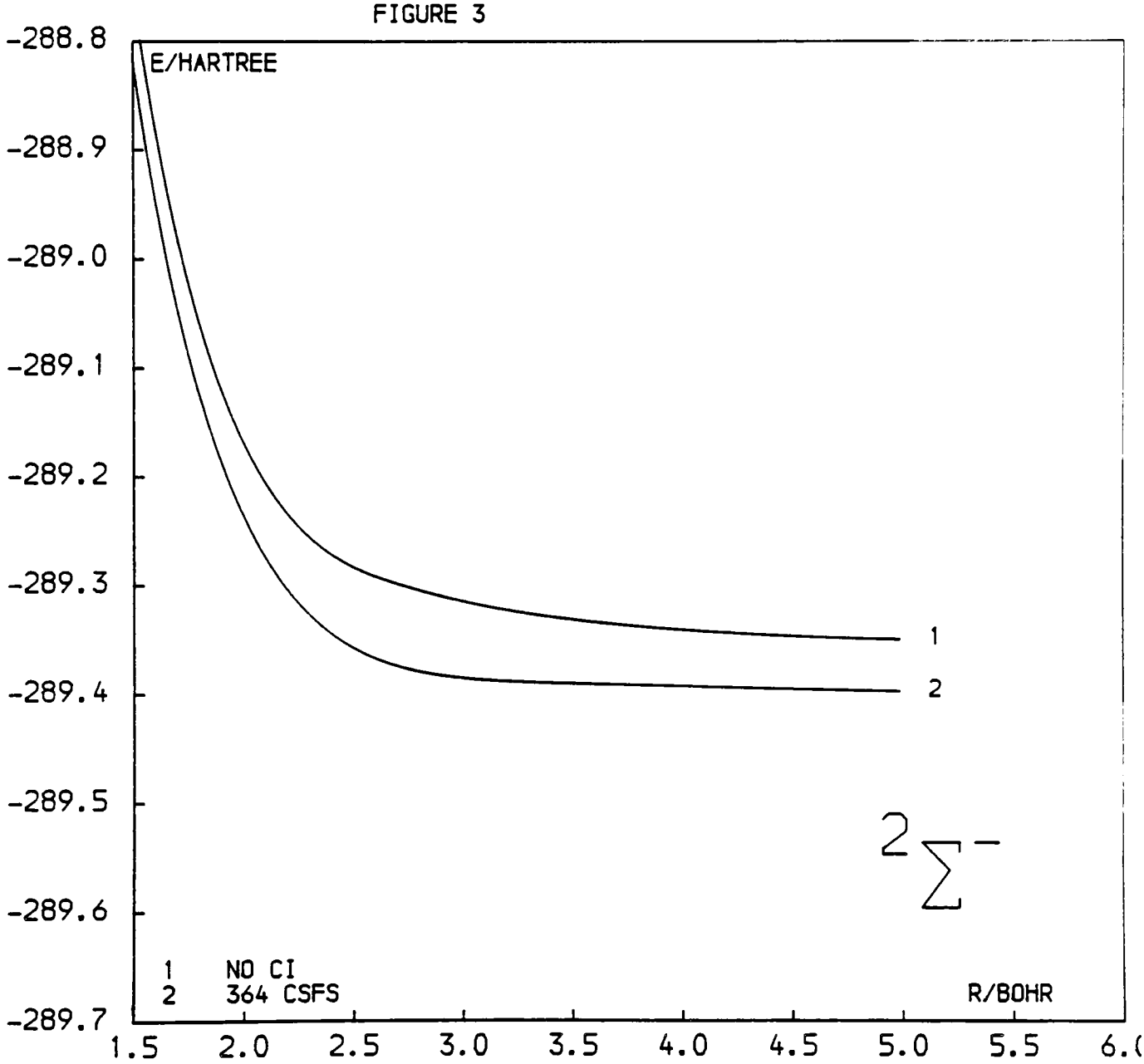
E/HARTREE
-288.8
-288.9
-289.0
-289.1
-289.2
-289.3
-289.4
-289.5
-289.6
-289.7
1
2
1 NO CI
2 364 CSFS
R/BOHR
1.5
2.0
2.5
3.0
3.5
4.0
4.5
5.0
5.5
6.0
$^2\Sigma^-$

Table VI Energy separations

$T_{\infty}(X^2\Pi - B^2\Sigma^+)/cm^{-1}$

Calculated	Wilson (1975)	33524.38
	This work	32874
Experiment	Bollmark et al. (1971)	31909.7

2.4 Diagonal spin-orbit coupling constant for SiH.

The spin-orbit coupling operator is taken from the two particle relativistic Breit hamiltonian and may be written:

$$H_{SO}= \frac{\alpha^2}{2}\sum_{i,N}\frac{Z_N}{r_{iN}^3}(\mathbf{r}_{iN}\times\mathbf{p}_i)\mathbf{s}_i - \frac{\alpha^2}{2}\sum_{i,j}\frac{1}{r_{ij}^3}(\mathbf{r}_{ij}\times\mathbf{p}_i)\cdot(\mathbf{s}_i+2\mathbf{s}_j)$$

where α is the fine structure constant; Z_N is the charge on nucleus N; i and j label electrons; r, p and s are one-electron position, linear momentum and spin angular momentum operators. We may recognise three separate parts in the above expression:

(1) the spin-orbit coupling of each electron in the Coulomb field of the nucleus;

(2) the spin-orbit coupling of each electron i in the Coulomb field of electron j;

(3) the interaction of the spin of electron j with the orbital angular momentum of electron i.

The selection rules for non-vanishing diagonal matrix elements of H_{so} differ from the rules for off-diagonal terms; they are

$$\Delta J=0,\ \Delta S=0,\ \Delta\Omega=\Delta\Lambda=\Delta\Sigma=0$$

Veseth (1970) has investigated the relation in a diatomic molecule between the simple phenomenological operator $AL\,S$ and the Pauli-Breit operator and has found that both operators lead formally to the same results.

The calculation of two electron integrals of H_{so} is simplified by the following symmetry relations:

$$\langle i\ j||k\ l\rangle=-\langle -i\ -j||-k\ -l\rangle \qquad \text{rule (1)}$$

$$\langle i\ j||k\ l\rangle=(-1)^{j+l}\langle i\ -l||k\ -j\rangle \qquad \text{rule (2)}$$

$$\langle i\ j||k\ l\rangle=(-1)^{k+i+l+j}\langle -k\ j||-i\ l\rangle \qquad \text{rule (3)}$$

Thus, for example,

$$\langle\sigma\ \pi^{-}||\sigma\ \pi^{-}\rangle=\langle\sigma\ \pi^{+}||\sigma\ \pi^{+}\rangle \qquad \text{by rule (2)}$$

but $$\langle\sigma\ \pi^{-}||\sigma\ \pi^{-}\rangle=-\langle\sigma\ \pi^{+}||\sigma\ \pi^{+}\rangle \qquad \text{by rule (1)}$$

so that $$\langle\sigma\ \pi^{+}||\sigma\ \pi^{+}\rangle=0$$

The calculation of the spin part of the matrix elements of H_{so} is trivial provided the spin-orbit coupling operator is rewritten in tensor form:

$$H_{so}=H_{so}^{(1)}+H_{so}^{(2)}$$

$$=\sum_{i} a_i^{(0)}s_i^{(0)}+\sum_{i\,j} b_{ij}^{(0)}(s_i+2s_j)^{(0)}$$

where a_i and b_{ij} are the purely spatial parts of the one- and two-electron parts of H_{so}. Thus

$$\langle H_{so}\rangle=\sum_{k}\langle k|a_i^{(0)}|k\rangle\sigma(k)+\sum_{k\,l}\langle k\ l|b_{12}^{(0)}|k\ l\rangle(\sigma(k)+2\sigma(l))$$

$$-\sum_{k\,l}\langle k\ l|b_{12}^{(0)}|l\ k\rangle(\sigma(k)+2\sigma(l))\delta_{\sigma(k)\sigma(l)}$$

Note that the summations for H_{so} are for all k and l since the operator is not symmetric but that the terms for k=l are self-cancelling. The spin part of the matrix elements depends only on the values of the spin quantum numbers $\sigma(i)$.

Wilson (1977) has developed a series of computer programs which calculate diagonal matrix elements of the spin-orbit coupling operator for CI wavefunctions constructed from large numbers of CSFs. These were used to investigate the effect of CI and also the importance of the inclusion of two-centre terms. The one-centre Hartree-Fock value for A at 2.8724 bohr is 127.12 cm^{-1} to be compared with a one- and two-centre value of 126.80 cm^{-1}. The difference between these values is about ¼% suggesting that use of only one-centre integrals would be a very good approximation. The two-centre two-electron integrals, unlike the two-centre one-electron integrals, cannot be evaluated analytically and are very expensive to compute. The one-centre approximation will be used for the corresponding off-diagonal matrix elements.

Different CI expansions were produced by allowing different number of electrons to take part and by allowing different numbers of these to be excited into the virtual orbitals $6\sigma-10\sigma$ and $3\pi-5\pi$. It can be seen from table VII that CI generally leads to a lower value than that obtained from a Hartree-Fock calculation and that convergence is slow.

The experimental value of A is 142.83 cm^{-1} so that there is a discrepancy of about 10%.

CSFs	CI virtuals		E(total) /hartree	$\frac{1}{2}A/cm^{-1}$
1	-	-	-289.4362	63.399
5	$4\sigma^2 5\sigma^2 2\pi$	0	-289.4461	60.887
16	$4\sigma^2 5\sigma^2 1\pi^4 2\pi$	0	-289.4462	60.986
90	$4\sigma^2 5\sigma^2 2\pi$	1	-289.4641	58.615
473	$4\sigma^2 5\sigma^2 1\pi^4 2\pi$	1	-289.4651	59.916

Table VII Effect of CI on the ground state of SiH.

Walker (1969) has calculated spin-orbit coupling constants for a number of second-row diatomics using Hartree-Fock wavefunctions and has consistently obtained values of smaller magnitude than experiment. Both Wilson (1975) and Walker have attributed part of the discrepancy to core polarisation: the outer $2\pi^1$ electron in SiH polarises the $1\pi^4$ core electrons and changes the net contribution of this closed shell. Within the restricted Hartree-Fock (RHF) method, pairs of electrons differing in only spin quantum number (eg $1\pi^+$ and $1\bar{\pi}^-$) have identical spatial parts. The problem is also one of electron correlation.

Lefèbvre-Brion et al. (1967) have used unrestricted Hartree-Fock (UHF) wavefunctions to correct constants for second-row atoms with open shells; they assumed that shielding effects were the same as for RHF wavefunctions and they neglected errors arising from the fact that UHF wavefunctions are not eigenfunctions of L^2 or S^2. Walker used these atomic values to correct calculated molecular

spin-orbit constants; his values for SiH before and after this correction are 129.5 cm^{-1} and 155.1 cm^{-1}, repectively. The values are roughly equidistant from the experimental value so that the core polarisation has been over-estimated.

Wilson recognised the importance of allowing CSFs into the CI wavefunction which arise from excitations of 1π electrons; he found that these CSFs may have large matrix elements of H_{so} but tend to have small coefficients in the CI expansion. The criterion for wavefunction improvement is that the energy is lowered (i.e. the variation principle). Molecular properties often do not vary monotonically with the decrease in energy. When deciding whether one wavefunction is better than another one, it is important to bear in mind what the wavefunctions are required for. For spin-orbit coupling matrix elements, best results often arise from fairly small CI expansions. The values in table VII do suggest that excitations from the $1\pi^4$ core are important. In particular, the energy change observed in going from 5 CFSs to 16 CSFs is very small compared with the change in the value of A.

It is very difficult to predict the importance of core polarisation in the calculation of off-diagonal matrix elements of the spin-orbit coupling operator. Because of this uncertainty, the ab initio values of p and q for SiH will be intrinsically rather less accurate than those obtained by Hammersley and Richards (1974) for CH and by

Cooper and Richards (1979) for OH. There is no $2\pi^1$ electron in the $B^2\Sigma^+$ or $^2\Sigma^-$ states to polarise the $1\pi^4$ core so that we might expect core polarisation to be rather less important in matrix elements between these $^2\Sigma$ states and the $X^2\Pi$ state.

2.5 The calculation of off-diagonal matrix elements of H_{so} and L^+S^-.

It has been shown by Löwdin (1955) that if determinants p and q are constructed from the same atomic basis set $\{\chi_a\chi_b\cdots\cdots\}$ and if Ω is an operator which can be expressed as a sum of one-electron operators ω then:

$$\langle\psi_p|\Omega|\psi_q\rangle = \sum_{iab} c_{ia}c_{jb}\,\Delta_{ij}(S_{pq})\,\langle\chi_a|\omega|\chi_b\rangle$$

where c_{ia} is the coefficient of basis function b in molecular spin orbital i. S is the matrix of overlap between molecular spin orbitals and Δ is the matrix of cofactors of S. The need to use this expansion arises because, for example, the $1\pi^+$ spin orbitals of $X^2\Pi$ and $B^2\Sigma^+$ are not identical so that Slater's rules do not apply.

Hall (1971) has produced the somewhat more complicated transformation equations which arise for two-electron operators and has written a program which calculates one-centre off-diagonal integrals of the spin-orbit coupling operator between Slater determinants constructed from the same atomic basis set but which have non-orthogonal

orbitals. Attention is restricted to pairs of determinants which differ in one spin orbital that is $\bar{\pi}^*$ in the first state and σ in the second. The matrix of cofactors is obtained by the method of Prosser and Hagstrom (1968) which involves diagonalisation of the overlap matrix by biorthogonalisation.

The operator L^* may also be expanded in terms of one-electron operators (l^*) and Hinkley (1971) has succeeded in reducing matrix elements to integrals over Slater-type orbitals. For one-centre terms, the operator may be expanded:

$$l^* = l_A^* - R_m \nabla^*$$

where R_m is the distance between centre A and the centre of mass. Using the fact that STOs centred on A are eigenfunctions of l_A^2 and using the formula given by Edmonds (1957) for the effect of the gradient operator on a spherical harmonic, it is possible to deduce an expression for $l^*|\sigma\rangle$ and thus reduce one-centre integrals $\langle\pi|l^*|\sigma\rangle$ to an analytic form.

The two-centre terms may be evaluated by expanding l^* as follows:

$$l^* = \frac{m_A}{m_A+m_B} l_A^* + \frac{m_B}{m_A+m_B} l_B^*$$

$$\langle\chi_A|l^*|\chi_B\rangle = \frac{m_A}{m_A+m_B}\langle\chi_B|l_A^-|\chi_A\rangle + \frac{m_B}{m_A+m_B}\langle\chi_A|l_B^+|\chi_B\rangle$$

The angular eigenfunctions are orthonormal and so all that remains is the radial integration which may be performed numerically using, for example, crossed Gaussian-Legendre quadrature.

Both the one-centre and two-centre terms can be seen to depend on the reduced mass of the system: $L^{\cdot}$, unlike H_{so}, gives slightly different matrix elements for SiH and SiD. These differences are small except when the matrix elements are very small as in certain highly excited terms arising in the CI expansion. Table VIII gives calculated Hartree-Fock matrix elements of $L^{\cdot}$ between the $X^2\Pi$ and the $B^2\Sigma^+$ states.

Table VIII Values of $\langle X^2\Pi|L^{\cdot}|B^2\Sigma^+\rangle$ for SiH and SiD.

R/bohr	SiH	SiD
2.2	0.986246	1.002595
2.4	1.029312	1.045238
2.6	1.085951	1.101314
2.8	1.154003	1.168300
3.0	1.234946	1.246721
3.2	1.316318	1.321154
3.4	1.330755	1.330560
4.0	1.297639	1.294602

2.6 Vibrational wavefunctions for bound levels.

Vibrational wavefunctions may be obtained in numerical form on points of a grid by solution of the radial Schrödinger equation by a Numerov procedure. An initial guessed eigenvalue is used to generate a trial solution that does not satisfy the boundary conditions - the deviation from these conditions is used to generate a better eigenvalue and the process is repeated until the boundary conditions are satisfied within a given tolerance. Convergence is usually achieved within a small number of iterations.

The present work uses a program based on a routine written by LeRoy which follows, in part, from the work of Cooley (1961) and Cashion (1963). This program has a number of advantages over various similar programs; in particular, the large number of arrays used by the routines of Redman (1970) to carry out a Newton-Raphson approximation are avoided. The potential used can be either analytic or numerical - in both cases it is extrapolated onto the grid of points corresponding to different R values. Redman preferred a logarithmic grid which has the advantage of being closely spaced at small internuclear distances where the potential varies most with R. A linear grid was used in this work: large, very closely spaced grids were used to ensure sufficient grid points at small R - the program reports the number of grid points per node. Care was also

taken to ensure that the lower limit of integration did not truncate the tail of the wavefunction at small R.

2.7 Vibrational wavefunctions for continuum levels.

The box normalisation procedure has been used by Gordon and Cashion (1966) and by Czarny et al. (1971) and more recently by Hammersley (1974) and Wilson (1975) to calculate pseudo-continuum wavefunctions. The system is treated as a bound state by placing a very steep potential barrier at large internuclear distance. Wilson placed the wall at 25 Å since the integrals were virtually unchanged when the barrier was moved out to larger R.

Czarny et al. have compared their results for the predissociation of O_2 with those obtained by other methods and have found good agreement. Unfortunately, a small percentage error in matrix elements involving continuum vibrational levels leads to large differences (in MHz) in the frequency prediction for the Λ-doubling transition in SiH. The box normalisation procedure was not used in this work.

It must be stressed that the problem with box normalisation is not the method per se. The potential is not generally well characterised beyond, say, 8 bohr so that it is not suprising that uncertainties arise at large R. The method can thus be very sensitive to the position of the

barrier simply because the potential is uncertain.

If a continuum wavefunction with energy E and rotational quantum number J is denoted by $\psi_{E,J}(R)$ then the appropriate radial Schrödinger equation is

$$\{d^2/dR^2+2\mu(E-V(R))/\hbar^2-J(J+1)/R^2\}\psi_{E,J}(R)=0$$

The boundary conditions at R=0 and $R\to\infty$ are:

$$\psi_{E,J}(0)=0$$

and $$\lim_{R\to\infty}\psi_{E,J}(R)=\left[\frac{2\mu}{\pi k\hbar^2}\right]^{1/2}\sin(kR-J\pi/2+\eta_J(E))$$

where $\eta_J(E)$ is the phase shift and $k^2=2\mu E/\hbar^2$.

Wilson (1977) has examined the two usual methods of imposing these boundary conditions. In the first of these, numerical integration is carried out to a value of R where the wavefunction is sinusoidal to within a reasonable tolerance. In the second method, due to LeRoy et al. (1976), the first-order WKB approximation is used for the wavefunction:

$$\psi_{EJ}(R)=A(R)[k(R)]^{-\frac{1}{2}}\sin\{\int^R k(R)dR+\eta_J(E))\}$$

where $k(R)^2=2\mu(E-V(R))/\hbar^2-J(J+1)/R^2$.

A(R) may be found by fitting the numerical wavefunction to this expression; the asymptotic amplitude is then given by:

$$A_{-}(R)^{4}=A(R)^{4}\left\{\frac{E-V(R)-\hbar^{2}J(J+1)/2\mu R^{2}}{E}\right\}$$

This method leads to a much smaller range of integration and thus also to the possibility of a more closely spaced grid.

The present work uses a program based on a routine written by Ashton which uses the method proposed by LeRoy. The programs for bound and continuum vibrational wavefunctions have been written in such a way that matrix elements of functions of R could be calculated between vibrational states. In particular, for SiH $\langle X^{2}\Pi\ v|H_{so}|^{2}\Sigma^{-}\ E_{u}\rangle$ and $\langle X^{2}\Pi\ v|BL^{+}|^{2}\Sigma^{-}\ E_{u}\rangle$ were calculated at various values of E_u, the energy of the continuum level relative to the asymptote of the $^{2}\Sigma^{-}$ potential curve.

For continuum levels, the summations over vibrational levels in the expressions for p and q (see section 2.2) must be replaced by integrals with respect to E_u. Thus, the contribution of the $^{2}\Sigma^{-}$ state to the Λ-doubling parameters for vibrational level v of the $X^{2}\Pi$ state may be written:

$$p_{v}=\frac{1}{2}\int_{0}^{\infty}\frac{\langle X^{2}\Pi\ v|H_{so}|^{2}\Sigma^{-}\ E_{u}\rangle\langle^{2}\Sigma^{-}\ E_{u}|BL^{-}|X^{2}\Pi\ v\rangle dE_{u}}{\Delta E_{v}+E_{u}}$$

$$q_{v}=2\int_{0}^{\infty}\frac{|\langle X^{2}\Pi\ v|BL^{+}|^{2}\Sigma^{-}\ E_{u}\rangle|^{2}dE_{u}}{\Delta E_{v}+E_{u}}$$

where E_u is the separation between the vth level of $X^{2}\Pi$ and the asymptote of the $^{2}\Sigma^{-}$ state.

In weakly bound states, the contribution to the Λ-doubling parameters may arise from both a sum over bound levels and an integral over continuum levels. In this case, it is easy to miss contributions from near the dissociation limit. A method which deals with this problem will be described in chapter 4. The lowest $^2\Sigma^-$ state of SiH is purely dissociative while the $B^2\Sigma^+$ state is quite strongly bound and so the problems of weakly bound states do not arise.

2.8 Terrestrial measurement of the Λ-doublet splitting.

Published spectroscopic constants not only differ with the resolution of the observed electronic spectrum but also with the method of analysis of the observed transitions. The values given in table IX are by no means a complete record of the experimental values of p and q but should give some idea of the uncertainty in the constants.

Rochester (1936) obtained p=0.079 cm^{-1} and q=0.0081cm^{-1}; Douglas (1957) accepted these values and suggested that the splitting is 0.098 cm^{-1} or 2940 MHz. Klynning et al. (1967) used a term value approach and obtained a value for the splitting of 2942 MHz with a standard deviation of 1%. However, Freedman and Irwin (1976) suggest that the term value approach gives biased estimates of molecular constants and so they used a direct fit procedure for the observed wavenumbers for the (0,0) and (1,0) bands of the $A^2\Delta - X^2\Pi$

transition. The splitting finally adopted by these authors was an average of the two sets of values - it is far from clear why such an average should be taken.

Table IX Terrestrial estimates of the Λ-doubling in SiH

Authors	p/cm^{-1}	q/cm^{-1}	(p+2q)/MHz
Rochester (1936) (1,0) band	0.079	0.0081	2854
Douglas (1957)	-	-	2940
Klynning et al. (1967)	0.080	0.00907	2942±30
Freedman and Irwin (1976)			
(0,0) band	0.08191	0.008310	2954
(1,0) band	0.0790	0.00828	2866
"average"			2932±18
Klynning et al. (1979)	0.08237	0.00831	2968±6

Klynning et al. (1979) have remeasured the (0,0) band of $A^2\Delta - X^2\Pi$ from high dispersion plates and suggest a value of 2968±6MHz. This value is more reliable than those from previous measurements and probably represents the best

terrestrial estimate of the Λ-doublet splitting in the ground state of SiH.

The calculations of the spin-orbit coupling constant by Walker (1969) and of various molecular constants by Wilson (1975) have already been mentioned. Wilson's electronic matrix elements were obtained using CI and are very reliable. However, box normalisation was used to obtain vibrational wavefunctions for the $^2\Sigma^-$ state. The Λ-doubling predicted was several percent larger than any of the terrestrial estimates.

2.9 Λ-doubling splitting in SiH.

The calculated electronic matrix elements of Wilson (1975) for the $^2\Sigma^-$ state (see table X) were extrapolated onto the grid used by the continuum wavefunction program (see section 2.7). The wavefunction for the $X^2\Pi$ state was obtained on an identical grid using the bound states program (see section 2.6) and values of vibronic matrix elements of H_{so}, and BL^+ were found between these two states. The integrals for p and q were then evaluated so as to obtain the contribution of the $^2\Sigma^-$ state to the Λ-doubling in the $v''=0$ level of the ground state of SiH. Values are given in table XI.

Table X Off-diagonal matrix elements as a function of internuclear distance.

R/bohr	$\langle X^2\Pi\|H_{so}\|^2\Sigma^-\rangle/cm^{-1}$	$\langle X^2\Pi\|L^+\|^2\Sigma^-\rangle$
2.4	25.934	1.683
2.6	26.093	1.736
2.8	26.071	1.717
3.2	24.356	1.569
3.4	23.187	1.511
3.6	22.135	1.344

	p/cm^{-1}	q/cm^{-1}
This work	0.053363	0.010200
Wilson	0.053927	0.012727

Table XI Contribution from the $^2\Sigma^-$ state

In principle, the summations for p and q extend over all $^2\Sigma$ states but, as is frequently the case, the summations can be limited to a very small number of states. In the case of SiH, we would expect from Van Vleck's pure precession approximation that only the $B^2\Sigma^+$ and $^2\Sigma^-$ states would be important.

The concept of pure precession is also important in terms of matrix elements of L^+ since these are not strictly defined for diatomic molecules: $|\Lambda\ S\ \Sigma\ J\ v\rangle$ is not an eigenfunction of L^2 and so L is not a good quantum number. Colbourn and Wayne (1979) have examined certain matrix elements of the operators L^2 and L^+ for triplet states of some diatomic molecules. They conclude that the pure precession hypothesis breaks down (i.e. many states have important contributions) for many non-hydride molecules; the hypothesis remains a useful concept for molecules which do not deviate markedly from the united-atom limit. For example, the value of $\langle^3\Sigma^-|L^-|^3\Pi\rangle$ for PF is two orders of magnitude greater than the value for PH.

An approximate value was obtained for the contribution from the state $(1-5)\sigma^2 6\sigma 1\pi^4$. At 3 bohr, the value of $\langle X^2\Pi|L^+|^2\Sigma^+\rangle$ was 0.2265 and the value of $\langle X^2\Pi|H_{so}|^2\Sigma^+\rangle$ was 66.46 cm^{-1}. Approximate vibrational matrix elements were obtained giving order of magnitude estimates

$$p\sim 4\times 10^{-4} cm^{-1} \quad q\sim 6\times 10^{-5} cm^{-1}$$

These values are not negligible in absolute terms but are small compared with the probable error in the energy separation between the $X^2\Pi$ and $^2\Sigma^-$ states.

The values obtained for the contribution from the $^2\Sigma^-$ state were combined with Wilson's values for the $B^2\Sigma^+$ state so as to obtain values of p and q . Ab initio values are collected in table XII. The magnitude of the splitting in the v''=0 level of $X^2\Pi$ is given by

$$-(p+2q)=0.10007 cm^{-1}=3000 MHz.$$

This value is appreciably lower than the previous ab initio value of 3168 MHz and is closer to the most recent terrestrial estimate than are many of the earlier experimental values.

Table XII Contributions to Λ-doubling in SiH.

	p_0 /cm^{-1}	q_0 /cm^{-1}
$B^2\Sigma^+$ state	0.028673	-0.001185
$^2\Sigma^-$ state	0.053363	0.010200
Total	0.08204	0.009015

2.10 Discussion.

The cosmic abundance of silicon suggests the presence of SiH in interstellar clouds. The molecule should be observable as a radiofrequency transition between the Λ-doublet components of the lowest rotational level - the lowest rotational transition of this molecule lies outside the range studied by radioastronomers. A search for this molecule has been hampered by the fact that the relevant terrestrial experiments are rather difficult. Furthermore, different spectroscopists use different fitting procedures and thus obtain very different results.

The true accuracy of the ab initio prediction of 3000 MHz will not be known until SiH is observed in the interstellar medium; however, the results suggest that core polarisation does not pose a serious problem.

Ultra-violet observations on diffuse clouds suggest significant depletion of Si relative to normal solar abundance. This is often taken to mean that silicon resides mostly in interstellar grains with only a small fraction available for molecule formation. Other molecules containing depleted elements will be considered in chapter 3. It is interesting that recent ultraviolet studies of the interstellar material in the halo and spiral arms of our Galaxy suggest the presence of a high velocity gas with nearly normal abundances of elements such as silicon (Pettini, private communication, 1981).

CHAPTER THREE

Molecules containing depleted elements.

CHAPTER 3 Molecules containing depleted elements.

Before a search can be made in interstellar space for a new molecule, accurate frequency predictions are required - these might come from terrestrial spectroscopy or from ab initio calculations. In chapter 2, we predicted the Λ-doubling frequency of SiH. At present the only known silicon molecules are SiO and SiS whereas sulphur (a factor of two less abundant) has been detected in ten molecules. The detection of SiH would appreciably alter the present estimates of gas-phase silicon abundance. A number of other elements, particularly the alkali metals and alkaline earth metals, are also apparently depleted in the interstellar medium. The most heavily depleted element is calcium and we shall consider spin-splitting in CaH. We shall also consider spin-splitting in BH^+ and Λ-doubling in LiO. Very accurate radiofrequency data exists for LiO but ab initio calculations will be seen to be very important.

3.1 Spin-orbit coupling and Λ-doubling in LiO.

This molecule has a $^2\Pi$ ground electronic state with radiofrequency transitions between the Λ-doublet components observable in the laboratory and, conceivably, also astrophysically. Accurate data is available from molecular beam studies but only for a fairly limited number of transitions. There are very large uncertainties in the fitting procedure and high correlation between fitted

molecular constants. This is unfortunate in view of the quality of the data.

Freund et al. (1972) have observed radiofrequency and X-band microwave transitions of LiO in both components ($\Omega = \frac{3}{2}$ and $\Omega = \frac{1}{2}$) of the $X\,^2\Pi$ state using an electric resonance molecular beam spectrometer. Analysis of the radiofrequency spectrum requires some prior knowledge of the fine structure. Values for various molecular constants were taken from theoretical calculations of Wahl. The configuraction interaction (CI) calculations of Yoshimine (1972) give rather different values, particularly for the energy separation between the $X\,^2\Pi$ and $A^2\Sigma^+$ states.

Yoshimine used the ALCHEMY program to calculate self-consistent field (SCF) and CI wavefunctions using a large number of Slater-type orbitals (STOs) and about 1500 symmetrised configurations. Remarkable agreement was found between molecular properties calculated using SCF and CI wavefunctions. In particular, the change in dipole moment was less than 2% indicating a very small influence on charge distribution.

The basis set in table I was taken from that used by Yoshimine and consists of 26 STOs of σ symmetry and 12 STOs of π symmetry. Separate SCF procedures were carried out on both the $X^2\Pi((1-3)\sigma^2 4\sigma^2 1\pi^3)$ and $A^2\Sigma^+((1-3)\sigma^2 4\sigma 1\pi^4)$ states using the ALCHEMY program. Matrix elements of H_{so} and L^+ were

then calculated at 3.3 bohr (i.e. close to the minimum of the ground state).

	Li	O
1s	4.699, 2.478	12.418, 6.995
2s	1.5, 0.81, 0.643	3.9, 2.922, 1.818
3s	2.681, 0.5	8.681, 1.6
2p	3.9, 3.0, 2.111	8.450, 4.7, 3.744
	1.076, 0.736	2.121, 1.318
3p	0.6	1.3
3d	3, 2, 1	4, 3, 2

Table I Zeta values used in the LiO calculations.

The R-centroid approximation recognises that if the electronic matrix elements do not vary rapidly with internuclear distance, then it is reasonable to factorise vibronic matrix elements into separate vibrational and electronic parts. In the case of a simple harmonic oscillator the factorisation is still valid even if the matrix elements vary rapidly with distance provided that the change is linear. The R-centroid approximation was used in this work to rewrite the expressions for p_v and q_v as:

$$p_v = 4\langle {}^2\Pi|\hat{H}_{SO}|{}^2\Sigma\rangle\langle {}^2\Pi|\hat{B}(\hat{L}^+ - \hat{L}^-)|{}^2\Sigma\rangle \sum_v \frac{\langle v\,v'\rangle\langle v|\hat{B}|v'\rangle}{E_{\pi,v} - E_{\Sigma,v}}$$

$$q_v = 2|\langle {}^2\Pi|\hat{B}(\hat{L}^+ - \hat{L}^-)|{}^2\Sigma\rangle|^2 \sum_v \frac{|\langle v|\hat{B}|v'\rangle|^2}{E_{\Pi,v} - E_{\Sigma,v}}$$

The electronic matrix elements need thus only be calculated at one internuclear distance: the R-centroid has been

approximated as 3.3 bohr. It is common to use R_e for this quantity.

Vibrational wavefunctions were obtained by numerical solution of the radial Schrödinger equation using a Numerov procedure. The potentials used were taken from the CI calculations of Yoshimine. The vibrational and electronic matrix elements were combined to give the calculated values in table II. LiO is very close to pure precession so that the summations for p and q may be limited to the interaction of the $X^2\Pi$ and $A^2\Sigma^+$ states.

The most reasonable level on which to test the calculated Λ-doubling parameters is $\Omega=\frac{1}{2}$, $J=\frac{3}{2}$, $v''=0$. The Λ-doublet splitting is predicted to be 12480 MHz for which Freund et al. have measured four lines at 12325.6 MHz, 12321.51 MHz, 12327.41 MHz and 12319.93 MHz. Transitions in the $\Omega=\frac{3}{2}$ manifold depend fairly strongly on the value chosen for A_π, B_π.

The diagonal spin-orbit coupling constant was calculated and the various contributions are listed in table III. The results confirm the validity of the one-centre approximation for the corresponding off-diagonal matrix elements. The observed value of A is -112.0 cm^{-1} but Freund et al. admit extensive correlation among their fine structure constants so that both A_n and the corresponding off-diagonal quantities are only known experimentally to

Table II. Computed values of molecular parameters.

Quantity	Value
$\langle X\,^2\Pi \mid H_{SO} \mid A\,^2\Sigma^+ \rangle$	83.56 cm^{-1}
$\langle X\,^2\Pi \mid L^+ \mid A\,^2\Sigma^+ \rangle$	1.401
p_0	0.2127 cm^{-1}
q_0	−0.002 167 cm^{-1}

Table III. Spin–orbit coupling constant for LiO ($X\,^2\Pi$).

	one-center	one-center and two-center
one-electron term (in cm^{-1})	−193.58	−194.58
two-electron term (in cm^{-1})	70.18	70.60
Total (in cm^{-1})	−123.40	−123.98

Table IV Observed and calculated radio frequency spectroscopic splittings.

State $\mid v, \Omega, J \rangle$	Observed (in MHz)	Calculated (in MHz)
$\mid 0\ \frac{3}{2}\ \frac{3}{2} \rangle$	11.282(10)	10.8
$\mid 0\ \frac{3}{2}\ \frac{5}{2} \rangle$	45.02(3)	43.1
$\mid 0\ \frac{3}{2}\ \frac{7}{2} \rangle$	112.237(2)	107.7
$\mid 0\ \frac{3}{2}\ \frac{9}{2} \rangle$	223.721(3)	215.0
$\mid 0\ \frac{1}{2}\ \frac{3}{2} \rangle$	12 325.82(3)	12 481.9

$\pm 10 cm^{-1}$.

The calculated values, A=-123.98 cm^{-1} and B=1.202 cm^{-1} were used to calculate Λ-doublet splittings for various J values of $\Omega = \frac{3}{2}$. The various calculated splittings are compared in table IV with the F' =3 → F'' = 3 transition frequencies (these values are very little different from the other components observed; this transition is common to all the J values considered here). Agreement between the calculated and experimental values is remarkably good.

Veseth (1976) has reanalysed the high precision molecular beam spectrum in terms of an unperturbed model denoted coupling case c_α and has found that fine-structure corrections beyond second-order do not have significant influence on the Λ-doubling despite the small energy separation. In view of this, the most important source of error remaining in these calculations is the uncertainty in the energy separation between the two electronic states. The remarkable accuracy of the predicted Λ-doublet splittings suggests that the experimental radiofrequency spectrum of LiO should be re-examined. Clearly the Yoshimine value for the separation of the electronic states should be used. Use of the ab initio spin-orbit coupling constant would break the extensive correlation between molecular parameters.

3.2 Spin-splitting in $^2\Sigma$ states.

Part of the Breit hamiltonian causes a direct interaction between the spin and rotational angular momenta. However, this effect is usually small compared with an indirect interaction due to the spin-orbit coupling operator, H_{so}. This operator mixes orbital angular momentum with spin angular momentum; this in turn leads to a coupling between the spin and rotational angular momenta.

The spin-doubling in a $^2\Sigma$ state may be described using an effective hamiltonian

$$H_{sr}=\gamma \mathbf{N}\cdot\mathbf{S}$$

where N is the rotational angular momentum of the nuclear framework, S is the total electron spin angular momentum and γ is the spin-rotation coupling constant. The first-order correction is due to the direct interaction and is given by (Green and Zare, 1976)

$$\gamma_v^{(1)}=\frac{-ge\hbar^2}{2m_e c^2\langle I\rangle}\langle {}^2\Sigma\ v|\sum_K\sum_i\frac{Z_K\cos\theta_{Ki}}{r_{iK}^2}|{}^2\Sigma\ v\rangle$$

where the summation extends over all nuclei, K, and over all unpaired electrons, i, and where <I> is the vibrational expectation value of the moment of inertia.

The second-order contribution to the spin-rotation coupling constant in a $^2\Sigma$ state may be derived by considering the interaction of this state with a $^2\Pi$ state using second-order perturbation theory (Van Vleck, 1929;

Kovács, 1969). The expression obtained closely resembles the expression for the Λ-doubling parameter p except that the summation is now over all $^2\Pi$ states

$$\gamma_v^{(2)} = 4 \sum_{n' v'} \frac{\langle {}^2\Sigma \; v | BL^+ | n'v' \rangle \langle n'v' | H_{so} | {}^2\Sigma \; v \rangle}{E_{n'v} - E_{\Sigma v}}$$

Wilson (1978) has calculated values of $\gamma_v^{(1)}$ and $\gamma_v^{(2)}$ for the $A^2\Sigma^+$ state of HF^+. The ratio $\gamma_v^{(1)}/\gamma_v^{(2)}$ was less than 10^{-4} so that the contribution from $\gamma_v^{(1)}$ was negligible. Here this work is extended to CaH. Apart from the effects introduced by a third-row atom, CaH is of intrinsic interest as its spectrum is of importance in resolving the apparent depletion of Ca in the interstellar medium relative to its abundance in stars.

There is a high correlation between γ and the centrifugal distortion in the spin-orbit coupling constant, A_D. Only in special cases where high quality spectra are available for isotopic molecules have separate determinations of these two constants been possible. The description of Zeeman spectra is strongly affected by the choice of γ_v or A_D - this leads to different fitted g values in ESR. Ab initio calculations are obviously of some importance to the experimentalist.

3.2.1 CaH

The basis set for CaH was taken from the values for CaO and MgH and is given in table V. The basis set consists of 19 σ STOs and 9 π STOs.

	Ca			H	
σ:	1s	16.7159	21.7744	σ: 1s	Ø.9151 1.450
	2s	7.6735	9.2638	2s	1.850
	3s	2.90954	4.10282	2p	1.4555
	4s	Ø.87095	1.46516		
	2p	7.2468	13.24497		
		3.68515			
	3p	2.34465			
	4p	Ø.83413			
	3d	2.21403			
	4f	2.90000			
π:	2p	7.2468	13.24497	π 2p	1.3000
	3p	3.68515	2.34465	3d	1.850
	4p	1.06184			
	3d	1.14926			
	4f	1.03702			

Table V STO exponents for CaH.

Separate SCF procedures were carried out for the $X^2\Sigma^+$ $((1-6)\sigma^2 7\sigma 1\pi^4 2\pi^4)$ and $A^2\Pi_r (1-6)\sigma^2 1\pi^4 2\pi^4 3\pi$ states using the ALCHEMY program. Matrix elements calculated at 3.7842 bohr are

$$\langle A^2\Pi | H_{so} | X^2\Sigma^+ \rangle = 39.952 cm^{-1}$$

$$\langle A^2\Pi | L^+ | X^2\Sigma^+ \rangle = 0.7736$$

Vibrational curves were constructed from Dunham curves generated from experimental data. Values for the dissociation energy were not available for some of the curves and so estimates were made. The coefficients used are listed in table VI.

State	R_e/Å	D_e/cm^{-1}	A_1/Å^{-1}	A_2/Å^{-2}	A_3/Å^{-3}	A_4/Å^{-4}
$X^2\Sigma^+$	2.0025	14000	0.32567	-1.75921	1.00265	-0.18542
$A^2\Pi$	1.974	15000	0.54617	-1.69568	0.86502	-0.15996
$E^2\Pi$	2.001	12000	1.51270	-0.17030	-0.78962	-0.16699

Table VI Dunham coefficients for CaH.

In Van Vleck's limit of pure precession, only the interaction of $X^2\Sigma^+$ and $A^2\Pi$ is important to the value of γ. The R-centroid approximation was used to factorise the vibronic matrix elements into separate vibrational and electronic components; vibrational wavefunctions were then obtained using a Numerov procedure (as described in chapter 2). Very few of the vibrational levels of the $A^2\Pi$ state were found to have significant contributions. Use of Dunham curves generated using different values for the dissociation energy caused very little change. The electronic and vibrational matrix elements were combined with experimental term values and the value labelled γ_{X-A} in table VII was obtained. This value is about 13% lower than experiment

suggesting that other states are also important in the summation. The error limit quoted for the experimental value (Berg and Klynning, 1974) is actually the standard deviation in the last figure.

Spin-doubling in CaH ($X^2\Sigma^+$, $v'' = 0$)

		$\gamma_0^{(2)}/cm^{-1}$
Calculated	γ_{X-A}	0.03638
	γ_{X-E}	0.00771
Total		0.0441
Experiment (Berg *et al.*)		0.0424(10)

The figure in brackets is the quoted error in the last figure

Table VII

Considerable difficulty was experienced in obtaining electronic wavefunctions for the $E^2\Pi$ and $L^2\Pi$ states and so the real and virtual orbitals of the ground state were used to generate these excited states. The magnitude of the electronic matrix elements between the ground state and these $^2\Pi$ states suggest that the summation needs to be extended over the E state but not over the L state. The contribution from $E^2\Pi$ is labelled γ_{X-E} in table VII.

The final calculated value for γ_0 is within about 5% of experiment and is only just outside the experimental error limit. Clearly, the calculated value would be improved by the inclusion of CI, by the use of better potential curves and by the use of separate SCF procedures for each state. The error introduced by the R-centroid approximation is likely to be of the order of 1%.

The results for CaH suggest that the calculations of spin-splitting could be made as accurate as Λ-doubling calculations provided similar procedures are adopted. Even at this level, the results should be of predictive value to experimentalists, even those working in the radiofrequency range.

3.2.2 BH^+.

BH^+ can be produced in a hollow cathode and the emission spectrum $A^2\Pi - X^2\Sigma^+$ has been measured by Almy and Horsfall (1937). Because of low resolution and uncertainties in the fitting, molecular constants obtained from this experiment are not expected to be particularly good. Application of the Hill and Van Vleck (1928) theory failed to give a value of A/B which was constant with increasing J. This situation was not greatly improved by the inclusion of centrifugal distortion constants, D_v. The remaining discrepancy was attributed to unobserved $^2\Sigma$ doubling; it was impossible to obtain an accurate value for the spin-rotation constant - a pure precession argument suggested that γ_0 was of the order of $0.02 cm^{-1}$. Calculation of an accurate value using ab initio methods would be very worthwhile.

Gerratt and Raimondi (1980) have applied the spin-coupled valence bond theory of molecular electronic structure to the $^2\Sigma^+$ state of BeH, which is isoelectronic with BH^+. The single-configuration spin-coupled wavefunction

for BeH is of the form:

$$\Psi^{(0)}_{SM_s} = |\{\phi_1\phi_2 \ldots \phi_N\}\ S,\ M_S\rangle$$

$$= |\{\sigma_1\sigma_2\sigma_3\sigma_4\sigma_5\}\ \tfrac{1}{2}, \pm\tfrac{1}{2}\rangle$$

where σ_1 and σ_2 correspond to two Be atom core orbitals which are permanently coupled to give a singlet spin; σ_3 and σ_4 are distorted sp hybrid orbitals on Be; σ_5 is a distorted 1s orbital on H. There are two linearly independent spin functions. A sharp change occurs in the spin-coupling coefficients, c_1 and c_2, from essentially atomic coupling above 5 bohr to a molecular description below 4 bohr (see figure 1).

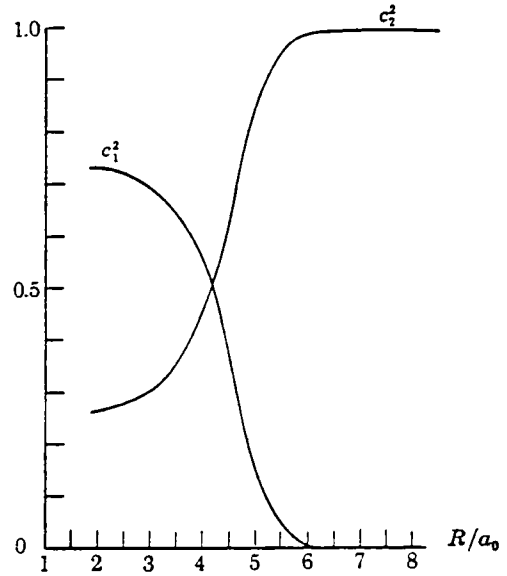

Figure 1
Spin-coupling coefficients for BeH ($X^2\Sigma^+$).

The calculated potential curve varies smoothly throughout. Using molecular orbital theory, this change corresponds to intersection of curves corresponding to configurations $1\sigma^2 2\sigma^2 3\sigma$ and $1\sigma^2 3\sigma^2 2\sigma$. This leads to a discontinuity in the SCF-CI energy.

Separate SCF procedures were carried out for the $X^2\Sigma^+$ $(1\sigma^2 2\sigma^2 3\sigma)$ and $A^2\Pi$ $(1\sigma^2 2\sigma^2 1\pi)$ states of BH^+ using the ALCHEMY program. The basis set is that used by Trivedi and Richards

(1980) and is given in table VIII.

	B			H	
1s	3.91385	7.32757	1s	1.18274	2.90014
2s	0.97964	1.56574	2s	1.98224	
3s	4.78275		2p	1.69999	
2p	0.91077	1.54007			
	2.14447	5.62328			
3d	1.08034	1.86930			
4f	1.25224				

Table VIII STO exponents for BH^+.

A CI expansion was carried out for both states. The active electrons were all but the the $1\sigma^2$ core; excitations were allowed up to 6σ and 3π with up to three electrons in virtual orbitals. This generated 85 CSFs for $X^2\Sigma^+$ and 102 CSFs for $A^2\Pi$. The potential curves are given in tables IX and X. The CI curves are shown in figure 2 and, as suggested by the discussion of BeH, there are discontinuities between 3 bohr and 4 bohr.

The SCF wavefunctions were used to calculate off-diagonal matrix elements of H_{so} and L^+S^- between the two states (see table XI). From figures 3 and 4 it can be seen that there are physically unreal discontinuities in the calculated quantities between 3 bohr and 4 bohr. It seems reasonable to attribute these to spin-recoupling as in BeH.

R/bohr	E(total)/hartree	
	no CI	85 CSFs
1.20	-24.38486	-24.39842
1.40	-24.60058	-24.61439
1.60	-24.71997	-24.73451
1.80	-24.78295	-24.79872
2.00	-24.81220	-24.82989
2.20	-24.82109	-24.84176
2.30	-24.82057	-24.84324
2.40	-24.81775	-24.84274
2.50	-24.81318	-24.84079
2.55	-24.81038	-24.83940
2.60	-24.80731	-24.83779
2.65	-24.80401	-24.83601
2.70	-24.80051	-24.83410
2.75	-24.79685	-24.83208
2.80	-24.79307	-24.82999
2.85	-24.78918	-24.82786
2.90	-24.78522	-24.82572
2.95	-24.78121	-24.82359
3.00	-24.77717	-24.82149

Table IX $X^2\Sigma^+$ state of BH^+

R/bohr	E(total)/hartree	
	no CI	85 CSFs
3.10	-24.76907	-24.81750
3.20	-24.76109	-24.81389
3.30	-24.75343	-24.81091
3.40	-24.74771	-24.81077
3.60	-24.74457	-24.80686
3.80	-24.74315	-24.80411
4.00	-24.74234	-24.80219
4.20	-24.74179	-24.80082
4.40	-24.74135	-24.79982
4.60	-24.74097	-24.79904
4.80	-24.74060	-24.79840
5.00	-24.74025	-24.79784
5.50	-24.73946	-24.79665
6.00	-24.73879	-24.79566
7.00	-24.73789	-24.79421
8.00	-24.73743	-24.79350
9.00	-24.73722	-24.79370
10.00	-24.73713	-24.79548
15.00	-24.73706	-24.79607
20.00	-24.73705	-24.79607
25.00	-24.73705	-24.79606

Table IX $X^2\Sigma^+$ state of BH^+

R/bohr	E(total)/hartree	
	no CI	102 CSFs
1.20	-24.23684	-24.25109
1.40	-24.45479	-24.47015
1.60	-24.57586	-24.59319
1.80	-24.64049	-24.66075
2.00	-24.67167	-24.69597
2.20	-24.68291	-24.71243
2.30	-24.68374	-24.71621
2.40	-24.68238	-24.71791
2.50	-24.67937	-24.71796
2.55	-24.67738	-24.71749
2.60	-24.67514	-24.71673
2.65	-24.67268	-24.71573
2.70	-24.67004	-24.71453
2.75	-24.66726	-24.71315
2.80	-24.66435	-24.71162
2.85	-24.66134	-24.70996
2.90	-24.65826	-24.70820
2.95	-24.65512	-24.70636
3.00	-24.65194	-24.70445

Table X $A^2\Pi_r$ state of BH^+

R/bohr	E(total)/hartree	
	no CI	102 CSFs
3.10	-24.64552	-24.70048
3.20	-24.63910	-24.69379
3.30	-24.63275	-24.69223
3.40	-24.62653	-24.68808
3.60	-24.61465	-24.67992
3.80	-24.60366	-24.67214
4.00	-24.59368	-24.66486
4.20	-24.58472	-24.65817
4.40	-24.57676	-24.65212
4.60	-24.56974	-24.64672
4.80	-24.56360	-24.64198
5.00	-24.55826	-24.63785
5.50	-24.54791	-24.62899
6.00	-24.54092	-24.62151
7.00	-24.53338	-24.61545
8.00	-24.53039	-24.61487
9.00	-24.52929	-24.61706
10.00	-24.52891	-24.61695
15.00	-24.52882	-24.61626
20.00	-24.52891	-24.61686
25.00	-24.52895	-24.61704

Table X $A^2\Pi_r$ state of BH^+

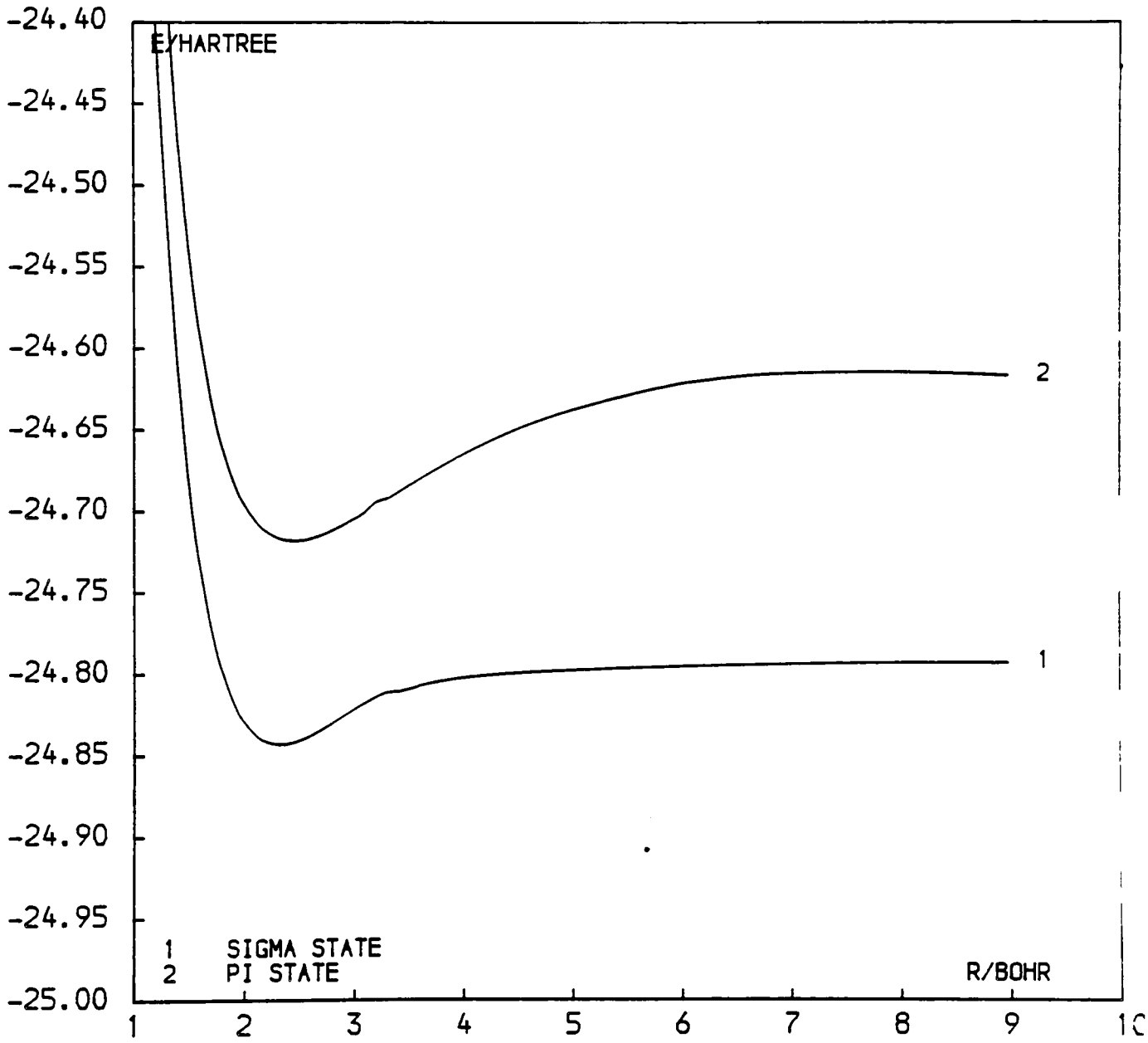

Figure 2 Potential curves for BH^+.

R/bohr	$\langle A^2\Pi\|L^+\|X^2\Sigma^+\rangle$	$\langle A^2\Pi\|H_{so}\|X^2\Sigma^+\rangle/cm^{-1}$
1.20	-1.14073	-28.67083
1.40	-1.16696	-28.31802
1.60	-1.19172	-27.85645
1.80	-1.21413	-27.37496
2.00	-1.23369	-26.92025
2.20	-1.24965	-26.50631
2.30	-1.25598	-26.30969
2.40	-1.26109	-26.11300
2.50	-1.26497	-25.90940
2.55	-1.26647	-25.80253
2.60	-1.26768	-25.69115
2.65	-1.26826	-25.57446
2.70	-1.26930	-25.45104
2.71	-1.26940	-25.42547
2.75	-1.26971	-25.32012
2.80	-1.26985	-25.18071
2.85	-1.26972	-25.03102
2.90	-1.26929	-24.86974
2.95	-1.26852	-24.69422
3.00	-1.26736	-24.50191

Table XI Off-diagonal matrix elements

R/bohr	$\langle A^2\Pi\|L^+\|X^2\Sigma^+\rangle$	$\langle A^2\Pi\|H_{so}\|X^2\Sigma^+\rangle/cm^{-1}$
3.10	-1.26341	-24.04743
3.20	-1.25591	-23.44126
3.30	-1.23939	-22.46006
3.40	-0.99204	-13.74987
3.60	-0.86518	-10.23023
3.80	-0.79358	-8.44771
4.00	-0.73698	-7.16082
4.20	-0.68770	-6.13796
4.40	-0.64279	-5.28789
4.60	-0.60088	-4.56477
4.80	-0.56130	-3.94176
5.00	-0.52371	-3.40122
5.50	-0.43764	-2.33684
6.00	-0.36260	-1.58613
7.00	-0.24534	-0.70447
8.00	-0.16751	-0.30110
9.00	-0.11978	-0.12566
10.00	-0.09250	-0.05195
15.00	-0.07640	-0.00066
20.00	-0.09736	-0.00000
25.00	-0.11961	0.00001

Table XI Off-diagonal matrix elements

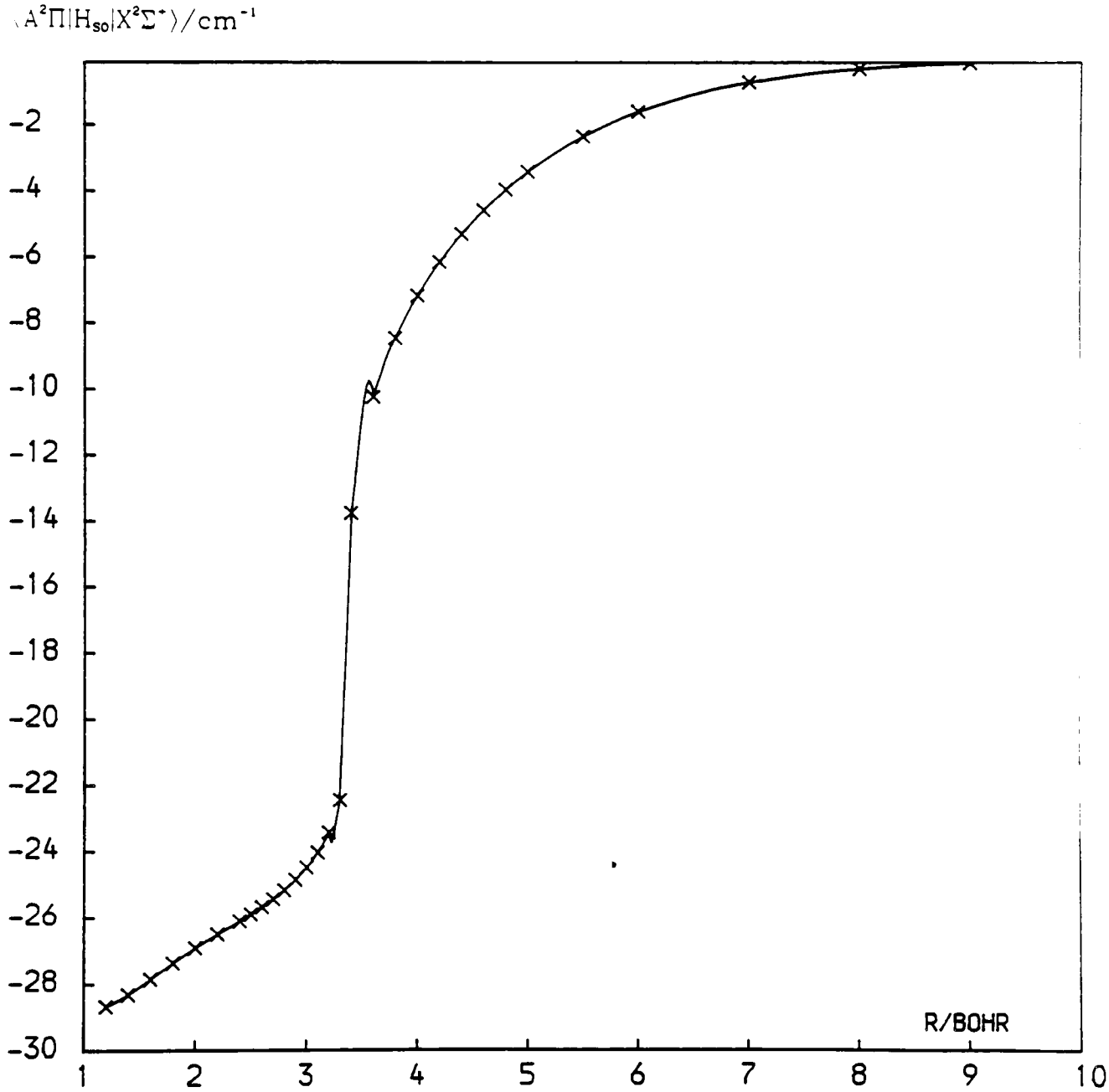

Figure 3 Off-diagonal matrix elements of H_{so}.

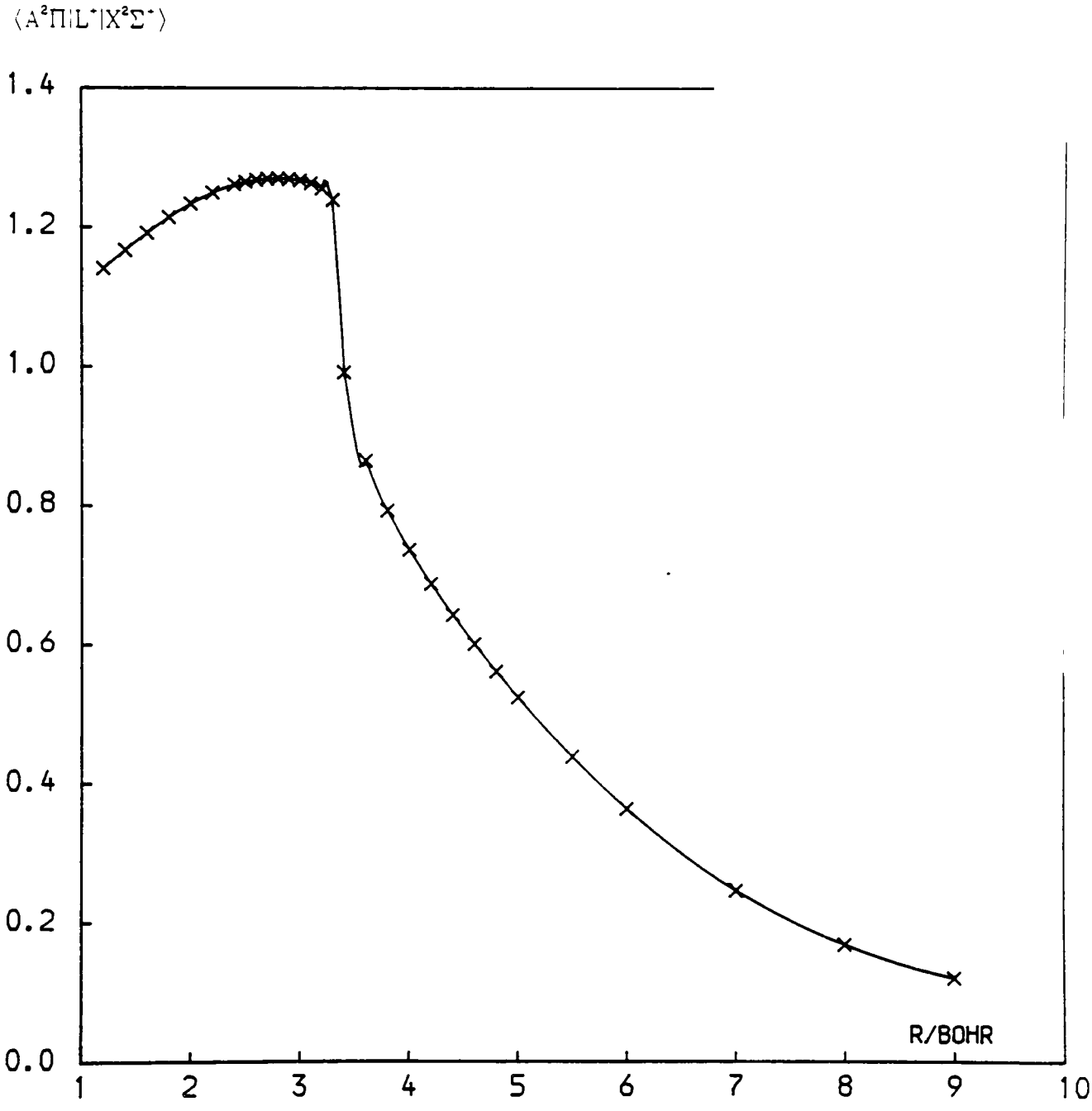

Figure 4 Off-diagonal matrix elements of L^+.

Before calculating a value for the spin-splitting parameter it is necessary to obtain some idea of the quality of the potential curves. No attempt was made to smooth these curves and so the calculated constants might be poorer than usual. The various values are collected in table XII. The results will certainly be less reliable than the CEPA calculations of Rosmus and Meyer (1977) but they do suggest that the CI curves are reasonable to within a few percent.

	Experiment	Calculation
B_o''/cm^{-1}	12.374	11.85
D_o''/cm^{-1}	-0.00125	-0.00132
$R_e''/Å$	1.228	1.21
B_o'/cm^{-1}	11.565	10.65
D_o'/cm^{-1}	-0.00124	-0.00124
$R_e'/Å$	1.298	1.26

Table XII Constants for BH^+.

The direct summation method described in chapter 4 was used to calculate a value for γ. The expression for the spin-rotation constant was factorised into separate components:

$$\gamma_o \sim \langle A^2\Pi|L^+S^-|X^2\Sigma^+\rangle\langle A^2\Pi|H_{so}|X^2\Sigma^+\rangle\gamma_o^{vib}$$

where $$\gamma_o^{vib} = 4\sum_{v'} \frac{\langle v''=0|B|v'\rangle\langle v'|v''=0\rangle}{\nu(^2\Pi\ v',^2\Sigma^+\ v'')}$$

The summation extends over all vibrational levels of the $A^2\Pi$ state. The value for γ_{vib}^0 is $0.001773\,cm^{-1}$, so that using matrix elements at 2.3 bohr (i.e. close to R_e''), the value

of γ_0 is 0.0586 cm^{-1}.

A value for γ_0 was also calculated without factorisation to take into account the somewhat unusual variation of electronic matrix elements with distance. The value thus obtained was 0.0584 cm^{-1}. The similarity between the two calculated values suggests that the discontinuities in figures 3 and 4 do not significantly affect the result.

There are clearly uncertainties in the ab initio value for the spin-splitting due to physically unreal discontinuities in the wavefunctions. Calculated constants for the two curves suggest that the shapes of the potentials may introduce an error of a few percent. The spectrum of BH^+ was analysed in 1937 and a renewed investigation is long overdue.

CHAPTER FOUR

Direct summation over vibrational levels.

CHAPTER 4 Direct summation over vibrational levels.

A method due to Hutson and Howard (1980) allows the direct evaluation of sums such as those encountered for the Λ-doubling parameters p and q. Explicit calculation of the vibrational wavefunctions in the perturbing states is not required.

Starting from the basic equations of Rayleigh-Schrödinger perturbation theory, it is possible to obtain a differential equation for a function $|n' \omega'\rangle$ which satisfies the equation

$$|n' \omega'\rangle = \sum_{v'} \frac{|n' v'\rangle\langle n'v'|B(R)(L^+S^- + L^-S^+)|^2\Pi\ v\rangle}{E_{\pi v} - E_{n'v'}}$$

$|n' \omega'\rangle$ is the first order correction to the state $|^2\Pi\ v\rangle$ due to the perturbation by the electronic state n'. It is not a normalised function (although it must satisfy the usual boundary conditions) and ω' is simply a label. The summations for p and q are reduced to:

$$p = 4 \sum_{n'} (-1)^k \langle^2\Pi\ v|H_{so}|n'\ \omega'\rangle$$

$$q = 2 \sum_{n'} (-1)^k \langle^2\Pi\ v|B(R)(L^+S^- + L^-S^+)|n'\ \omega'\rangle$$

The electronic part of the ket $|n' \omega'\rangle$ is just the appropriate electronic wavefunction, $\phi_{n'}$, whereas the vibrational part $\chi_{n'\omega'}$ is defined by

$$\left[-\frac{\hbar^2}{2\mu}\frac{d^2}{dR^2} + V_{n'}(R) - E_{\pi v} \right] \chi_{n'\omega'}(R) = -B(R)H'_{n'}(R)\chi_{\pi v}(R)$$

where $V_{n'}$, is the effective potential curve for the electronic state n'; $\chi_{\pi v}$ is the vibrational part of the ket $|^2\Pi\ v\rangle$; $H'_{n'}$, is the electronic part of the matrix element of the shift operators

$$H'_{n'}(R) = \int \phi^*_{n'} (L^+S^- + L^-S^+)\phi_\pi \, d\tau_e$$

where $d\tau_e$ denotes integration over all electronic coordinates but not over the internuclear distance.

4.1 Numerical solution.

The linear, inhomogeneous differential equations to be solved are of the form

$$\chi^{(2)}(R)=V(R)\chi(R)+g(R) \qquad (1)$$

where $\chi^{(2)}$ is the second derivative of χ with respect to R and where $g(R)$ has boundary value zero at R equal to zero and as R tends to infinity. For the wavefunction to be quadratically integrable, χ must also tend to zero at these limits.

If all the functions are specified on an equally spaced grid, then equation (1) can be replaced by a finite difference approximation at each grid point. Expanding about grid point i:

$$\chi_{i-1}+\chi_{i+1}=\sum_{k=0}^{\infty}\frac{2h^{2k}}{(2k)!}\chi_i^{(2k)}$$

$$=2\chi_i+h^2\chi_i^{(2)}+\frac{h^4}{12}\chi_i^{(4)}+\ldots$$

where $\chi^{(2k)}$ is the (2k)th derivative of χ and h is the step size on the grid.

Define W_i and Y_i such that

$$W_i = \left(\frac{h^2}{12} V_i\right)\left(1-\frac{h^2}{12} V_i\right)$$

$$Y_i = \chi_i - \frac{h^2}{12}\chi_i^{(2)} = \chi_i\left[1-\frac{h^2}{12} V_i\right] - \frac{h^2}{12} g_i \qquad (2)$$

Boundary conditions are $Y_0 = Y_{n+1} = 0$.

Thus

$$\begin{aligned} Y_{i-1} - 2Y_i + Y_{i+1} &= h^2 \chi_i^{(2)} \\ &= h^2 V_i \chi_i + h^2 g_i \\ &= 12 W_i Y_i + h^2 g_i [1 - W_i] \end{aligned}$$

The set of n simultaneous equations for Y_i may be written

$$\mathbf{AY} = \mathbf{G}$$

where $A_{ii} = -2 - 12W_i$, $A_{ij} = 1$ for $i \neq j$,

and $G_i = h^2 g_i [1 - W_i]$.

The Y_i may be obtained by Gaussian elimination; the function χ is obtained using the inverse of equation (2). The method is numerically stable unless there is a degenerate perturbing level, in which case **A** becomes singular.

4.2 Numerical comparisons.

In these numerical comparisons we shall use the R-centroid approximation to separate the vibronic matrix

elements into purely vibrational and purely electronic parts. It is convenient to define reduced quantities p^{vib} and q^{vib} which correspond to the vibrational sums only:

$$p^{vib}_{n'} = 4 \sum_{v'} \frac{\langle v|v'\rangle\langle v'|B(R)|v\rangle}{E_{\pi v} - E_{n'v'}} = 4\langle v|\omega'\rangle$$

$$q^{vib}_{n'} = 2 \sum_{v'} \frac{|\langle v|B(R)|v'\rangle|^2}{E_{\pi v} - E_{n'v'}} = 2\langle v|B(R)|\omega'\rangle$$

It must be emphasised that the direct solution method is still valid when the R-centroid approximation is not used. Indeed, the computational advantages are greater when $H'_{n'}$ is a fast varying function of R. We shall approximate the R-centroid as R_e for the perturbed state.

4.2.1 OH.

As shown by Hinkley et al. (1973) the vibrational elements in the sums for p and q can be accurately reproduced using Morse curves for the $X^2\Pi$ and $A^2\Sigma$ states

$$V(R) = D\left[1 - \exp(-\beta(R-R_e))\right]^2 + \Delta V$$

where values for the various parameters are given in table I. Contributions to Λ-doubling from higher states have been found to be negligible (Cooper and Richards, 1979).

	D/cm^{-1}	$\beta/\text{Å}^{-1}$	$R_e/\text{Å}$	$\Delta V/cm^{-1}$
OH $X^2\Pi$	37296.9	2.29337	0.9706	0.0
OH $A^2\Sigma^+$	20292.0	2.64746	1.0121	32684.1
Unbound	30000.0	10.0	0.9706	2844.24

Table I. Potential parameters for model problems

These curves are illustrated in figure 1, together with the ground state vibrational wavefunction χ_{π_O}. The expressions for $p^{v'b}$ and $q^{v'b}$ were evaluated by both the conventional 'sum over states' method and by the direct method. OH is a favourable case for the explicit summation approach and the sum converges to within five significant figures when only nine vibrational levels of the $A^2\Sigma^+$ state are included. The results of the direct calculation agree to within the convergence of the summations (see table II).

Also shown in figure 1 is the function $\chi_{A\omega}$ obtained as solution of the equation

$$\left[\frac{h^2}{2\mu} \frac{d^2}{dR^2} + V_A(R) - E_{\pi_O} \right] \chi_{A\omega}(R) = -B(R)\chi_{\pi_O}(R) \quad (3)$$

Although it contains contributions from several vibrational levels of the $A^2\Sigma^+$ state, $\chi_{A\omega}$ is a slowly varying function.

4.2.2 LiO.

This is another case where the summations over n' can be limited to one strongly bound state. In this case, numerical potentials were taken from the large CI calculations of Yoshimine (1972). Explicit evaluation of the summations for $p^{v'b}$ and $q^{v'b}$ gave convergence to within six significant figures with only ten vibrational levels included; the direct method gave agreement to within the limits set by this convergence (see table II).

Table II. Comparison between explicit summation and direct solution results

v'_{max} for sum	$p^{vib}/10^{-3}cm^{-1}$	$q^{vib}/10^{-3}$ cm^{-1}
	OH	
0	-1.96912	-17.44792
1	-2.22128	-20.55588
2	-2.25171	-21.07396
3	-2.25612	-21.17430
5	-2.25716	-21.20487
7	-2.25725	-21.20814
9	-2.25726	-21.20856
Direct	-2.25728	-21.20922
	LiO	
10	-1.81681	- 1.10381
Direct	-1.81673	- 1.10377
	Unbound perturbing state	
Integration mesh size/cm^{-1}		
200	-3.023853	-26.03853
100	-3.023847	-26.03849
Direct	-3.023837	-26.03842

Figure 1. Morse curves used to represent potential curves for OH. Also shown are the ground state vibrational wavefunction $\chi_{\pi o}(R)$, and the correction function $\chi^{(1)}_{\Sigma\omega}(R)$, which has been enlarged by a factor of 500 relative to $\chi_{\pi o}(R)$.

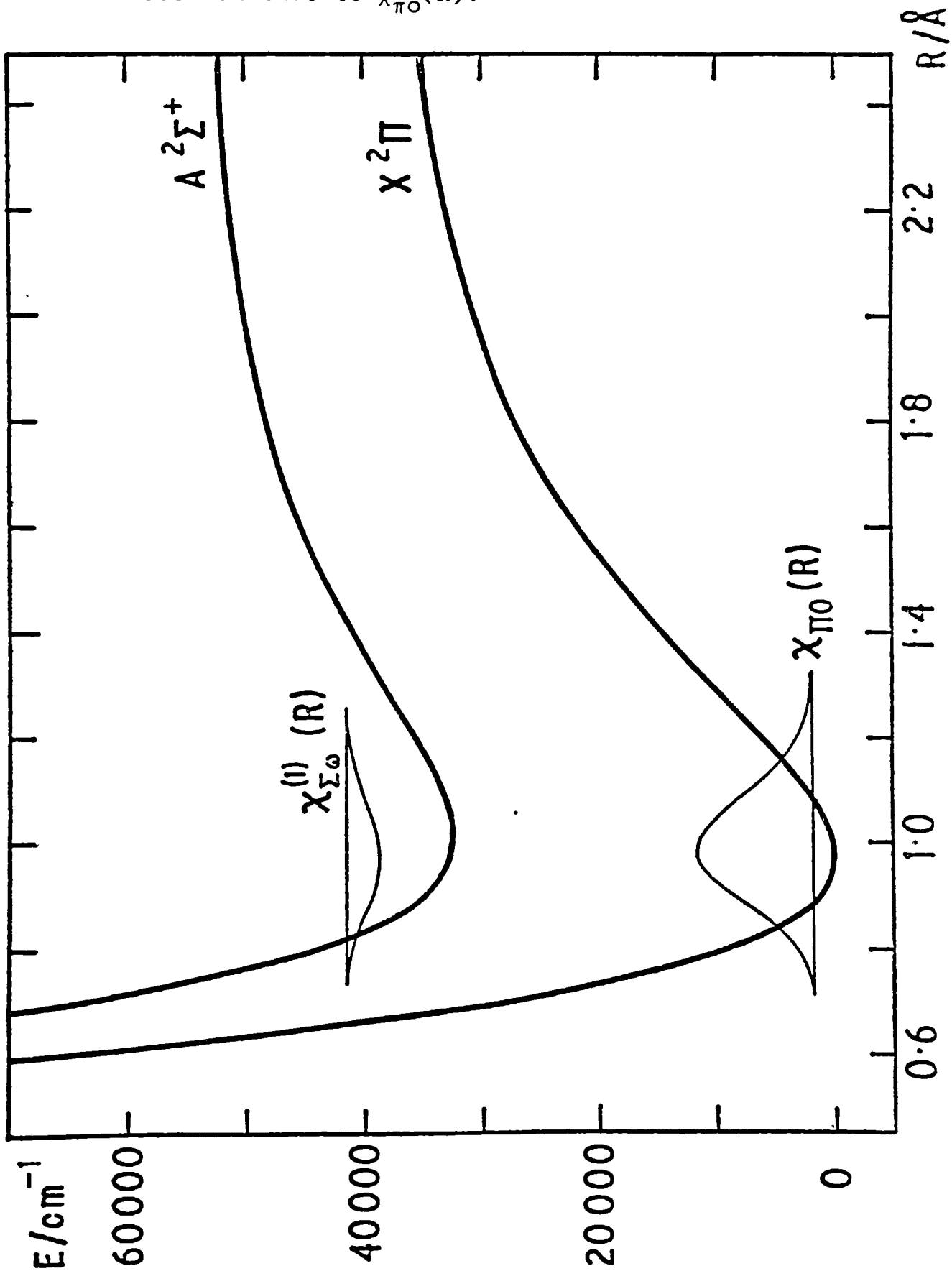

As in the case of OH, the major advantage of the direct method over the conventional method is that it is computationally convenient and inexpensive.

4.2.3 Unbound perturbing state.

In this case, the summations for p and q are replaced by integrals over continuum states. These are computationally expensive to calculate - particularly for high energy states where the wavefunction is a very fast oscillating function of internuclear distance so that very small step sizes are required by the usual integration techniques. For the direct method, the differential equation (3) takes the same form as in the bound state case and is no more difficult to solve. The boundary conditions still mean that χ tends to zero at R equal to zero or infinity so that continuum contributions cancel one another at large R. A model problem was constructed using the $X^2\Pi$ state of OH for the perturbed state and a repulsive exponential

$$V(R) = D \exp(-\beta(R-R_e)) + \Delta V$$

for the perturbing state. Potential parameters are given in table I; the aymptotic limit of the dissociative curve lies exactly $1000 cm^{-1}$ above the ground state energy $E_{\pi o}$.

The integrals over the continuum needed for the conventional method were performed by evaluating the integrands at 2000 values of E_{Av}, at $100 cm^{-1}$ intervals

starting at 10 cm^{-1} above the dissociation limit of the unbound curve, and integrating using Simpson's rule. As a check on the convergence of this integration, the calculations were also performed using a 200 cm^{-1} step size over the same energy range, and the results are given in table II. The integrals p^{vlb} and q^{vlb} obtained in this way are converged to within five significant figures with respect to step size. The results from direct solution of equation (3) agree to within this tolerance, but take several orders of magnitude less computer time.

The function $\chi_{\lambda\omega}$ is illustrated in figure 2; despite the grossly different form of the perturbing potential from the OH case, the $\chi_{\lambda\omega}$ functions are remarkably similar for the two cases. Despite contributions from highly oscillatory continuum wavefunctions, $\chi_{\lambda\omega}$ is a slowly varying function of R allowing a relatively large step size to be used.

4.3 Λ-doubling in HF^+.

This molecule is isoelectronic with OH but Wilson (1978) found differences between the two systems mainly due to the fact that the $A^2\Sigma^+$ potential for HF^+ is much shallower than that for OH. Wilson calculated Λ-doubling and spin-doubling parameters in HF^+ and found that it was necessary to include both bound and continuum vibrational levels in the perturbation series used for p and q but that only bound levels contributed to the spin-rotation constant,

Figure 2. Potential curves used for testing direct solution method with an unbound perturbing state, together with the ground state wavefunction $\chi_{\pi o}(R)$ and correction $\chi^{(1)}_{\Sigma\omega}(R)$ from the perturbing electronic state. $\chi^{(1)}_{\Sigma\omega}(R)$ has been enlarged by a factor of 500 for clarity.

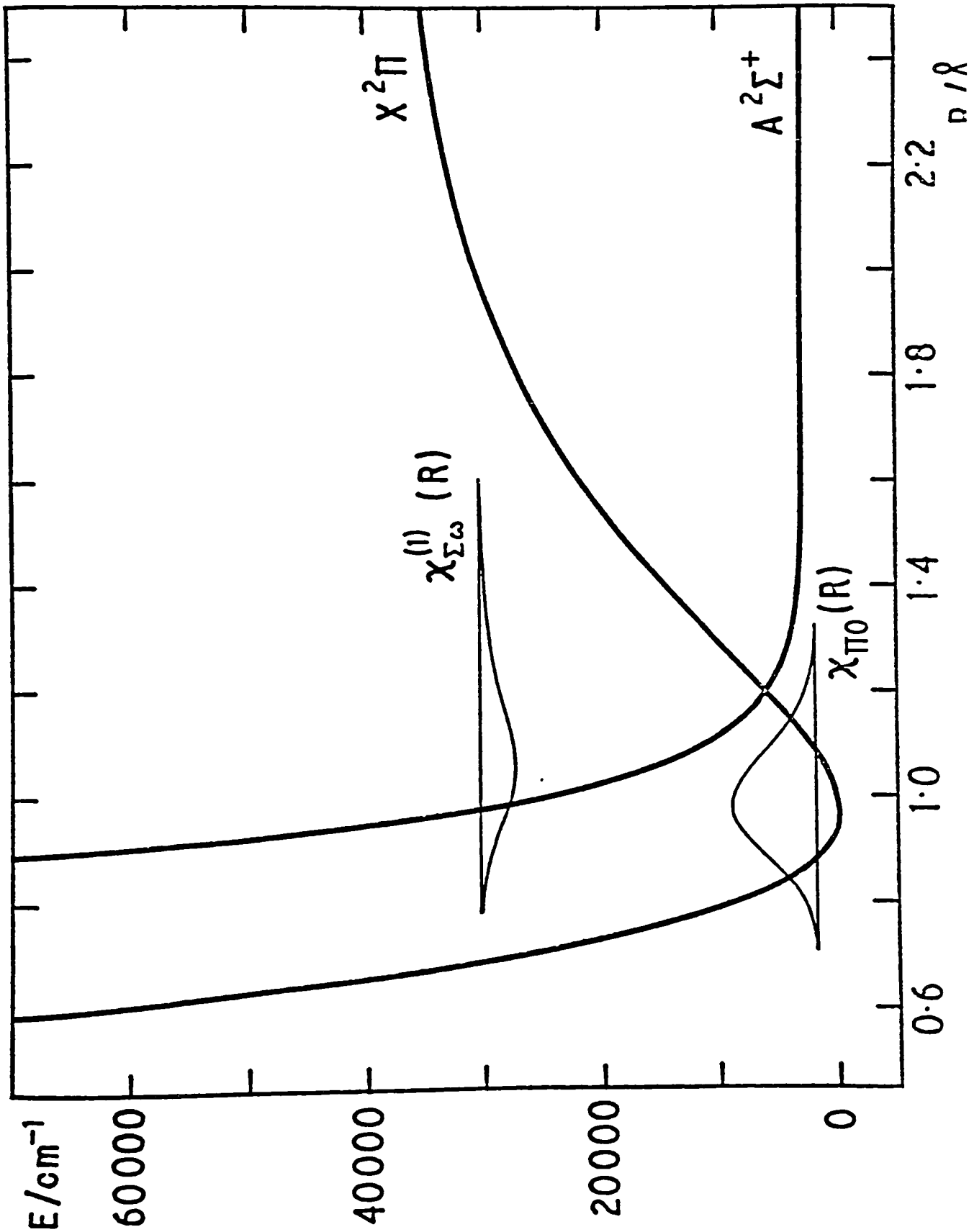

$\gamma_{..}$ Pure precession is a good approximation for the $X^2\Pi$ and $A^2\Sigma^+$ states so that the summations over n' can be truncated after one electronic state, as in OH.

The $A^2\Sigma^+$ state has only four vibrational levels. Except for the v''=0 level of $X^2\Pi$, the contributions of these four levels to p and q are less important than contributions from the continuum. Wilson treated the continuum by numerical solution of the radial Schrödinger equation at a number of energy separations, followed by integration of these values using Gauss-Legendre quadrature. The bound levels were included by the conventional sum-over-states method. The major problem with Wilson's calculations is that it is easy to miss contributions from the top of the ladder of bound states and from the bottom of the continuum. The resulting basis set may not be complete. The direct method works for both bound and unbound perturbing states and, in the case of a weakly bound perturbing state, includes all contributions.

Potential curves for the $X^2\Pi$ and $A^2\Sigma^+$ states were constructed from the parameters given by Wilson (1978) (and reproduced in table III). The curves used were of the form

$$V(R) = D_e [1-(1+a_1(R-R_e) + a_2(R-R_e)^2 + a_3(R-R_e)^3 + a_4(R-R_e)^4) \times \exp(-a_1(R-R_e))]$$

Values of p^{v_b} and q^{v_b} obtained by direct solution of equation (3) were combined with Wilson's electronic matrix elements

$$\langle X^2\Pi|H_{so}|A^2\Sigma^+\rangle = -173.997 cm^{-1} \quad \langle X^2\Pi|L^+|A^2\Sigma^+\rangle = 1.375$$

	$X^2\Pi$	$A^2\Sigma^+$
D_e/cm^{-1}	29113.71	3929.80
$R_e/Å$	1.00103	1.22415
$a_1/Å^{-1}$	3.84731	4.53676
$a_2/Å^{-2}$	2.72537	2.21584
$a_3/Å^{-3}$	3.09743	-1.49472
$a_4/Å^{-4}$	1.31629D-5	-6.79798

Table III Potential parameters for HF^+.

v	Calculation Wilson	Calculation This work	Experiment p_v	$\bar{p}_v$
0	0.5771	0.589	0.64 ± 0.06	0.594
1	0.5327	0.580	0.63 ± 0.08	0.585
2	0.5234	0.573	0.66 ± 0.08	0.567

Table IVa Values of p_v for HF^+.

v	Calculation Wilson	Calculation This work	Experiment q_v	$\bar{q}_v$
0	-0.0374	-0.0402	-0.046 ± 0.008	-0.0314
1	-0.0324	-0.0382	-0.046 ± 0.008	-0.0296
2	-0.0298	-0.0363	-0.049 ± 0.010	-0.0270

Table IVb Values of q_v for HF^+.

Figure 3. Potential curves derived from RKR potential for HF^+. Also shown are the vibrational wavefunctions for the lowest vibronic states.

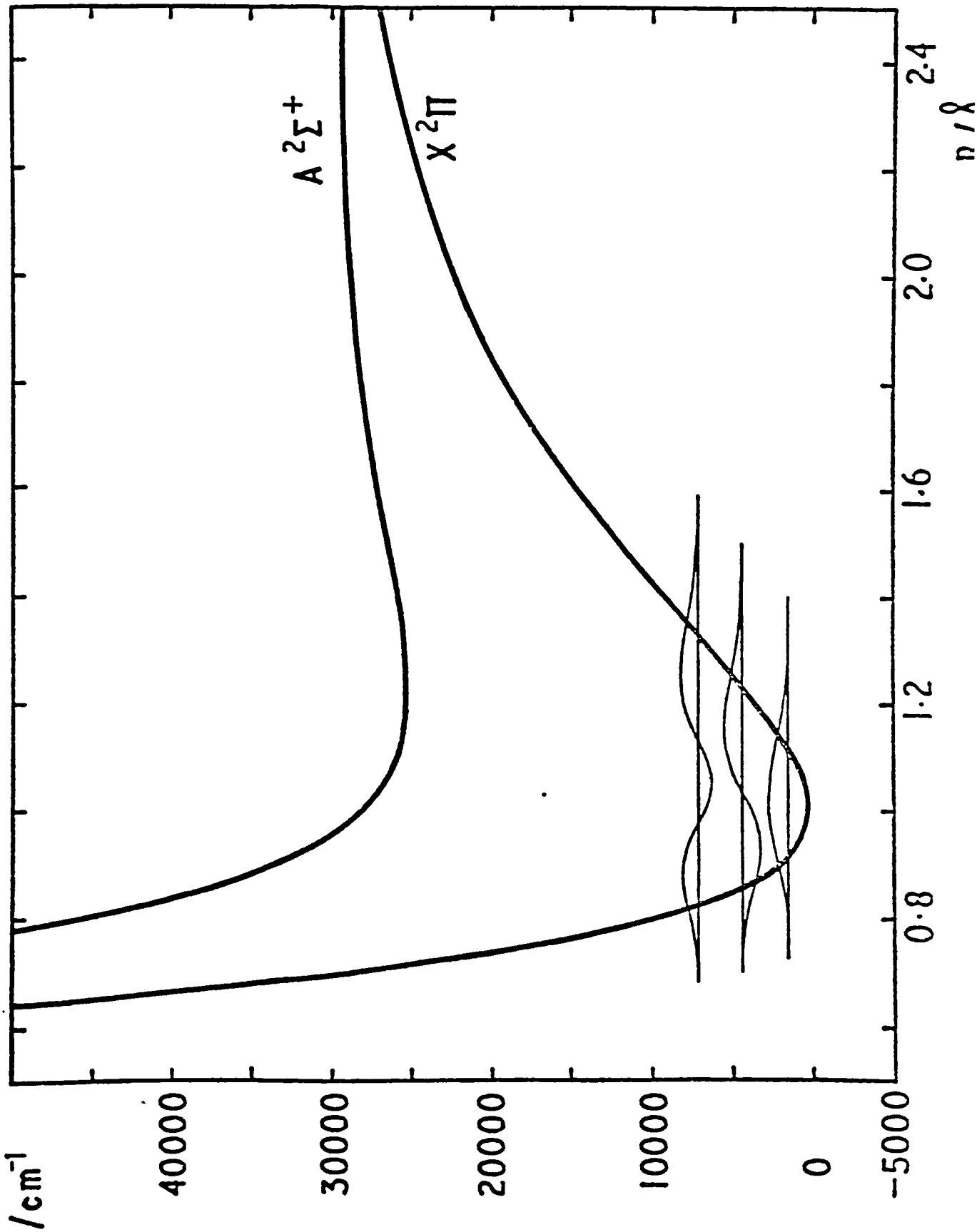

to produce the Λ-doubling constants in tables IVa and IVb. The experimental results are taken from Gewurtz et al. (1975) and are of two types. The sets with large error limits are the more reliable. It can be seen that the new calculated values are within, or are close to, the experimental error limits and are approximately 10% larger than Wilson's values. The quantities $\bar{p}_v$ and $\bar{q}_v$ were obtained by ascribing the Λ-doubling to the interaction of the $X^2\Pi$ state with a single effective $^2\Sigma$ vibronic level whose relative energy is an adjustable parameter. This type of procedure does not, in general, form a suitable basis for a theoretical discussion of Λ-doubling. It can be seen from tables IVa and IVb that these 'effective' parameters lie well outside the experimental error bars in the case of q.

The discrepancy between the new calculated values and the values of Wilson probably arises because of neglected contributions from near the dissociation limit of the $A^2\Sigma^+$ state. As well as being computationally more convenient, the direct method is also more reliable for this sort of system. The new calculated values suggest the need for a new experimental study of HF^+ which is a potential interstellar maser. Even if it is not experimentally feasible to obtain better high resolution electronic spectra, reanalysis of the existing data is necessary.

The direct evaluation of perturbation sums without explicit calculation of vibrational wavefunctions in the

perturbing states has been shown, in the cases of OH, LiO and a model repulsive potential, to be equivalent to the sum-over-states approach. In the case of HF^+, results from the sum-over-states method do not agree with those from the direct summation method ..... this is due to an incomplete basis set in the explicit summation method. The direct summation method has already been applied to spin-doubling in BH^+ in chapter 3 and will be applied to Λ-doubling in NaAr in chapter 5.

CHAPTER FIVE

The variation of spin-orbit coupling energy with distance.

CHAPTER 5

The variation of spin-orbit coupling energy with distance.

The spin-orbit coupling energy varies with internuclear separation for two distinct reasons. Firstly, there is the variation of spin-orbit coupling matrix elements with distance. In the case of the $X^2\Pi_g$ state of O_2^+ (Raftery and Richards, 1975), the change in the $1\pi_g$ orbital is responsible for the change in A. On the other hand, it is the different relative importance of certain CSFs in the CI wavefunction for the $A^2\Pi_u$ state of O_2^+ that causes the variation of A in this state. The second effect is the change in the dependence of the spin-orbit coupling energy on the spin-orbit coupling constant. It is this second effect that we shall consider here.

The spin-orbit coupling energy in an atom is given by

$$\langle S\ L\ J\ M|H_{so}|S\ L\ J\ M\rangle = A\ W(J,L,S)$$

where W(J,L,S) is the eigenvalue of $\mathbf{L}\,\mathbf{S}$

$$W(J,L,S) = \tfrac{1}{2}[J(J+1)-L(L+1)-S(S+1)]$$

Thus, the energy separation between the J and (J-1) levels arising from the same $^{(2S+1)}L$ term is JA. This is the Landé interval rule.

The spin-orbit coupling energy in a diatomic molecule is $A\Lambda\Sigma$ so that the energy separation between the Ω and $(\Omega-1)$ levels arising from the same $^{(2S+1)}\Lambda$ term is $2A\Lambda\Sigma$. Consider a $^2\Pi$ molecule dissociating to a closed shell $^1S_0$ atom and to an

open shell ^2P atom. In the molecule, the splitting between the $^2\Pi_{3/2}$ and $^2\Pi_{1/2}$ levels is A - even at infinite bond-length. Obviously, the system at infinite separation is not a molecule but is two separate atoms with spin-splitting $\frac{3}{2}A$. Clearly, there must be some transition region in which the spin-orbit coupling energy changes between these two extremes.

5.1 Spin-orbit coupling in $HeNe^*$.

The neon lasing transition of the helium-neon laser is pumped through excitation transfer from metastable helium to neon. The pumping collisions are not well understood but are presumed to be

$$He^*(2^1S) + Ne \rightarrow He + Ne^*(2p^5 5s)$$

$$He^*(2^3S) + Ne \rightarrow He + Ne^*(2p^5 4s)$$

Both Ne* species have an electron in a diffuse Rydberg orbital so that it is usual to interpret scattering data of metastable helium from neon in terms of an outgoing potential which is $HeNe^*$ rather than $HeNe^*$. RKR potentials for the $X^2\Sigma^+$ and $A^2\Pi_{1/2}$ curves are available from the spectroscopic study of Dabrowski and Herzberg (1978). The $A^2\Pi_{3/2}$ potential may be obtained from the $A^2\Pi_{1/2}$ values by assuming that the spin-orbit coupling is constant and equal to that in the free Ne^+ ion (728 cm^{-1}). An ab initio study of the variation of spin-orbit coupling matrix elements with internuclear should give some idea of the validity of this

assumption.

A basis set for $HeNe^+$ was constructed from accurate atomic basis sets for He and Ne ground state atoms (see table I) and SCF procedures were carried out at a number of internuclear separations of the $A^2\Pi$ state $((1-4)\sigma^2 1\pi^3)$ using the ALCHEMY program. The Hartree-Fock wavefunctions thus obtained were used to calculate off-diagonal matrix elements of H_{so}. The interaction between He and Ne^+ is not expected to be very strong and so the one-centre approximation should be particularly good for $HeNe^+$. Energies and matrix elements are collected in table II.

From ionisation potential measurements, the energy separation between Ne^+ ($^2P_{3/2}$) and Ne^+ ($^2P_{1/2}$) is 728 cm^{-1} so that the spin-orbit coupling constant for Ne^+ ($^2P_1$) is -521 cm^{-1}. It can be seen that the ab initio value at 4500 bohr agrees well with this experimental value and that the change in spin-orbit coupling constant between 4.5 bohr and 4500 bohr is only 0.1cm^{-1}. Even when the He and Ne^+ atoms are very close, the change in A is very small (ca. 1%) showing very little interaction.

Basis sets of double zeta (DZ) quality frequently give poor estimates of binding energy. The inclusion of polarisation functions (P) in the basis set often leads to a large energy improvement; these functions are usually d and f orbitals whose exponents are optimised during the SCF

Table I STO exponents for HeNe*

He		Ne	
1s	1.450	1s	15.439
			8.806
2s	2.641	2s	3.764
			2.301
		3s	10.995
		2p	10.542
			4.956
			2.793
			1.623

Table II SCF energies and spin-orbit coupling matrix elements for HeNe*

R/bohr	SCF energy (in hartrees)	Spin-orbit coupling matrix elements (in cm^{-1})	
		no polarisation functions	polarisation functions
1.5	-142.95	-507.34	-507.61
2.0	-140.34	-509.37	-509.26
2.5	-138.57	-514.85	-514.75
3.0	-137.31	-518.07	-518.02
3.5	-136.38	-519.53	-519.51
4.5	-135.12	-520.33	-520.31
6.5	-133.75	-520.43	-520.43
4500	-130.68	-520.43	-520.43

calculations. For molecules where the chemical binding is weak, a DZ basis set may predict that the system is unbound while a DZ+P basis set may correctly predict a binding energy of, say, a few hundred wavenumbers. The $A^2\Pi$ state of $HeNe^+$ is known to be weakly bound from the work of Dabrowski and Herzberg (1978). The basis set of table I was used to calculate SCF and CI energies as a function of internuclear distance; the calculated curve was found to be repulsive so that this is clearly a case where a basis set of at least DZ+P quality is required.

It is important to ask what effect the inclusion of polarisation functions would have on the ab initio value for the spin-orbit coupling constant. It seems likely that the inclusion of polarisation functions will have a negligible effect since the contribution from d orbitals to the value of A in molecules containing only light atoms is generally very small indeed. The basis set in table I was augmented with three d orbitals on Ne with exponents 0.5, 1.0 and 1.5. The percentage change in A (see table II) is negligible but suggests that polarisation functions may be necessary to accurately reproduce the variation of $A(R)$.

In a molecule, the spin-orbit splitting is $2A\Lambda\Sigma$ and if $A(R)$ is constant then the $^2\Pi_{3/2}$ and $^2\Pi_{1/2}$ curves will be parallel. As the internuclear distance is increased, the electrostatic axis-orbit interaction becomes comparable to the spin-orbit interaction. The $^2\Pi_{3/2}$ state remains a pure $^2\Pi$

state but the $^2\Pi_{1/2}$ state gains a $^2\Sigma$ component which adds a component to the energy. The curves cease to be parallel until the internuclear distance is sufficiently large for the system to behave as separated atoms. The situation in which A(R) is constant is illustrated schematically in figure 1; the shaded area is the contribution to the splitting from the $^2\Sigma$ component. There is a recoupling of angular momentum in the transition region causing a change in the spin-orbit coupling energy.

$$|^2\Pi_{1/2}\rangle \sim |L\ \Lambda=1\rangle\ |S\ -\tfrac{1}{2}\rangle \qquad \text{for small } R$$

$$= \sqrt{\tfrac{2}{3}}|L\ \Lambda=1\rangle\ |S\ -\tfrac{1}{2}\rangle - \sqrt{\tfrac{1}{3}}|L\ \Lambda=0\rangle\ |S\ +\tfrac{1}{2}\rangle \qquad \text{for } R\to\infty$$

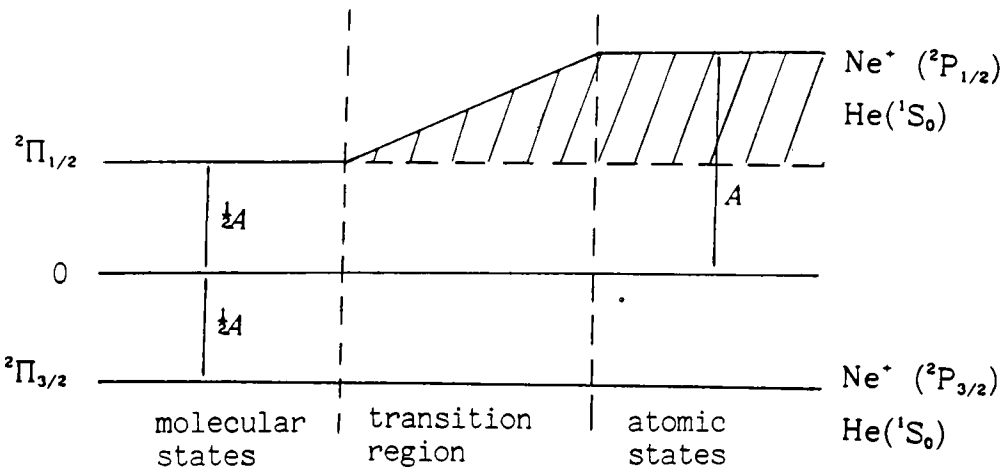

Figure 1 Schematic representation of the variation of spin-orbit coupling matrix element with internuclear separation.

According to Haberland (private communication, 1980), the minimum in the $A^2\Pi$ potential is definitely in the transition region since the $A^2\Pi_{1/2}$ and $A^2\Pi_{3/2}$ curves are not parallel. Haberland has suggested comparing data from photodissociation experiments with calculated potential curves (obtained neglecting spin-orbit coupling effects) so as to examine the change in spin-coupling energy with distance. From the calculations presented here, it is clear that the change in spin-orbit coupling energy will be almost entirely due to the recoupling of angular momenta.

5.2 Spin-orbit coupling and Λ-doubling in NaAr.

Supersonic free expansions have been widely used to form a number of weakly bound van der Waals molecules. Under the extremely low translational temperatures that may be achieved, even the most weakly bound van der Waals molecules are quite stable. Smalley et al. (1977) and Tellinghuisen et al. (1979) have prepared NaAr in a supersonic expansion of sodium vapour plus a few percent argon in a helium carrier gas and have measured the fluorescence excitation spectrum of the $X^2\Sigma^+$-$A^2\Pi$ optical transition.

The $X^2\Sigma^+$ ground state which dissociates to Na ($^2S_{1/2}$) and Ar ($^1S_0$) is only weakly attractive and only the v''=0 to v''=4 levels are known. The $A^2\Pi_r$ state is much more strongly bound and transitions to vibrational levels v' =7 to v' =11 have been observed. A mainly repulsive $B^2\Sigma^+$ state has been

studied indirectly by the Λ-doubling in the $A^2\Pi_{1/2}$ state. These states both dissociate to Na ($^2P_{1/2}$) and Ar ($^1S_0$) and are close in energy - the $A^2\Pi$-$B^2\Sigma^+$ interaction should dominate the contributions due to other $^2\Sigma$ states.

The ground state interatomic potential implied by the vibrational and rotational spectroscopic constants of Smalley et al. (1977) is consistent with curves measured or calculated by other workers. Smalley et al. used the potential curves calculated by Baylis and a rather crude model to account for the observed Λ-doubling in the $A^2\Pi_r$ state; the conclusion was that the calculated $B^2\Sigma^+$ potential was too repulsive. Saxon et al. (1977) have carried out large CI calculations on the three states using large STO basis sets. The $B^2\Sigma^+$ curve was indeed found to be less repulsive than had been previously believed. The crude model was correct in this respect but, obviously, ab initio calculations would be more convincing.

Separate SCF procedures were attempted on each of the $X^2\Sigma^+$, $A^2\Pi_r$ and $B^2\Sigma^+$ states using the ALCHEMY program. The basis set of 30 σ-STOs and 16 π-STOs was taken from the work of Saxon et al. (1977) and is given in table III. The wavefunctions for the $A^2\Pi_r$ state were used to calculate values for the spin-orbit coupling constant at a number of internuclear distances (see table IV). Vibrationally averaged values are given in table V together with fitted (experimental) values.

Table III STO exponents used for NaAr.

	Na		Ar
1s	18.704	1s	30.066
	11.153		18.157
2s	9.990	2s	16.041
	4.069		6.772
3s	3.081	3s	4.885
	1.186		3.620
	0.724		2.085
2p	7.943	2p	14.502
	4.264		8.129
	2.295	3p	6.396
3p	1.247		2.905
	0.591		1.610
3d	1.200	3d	2.200
	0.500		1.394
4d	0.500	4d	1.394

Table IV Spin-orbit coupling matrix elements for the $A^2\Pi$ state of NaAr.

Geometry (in bohr)	One electron contribution (in cm^{-1})	Two electron contribution (in cm^{-1})	Total (in cm^{-1})
3.0	24.30	-5.18	19.12
3.5	23.91	-5.21	18.70
4.0	22.65	-5.03	17.62
4.5	20.89	-4.74	16.15
5.0	19.03	-4.42	14.61
5.5	17.31	-4.12	13.19
5.7	16.69	-4.01	12.67
6.0	15.83	-3.86	11.97
6.3	15.08	-3.73	11.35
7.0	13.70	-3.48	10.21
8.0	12.47	-3.26	9.21
9.0	11.85	-3.15	8.69
10.0	11.55	-3.10	8.43
11.0	11.41	-3.07	8.34

Table V Calculated and experimental spin-orbit coupling constants (in cm^{-1}).

	Calculation		Experiment	
v	A	$\frac{3}{2}A$	rotational analysis	multiplet splitting
11	9.1	13.7		
10	9.3	14.0	12 ± 2	13.48
9	9.5	14.3	14 ± 2	13.87
8	9.7	14.6	11 ± 1	14.29
7	10.0	15.0	12 ± 2	14.79
6	10.3	15.5		

The splitting in a free ^2P sodium atom is 17.20 $cm^{-1} = \frac{3}{2}A$ so that the ab initio spin-orbit coupling constants for NaAr are very similar to the atomic value. They do suggest some polarisation of Na by Ar. An atomic population analysis was carried out at each geometry and no evidence was found to support the suggestion of Smalley et al. (1977) of perturbation of the Na 2p core electrons by the Ar atom. The spin-orbit coupling 'constants' of Smalley et al. are actually spin-orbit energies. The ab initio values of A (and of $\frac{3}{2}A$) suggest that it is not correct to equate the multiplet splitting to the spin-orbit coupling constant. It seems likely that NaAr is in the transition region described

earlier in this chapter and lies close to the atomic end.

Considerable difficulty was encountered when calculating wavefunctions for the $B^2\Sigma^+$ state and so occupied and virtual orbitals of the $A^2\Pi$ state were used. Off-diagonal matrix elements of H_{so} and L^+S^- were then calculated at 6 bohr, i.e. close to the potential minimum of the $A^2\Pi$ state. These matrix elements (see table VII) were combined with the vibrational quantities $\chi_{n\omega}(R)$ described in chapter 5; the potential curves were constructed from the CI calculations of Saxon et al.. The vibrational sums for $A^2\Pi$-$X^2\Sigma^+$ were very much smaller than those for $A^2\Pi$-$B^2\Sigma^+$. Calculated values of the Λ-doubling parameter ($\frac{1}{2}p+q$) are compared with experiment in table VIII. The magnitude of the splitting has been reproduced. This is to some extent fortuitous in view of the arbitrary choice of 6 bohr but the variation of the Λ-doublet splitting with vibrational quantum number is also in good agreement with observation.

Provided a reasonable model is used and provided accurate potential curves are available, it is possible to reproduce both the magnitude and vibrational variation of the Λ-doubling parameters. The interest in NaAr arises from the fact that the Λ-doubling in the $A^2\Pi$ state gives direct information about the Na+Ar interaction in the $B^2\Sigma^+$ state. The success of these calculations encourages the application of similar methods to other van der Waals species.

Geometry (in bohr)	Sodium 2p	Sodium 3p	Sodium 3d	Sodium 4d	Argon 2p	Argon 3p	Argon 3d	Argon 4d
3.0	0.30	93.60	3.04	0.24	0.07	1.91	0.35	0.50
3.5	0.37	94.23	2.44	0.20	0.06	1.82	0.41	0.47
4.0	0.43	95.28	1.77	0.12	0.06	1.59	0.37	0.39
4.5	0.47	96.42	1.14	0.05	0.05	1.31	0.28	0.28
5.0	0.51	97.39	0.66	0.01	0.04	1.04	0.18	0.18
5.5	0.53	98.11	0.33	0.00	0.03	0.79	0.10	0.10
5.7	0.54	98.33	0.25	0.00	0.03	0.70	0.08	0.08
6.0	0.55	98.59	0.15	0.01	0.02	0.58	0.05	0.05
6.3	0.56	98.78	0.08	0.01	0.02	0.48	0.04	0.03
7.0	0.56	99.07	0.02	0.02	0.01	0.29	0.01	0.01
8.0	0.57	99.27	0.00	0.02	0.01	0.13	0.00	0.00
9.0	0.57	99.36	0.00	0.01	0.00	0.06	0.00	0.00
10.0	0.57	99.40	0.00	0.00	0.00	0.02	0.00	0.00
11.0	0.57	99.42	0.00	0.00	0.00	0.01	0.00	0.00

Table VI Percentage utilisation of atomic basis functions in the 4π orbital in the $A^2\Pi_r$ state of NaAr.

Quantity	Value
$\langle A^2\Pi \vert H_{so} \vert B^2\Sigma^+ \rangle$	5.371 cm^{-1}
$\langle A^2\Pi \vert L^+ \vert B^2\Sigma^+ \rangle$	1.340
$\langle A^2\Pi \vert H_{so} \vert X^2\Sigma^+ \rangle$	10.198 cm^{-1}
$\langle A^2\Pi \vert L^+ \vert X^2\Sigma^+ \rangle$	0.785

Table VII Off-diagonal matrix elements at 6.0 bohr.

Table VIII Λ-doubling parameters for the $A^2\Pi$ state of NaAr

v	$-(\frac{1}{2}p+q) \times 10^2$/GHz Calculated	Experiment
11	14.30	13.420 ± 0.30
10	7.94	8.443 ± 0.103
9	5.46	5.592 ± 0.094
8	4.09	4.163 ± 0.179
7	3.41	2.838 ± 0.149
6	2.93	

5.3 Discussion.

The variation of spin-orbit coupling energy with distance is very important in NaAr. The calculations suggest that the observed multiplet splitting (ca. 14 cm^{-1}) is closer to $\frac{3}{2}A$ (as in atoms) than to A (as in molecules). In systems in which the interaction between the atoms is weak it is not reasonable to equate the observed multiplet splitting to the spin-orbit coupling constant.

When atomic spectra are perturbed by neutral atoms or molecules, the line shapes may be analysed to give information on the emitter-perturber interaction (see Peach, 1981). For the sodium - rare gas systems, different values of the asymmetry parameter are observed for the two lines and this gives direct information about the difference between the $A^2\Pi_{1/2}$ and $A^2\Pi_{3/2}$ potential curves. The variation of spin-orbit coupling energy in systems such as NaAr is thus very important to the understanding of line profiles.

The variation of spin-orbit coupling energy with distance may soon be measurable for $HeNe^*$ and it is clear that the spin-orbit coupling matrix element is almost constant with change in internuclear distance; in weakly bound molecules the geometry dependence of the spin-orbit coupling energy is mostly due to the recoupling of angular momenta between the separated atom and molecular limits.

CHAPTER SIX

Higher order corrections to Λ-doubling and spin-splitting in diatomic molecules.

CHAPTER 6

Higher order corrections to Λ-doubling and spin-splitting in diatomic molecules.

6.1 Expressions for higher order corrections.

The theoretical computation of Λ-doublet splittings has so far been considered in terms of parameters p and q. However, the observed Λ-doubling for high rotational quantum numbers shows marked deviation from the Mulliken and Christy (1931) formula. Indeed, the advent of high precision microwave and radiofrequency measurements has meant that these discrepancies are observable even for low rotational levels. Higher order terms are generally considered in terms of the phenomenological replacements

$$p_v \rightarrow p_v + p_J J(J+1)$$
$$q_v \rightarrow q_v + q_J J(J+1)$$

Occasionally, even more correction terms are required.

We have seen in section 2.2 that a Van Vleck transformation to second order yields the standard Λ-doubling matrix

$$\begin{pmatrix} \pm \frac{1}{2}(p_v+2q_v)(J+\frac{1}{2}) & \pm \frac{1}{2} q_v X(J+\frac{1}{2}) \\ \pm \frac{1}{2} q_v X (J+\frac{1}{2}) & 0 \end{pmatrix}$$

Neglecting terms which merely add insignificant corrections to p_v and q_v, a Van Vleck transformation to third order leads to the correction matrix

$$\begin{pmatrix} \pm \left(\frac{1}{2} p_J + \frac{1}{2} q_J\right) J(J+1)\left(J+\frac{1}{2}\right) & \pm \frac{1}{2} q_J J(J+1) \; X \left(J+\frac{1}{2}\right) \\ \pm \frac{1}{2} q_J J(J+1) \; X \left(J+\frac{1}{2}\right) & \pm \frac{1}{2} q_J X^2 \left(J+\frac{1}{2}\right) \end{pmatrix}$$

The new parameters p_J and q_J for vibrational level v of the $^2\Pi$ state are given by

$$p_J = 2 \sum_{2\Sigma,k} \sum_{u \neq v} (-1)^S \frac{B_{vu}(A_{uk}B_{vk} + B_{uk}A_{vk})}{\nu(v,u)\ \nu(\Pi v, \Sigma k)}$$

$$+ \sum_{2\Sigma\ k,\ell} \sum (-1)^S \frac{B_{k\ell}(A_{vk}B_{v\ell} + B_{vk}A_{v\ell})}{\nu(\Pi v, \Sigma k)\ \nu(\Pi v, \Sigma \ell)}$$

$$- 2\, B_v(^2\Pi) \sum_{2\Sigma,k} (-1)^S \frac{A_{vk}\, B_{vk}}{\nu(\Pi v, \Sigma k)^2} + 2\, q_J$$

$$q_J = 4 \sum_{2\Sigma,k} \sum_{u \neq v} (-1)^S \frac{B_{vu}\, B_{uk}\, B_{vk}}{\nu(v,u)\ \nu(\Pi v, \Sigma k)}$$

$$+ 2 \sum_{2\Sigma\ k,\ell} \sum (-1)^S \frac{B_{k\ell}\, B_{vk}\, B_{v\ell}}{\nu(\Pi v, \Sigma k)\ \nu(\Pi v, \Sigma \ell)}$$

$$- 2\, B_v(^2\Pi) \sum_{2\Sigma,k} (-1)^S \frac{B_{vk}^2}{\nu(\Pi v, \Sigma k)^2}$$

In the summations above the vibrational levels k and l always refer to the same $^2\Sigma$ state. $\nu(v,u)$ is a shorthand for the energy difference $E(\Pi,v) - E(\Pi,u)$. The new parameters p_J and q_J may be interpreted as representing effective

centrifugal distortion corrections to the standard Λ-doubling parameters p_v+2q_v and q_v. There are two distinct contributions. The first one arises from the mixing of the vibrational levels of the $^2\Pi$ state and represents a centrifugal distortion effect. This corresponds to the first term in the expressions for p_J, q_J and γ_N (see below). The other contribution stems form higher order non-adiabatic mixing of electronic states (cf p and q).

Clearly it would be useful if the correction matrix could be obtained from the second order Λ-doubling matrix by means of the phenomenological replacements used to fit observed spectra. This may be achieved by a slight transformation of the complete effective $^2\Pi$ matrix. The $^2\Pi_{3/2}-^2\Pi_{3/2}$ element is removed and is added to the $^2\Pi_{1/2}-^2\Pi_{1/2}$ element with no significant change of the $^2\Pi_{1/2}-^2\Pi_{3/2}$ element.

$$|^2\Pi_{1/2}\ v\rangle' = |^2\Pi_{1/2}\ v\rangle - c_{1/2}|^2\Pi_{3/2}\ v\rangle$$

$$|^2\Pi_{3/2}\ v\rangle' = |^2\Pi_{3/2}\ v\rangle - c_{3/2}|^2\Pi_{1/2}\ v\rangle$$

Orthogonality is preserved if $c_{1/2}=-c_{3/2}$; both coefficients are real and small compared with unity. In this new basis set

$$\langle^2\Pi_{3/2}\ v|H^{(1)}|^2\Pi_{3/2}\ v\rangle' = \langle^2\Pi_{3/2}\ v|H^{(1)}|^2\Pi_{3/2}\ v\rangle + 2c_{3/2}\langle^2\Pi_{3/2}\ v|H^{(1)}|^2\Pi_{1/2}\ v\rangle$$
$$= 0$$

The last condition will be satisfied if

$$c_{3/2}=-c_{1/2}=\mp\frac{q_J}{4B_v}X(J-\tfrac{1}{2})$$

The off-diagonal matrix elements now become

$$\langle {}^2\Pi_{1/2}\ v|H^{(1)}|{}^2\Pi_{3/2}\ v\rangle = \langle {}^2\Pi_{1/2}\ v|H^{(1)}|{}^2\Pi_{3/2}\ v\rangle \pm \frac{A_v - 2B_v}{4B_v} q_J X(J-\tfrac{1}{2})$$

The change of basis also adds an insignificant contribution to q_v

$$\langle {}^2\Pi_{1/2}\ v|H^{(1)}|{}^2\Pi_{1/2}\ v\rangle = \langle {}^2\Pi_{1/2}\ v|H^{(1)}|{}^2\Pi_{1/2}\ v\rangle \pm \tfrac{1}{2} q_J X^2(J-\tfrac{1}{2})$$

If insignificant corrections to p_v and q_v are neglected, then in the new basis the matrix takes the form

$$\begin{pmatrix} \pm\frac{1}{2}(p_J - 2q_J)J(J-1)(J-\frac{1}{2}) & \pm\frac{1}{2}q_J J(J-1)X(J-\frac{1}{2}) \\ \pm\frac{1}{2}q_J J(J-1)X(J-\frac{1}{2}) & 0 \end{pmatrix}$$

This new form of the correction matrix can be obtained from the standard Λ-doubling matrix by the phenomenological replacements mentioned above.

The spin-splitting (ρ-doubling) of $^2\Sigma$ states is given by

$$\Delta\nu_e = \gamma_k(N-\tfrac{1}{2}) + \gamma_N N(N-1)(N-\tfrac{1}{2})$$

This effect arises from an interaction of the relevant $^2\Sigma$ state with $^2\Pi$ states. Van Vleck transformations to the second and third order yield the following expressions for the parameters γ_k and γ_N

$$\gamma_k = 2 \sum_{^2\Pi, v} \frac{A_{vk}\ B_{vk}}{\nu(\Pi v,\ \Sigma k)}$$

$$\gamma_N = 2 \sum_{2\Pi,v} \sum_{\ell \neq k} \frac{B_{k\ell}(A_{v\ell} B_{vk} + B_{v\ell} A_{vk})}{\nu(k,\ell)\ \nu(\Pi v, \Sigma k)}$$

$$- \sum_{2\Pi} \sum_{u,v} \frac{B_{vu}(B_{uk} A_{vk} + A_{uk} B_{vk})}{\nu(\Pi u, \Sigma k)\ \nu(\Pi v, \Sigma k)}$$

$$+ 2 B_k(^2\Sigma) \sum_{2\Pi,v} \frac{A_{vk} B_{vk}}{\nu(\Pi v, \Sigma k)^2}$$

Despite the similarity of γ_k and p_v, the definition for γ_k more closely resembles that for $(p_i - 2q_i)$ than that for p_i. Note that the first order contribution to the spin-splitting (see section 3.2) has been neglected since it is swamped by the second order contribution.

6.2 Calculated values for OH, OD and SH.

Accurate experimental data exists for the Λ-doubling in each of these molecules. In each case the $X^2\Pi$ ground state is almost uniquely perturbed by the first excited $A^2\Sigma^+$ state. In view of the successful predictions of second order parameters p_v and q_v, it is interesting to attempt to calculate the higher order corrections. These provide a very sensitive test of the ab initio methods since rather more complex interactions are involved in the higher order terms.

Basis sets were taken from the calculations of Cade and Huo (1967a,b) and separate SCF procedures were carried out for the $X^2\Pi$ and $A^2\Sigma^+$ states of OH (or OD) and SH using the ALCHEMY program. The electronic wavefunctions were then used to calculate off-diagonal matrix elements of L^+S^- and of the spin-orbit coupling operator, H_{so}.

Hinkley et al. (1973) have shown that the vibrational matrix elements in the sums for p_v and q_v for OH can be accurately reproduced using Morse curves

$$V(R) = D\left[1 - \exp(-\beta(R-R_e))\right]^2 + \Delta V$$

with parameters as given in table I. RKR curves for SH were constructed from experimental data and the turning points were fitted to the expression

$$V(R)=D_e[1-(1-a_1x-a_2x^2+a_3x^3-a_4x^4)e^{-a_1x}]$$

where $x=R-R_e$. Values for the parameters are given in table II. This expression was then used to extrapolate the potential onto the grid used in the Numerov procedure (see section 2.6).

Vibrational wavefuntions were combined with the various electronic matrix elements and the necessary integrations were performed to obtain all the vibronic matrix elements required for calculation of the Λ-doubling and spin-splitting parameters.

Table I Potential parameters used for OH and OD.

OH/OD	D/cm^{-1}	$\beta/Å^{-1}$	$R_e/Å$	$\Delta V/cm^{-1}$
$X^2\Pi$	37296.9	2.29342	0.9706	0
$A^2\Sigma^+$	20292.0	2.64746	1.0121	32684.1

Table II Potential parameters used for SH.

SH	$a_1/Å^{-1}$	$a_2/Å^{-2}$	$a_3/Å^{-3}$	$a_4/Å^{-4}$	D_e/cm^{-1}	$R_e/Å$
$X^2\Pi$	4.35022	5.70373	4.08196	4.77566	28633	1.340
$A^2\Sigma^+$	2.94663	-1.95350	-7.05080	$5.05678 \cdot 10^{-7}$	6834	1.423

Table III Centrifugal distortion constants.

	$10^4 D_o$ ($^2\Pi$)/cm^{-1}		$10^4 D_o$ ($^2\Sigma$)/cm^{-1}	
	calculated	experiment	calculated	experiment
OH	19.2	19.38	20.4	20.39
OD	5.42	5.374	5.84	5.763
SH	4.93	4.8	8.65	6.3

The rotation-vibration energy of a diatomic molecule is conventionally expanded as

$$E_{v,J} = E_v^{(0)} - B_v J(J-1) - D_v J^2(J-1)^2 - H_v J^3(J-1)^3 - L_v J^4(J-1)^4 -$$

where $E_v^{(0)}$ corresponds to the rotationless molecule. If the effects of rotation are considered as a perturbation then, within the Born-Oppenheimer approximation, the centrifugal distortion constant, D_v, is given by

$$D_v = \sum_{u \neq v} \frac{B_{uv}^2}{\nu(u,v)}$$

Values of D_0 were calculated to test the quality of the various potentials and are given in table III. The results are generally good for OH and OD suggesting that the Morse curves used are adequate. The values for SH are less satisfactory and show that the potential used for the $A^2\Sigma^+$ state of SH is rather poor. It is not clear whether the discrepancy is also a reflection of the fact that the summation for D_v was restricted to bound levels.

The summations required for the various Λ-doubling parameters were carried out for all three molecules. Despite the shallow nature of the $A^2\Sigma^+$ potential for SH, the summations were restricted to bound levels. Convergence was fairly fast though a number of excited vibrational levels were important. In the case of the first summation in the expression for p_J, convergence to four significant figures required extending the summation up to v=5 for OH and up to v=7 for SH. The calculations were also performed for the

		OH		OD		SH	
		Calc.	Fitted	Calc.	Fitted[c]	Calc.	Fitted[d]
$^2\Pi$, v=0	p_v	6897.5	7050.11(2)[a]	3663.3	3796(14)	9502	9005.0(1)
	q_v	-1138.3	-1159.17(1)[a]	-321.8	-327.8(6)	-305.5	-284.17(4
	p_J	- 0.410	-0.6668 (2)[a]	-0.228	-0.38 (3)	-0.89	-2.1 1)
	q_J	0.412	0.4416 (2)[a]	0.0624	0.061(1)	0.057	0.043(2)
$^2\Sigma^+$,v=0	γ_k	6360.6	6762(10)[b]	3380	3601 (6)		
	γ_N	-1.34	-1.43 (5)[b]	-0.384	-0.358(7)		

Table IV Calculated and fitted parameters (in MHz) for OH, OD and SH.

a From fit to molecular beam, E.P.R., L.M.R., and optical data (Cooper and Veseth, 1981).

b Coxon (1980).

c Coxon (1975).

d From fit to molecular beam, E.P.R., and optical data (Cooper and Veseth, 1981).

spin-splitting of the $A^2\Sigma^+$ states of OH and OD. All the values for the higher order corrections were dominated by centrifugal distortion effects; the terms referring to third order non-adiabatic terms tended to be almost completely self-cancelling.

The ab initio values are compared with experiment in table IV. The results for OH and OD are very pleasing. Extensive calculations on OH by Cooper and Richards (1979) that included CI produced Λ-doublet splittings in excellent agreement with radioastronomical observations. However, agreement is apparently good for the higher order parameters even at the Hartree-Fock level. The results for SH are suprisingly good in view of the obvious limitations of the $A^2\Sigma^+$ potential; it should be mentioned that the existing data for SH yields a high correlation (0.99) between p_v and q_v so that the fitted values are probably more uncertain than is suggested by the standard deviations. For each of these molecules, the discrepancy in p_v is larger than in the other parameters. This is partly due to the fact that the computed result arises from the difference between two fairly similar quantities; indeed, values for the quantity (p_v-2q_v), which more closely resemble γ_N, are rather better.

6.3 Conclusions.

An attempt has been made to extend calculations of Λ-doubling and spin-splitting parameters to higher order. This has been very satisfactory. It has been possible to show that centrifugal distortion effects dominate third order non-adiabatic terms in the higher order corrections. Even at the Hartree-Fock level, agreement with fitted values is very good.

Those parameters which depend on matrix elements of the spin-orbit coupling operator (a two-particle operator) should be greatly improved by the inclusion of CI. There is clearly a need for more extensive calculations on SH; in the absence of suitable experimental potential curves, large CI calculations need to be carried out for both states. It may also be necessary to extend the summations to the continuum of the $A^2\Sigma^+$ state.

The calculated higher order parameters are very pleasing, particularly for OH and OD. The calculation of such quantities is likely to be very important in the future as high precision microwave and radiofrequency experiments become possible for other molecules.

CHAPTER SEVEN

Extensions to new problems.

CHAPTER 7 Extensions to new problems.

7.1 Larger systems.

The extension of the methods to small polyatomic species seems a logical step. The calculation of spin-orbit splittings in some linear triatomic systems has been attempted by Horsley and Hall (1973); the results were generally very good. Here we shall consider the molecules CCN and CNC which have very different spin-orbit coupling constants. Both the ground ($X^2\Pi$) and lowest excited ($A^2\Delta$) states of these molecules are linear.

Calculation of all the two-centre and three-centre integrals for these molecules would be very time consuming. The one-centre approximation is essential in studies of polyatomic systems. Hinkley (1971) used a small Gaussian-type orbital basis set to calculate spin-orbit coupling constants for these molecules within the one-centre approximation. His wavefunctions were not fully converged and the results obtained were too low by a factor of about two. GTOs are to be suspected in the region near the nucleus but this is unlikely to account for the massive discrepancies.

In the ground states, the spin-orbit coupling constant for CNC is 26.41 cm^{-1} (Merer and Travis, 1966) while that for CCN is 40.34 cm^{-1}. This is, at first sight, a little suprising since it is difficult to see why rearranging the

atoms should have such a large effect. Thomson (1973) has found that the unpaired electron in CCN (2π orbital) and the unpaired electron in CNC ($1\pi_g$ orbital) are mainly concentrated on the terminal carbon atoms with only small nitrogen populations.

The ATMOL3 programs of Saunders et al. (see Guest and Saunders (1974)) were used to obtain symmetry equivalenced RHF wavefunctions. The STO basis set (see table I) was minimal and was chosen so that comparison with Hinkley's results would be fair.

	C		N
1s	5.7	1s	6.7
2s	1.625	2s	1.95
2p	1.625	2p	1.95

Table I Exponents for CCN and CNC.

The one- and two-electron contributions to spin-orbit coupling are given in table II. Atomic values calculated by Blume and Watson (1963) are 13.4 cm^{-1} for carbon and 41.8 cm^{-1} for nitrogen. The coupling constant for nitrogen is greater than that for carbon by a factor of about three so that although the charge is not particularly concentrated on the terminal nitrogen atom in CCN, the contribution from this atom is quite large. Because of the symmetry of the $1\pi_g$ orbital of CNC, there is no contribution from the central

atom in this molecule. The contributions from all the terminal carbon atoms is very similar and so the difference between these two molecules arises from the nitrogen contribution. Despite the limitations of the basis set, agreement with experiment is very good. The results suggest numerical error in the earlier work of Hinkley.

	C_a	C_b	N	Total
C_aC_bN				
one-electron	25.79	1.28	46.95	74.02
two-electron	-13.29	-0.61	-20.75	-34.65
total	12.50	0.67	26.20	39.37
$C_aN\ C_b$				
one-electron	25.76	25.76	0	51.52
two-electron	-13.02	-13.02	0	-26.04
total	12.74	12.74	0	25.48

Table II Spin-orbit coupling matrix elements (in cm^{-1}).

For a $^2\Delta$ state that arises from a configuration $\sigma\pi^2$, many integrals are identically zero because of the spin part of H_{so}. A non-zero value of $^*A$ arises from the spin-other-orbit interaction between the outer electrons (Lefèbvre-Brion and Bessis, 1969) and so the spin-orbit coupling constants for $^2\Delta$ ($\sigma\pi^2$ configuration) states are frequently small and negative. Higher order spin-orbit effects become more important as the nuclear charge increases. These effects are dominant in many molecules containing a second row atom; for example, a small positive

value arises for A in the $A^2\Delta$ state of SiH. Veseth (1971) has considered a number of $^2\Delta$ states and has obtained information about perturbing states from the second order spin-orbit contribution.

The $A^2\Delta$ states of CCN and CNC arise from a configuration of the type $\sigma\pi^2$. The coupling constant for CCN is negative (-0.6 cm^{-1}) but for CNC it is positive (+0.33 cm^{-1}). It seems likely that this is due to higher order spin-orbit coupling effects. The energy separations between the $X^2\Pi$ and $A^2\Delta$ states are of the order of 30 000 cm^{-1} so it must be interactions with other states that are important.

The calculation of off-diagonal matrix elements for polyatomic systems is another obvious extension. The calculation of electronic off-diagonal matrix elements presents no problems but calculation of vibrational matrix elements is rather difficult. Unless the effects of bending are neglected, it is necessary to know the complete potential surface fairly accurately. Such information is only rarely available for open shell systems. This will also be a problem in the calculation of spin-orbit effects in non-linear molecules. Rather more important in this case, most of the present theory is developed around the cylindrical symmetry of the system; the form of the spin-orbit coupling operator will be somewhat different for the non-linear case. Most of the existing ab initio techniques used in spin-orbit coupling calculations use

complex orbitals such as π^- and π . Clearly, real orbitals with rather more complicated spatial dependence will arise in non-linear systems. However, it may be possible to express the molecular orbitals in simple planar systems in terms of complex basis functions.

The calculation of diagonal spin-orbit coupling constants for linear systems seems to be relatively straightforward. Problems arise in the corresponding off-diagonal matrix elements because of the need to know the potential surface. It may, however, be a reasonable approximation to restrict attention to linear geometry and to neglect bending. The problems presented by non-linear, and particularly non-planar systems, would appear to be rather more severe.

7.2 Noble gas molecular ions.

Inert gas positive ions have been observed to show a high degree of reactivity with other atoms and molecules. Unlike the neutral inert gas atoms, the positive ions have an unpaired valence electron. The HeH^+ ion, for example, is known to be very stable although simple arguments based on ionisation potentials would not predict this. Reactions involving inert gas ions have been observed in a number of experiments including ion cyclotron resonance, stationary and flowing afterglows, and molecular beams.

Helium is the least reactive of the noble gases having the highest ionisation potential of any element. It is, however, the most abundant element in the interstellar medium other than hydrogen so that if helium forms simple stable molecular ions it is plausible that these might be present in the interstellar medium in detectable abundances. It would be very worthwhile to consider whether the helium analogues of OH and CH might be detectable in the molecular clouds via Λ-doubling transitions.

Calculations were performed for the diatomic ions of the form AHe^+, where A is C, N or O, using the ALCHEMY programs; the STO basis sets were based on those used by Cade and Huo (1967a) for the neutral hydrides. Potential curves were obtained for that state which corresponds to the ground state in the analogous hydride. OHe^+ ($^2\Pi$) is more strongly bound than NHe^+ ($^3\Sigma^-$) which in turn is more strongly bound than CHe^+ ($^2\Pi$). Approximate well depths are 3000 cm^{-1}, 600 cm^{-1} and 200 cm^{-1} for OHe^+, NHe^+ and CHe^+, respectively. Atomic population analyses were carried out close to the equilibrium geometries; there is a decrease in the electron density on He from 1.973 in CHe^+ through 1.889 in NHe^+ to 1.690 in OHe^+. This mirrors the trend in stability (and also in geometry). Calculations on the $^2\Sigma^+$ state of CHe^+ confirmed a $^2\Pi$ ground state but the $^4\Sigma^-$ state of OHe^+ was found to cross the $^2\Pi$ state between 2.0 and 2.5 bohr. A repulsive $^4\Sigma^-$ ground state has been observed in a minimum basis set CI study of OHe^+ by Augustin et al.

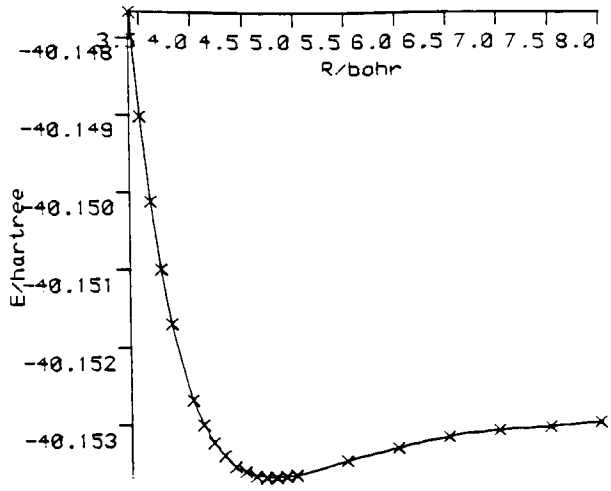

(C-He)+ 2-PI

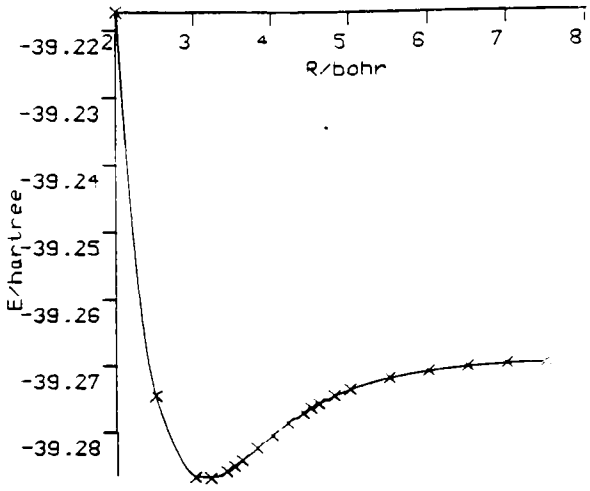

(C-He)2+ 1-SIGMA+

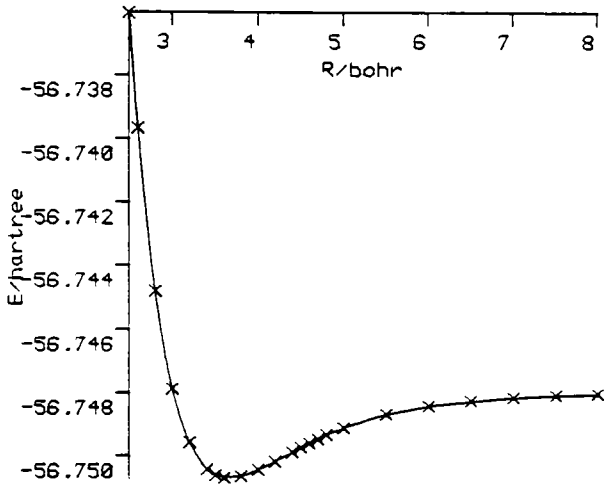

(N-He)+ 3-SIGMA-

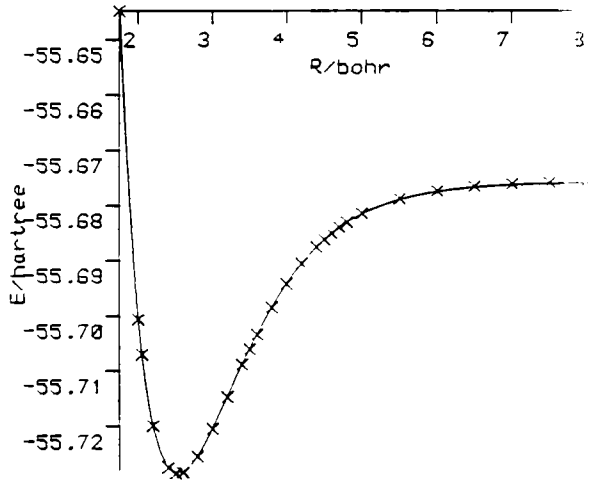

(N-He)2+ 2-PI

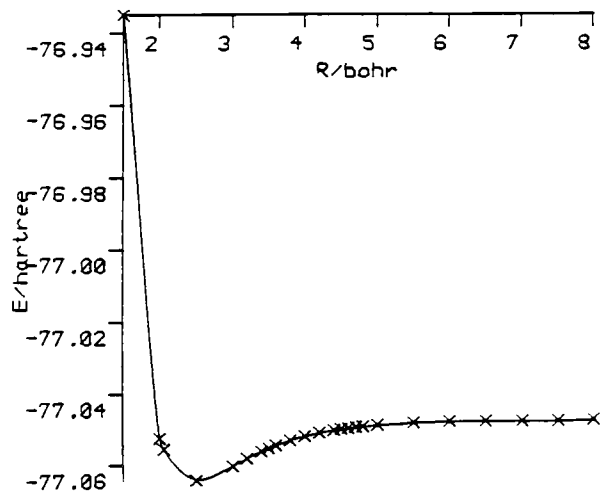

(O-He)+ 2-PI

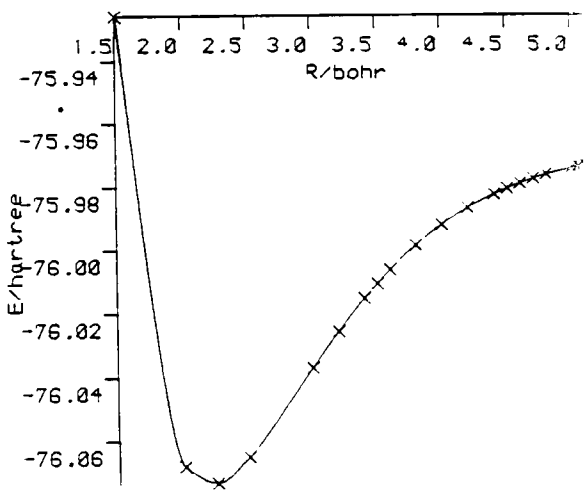

(O-He)2+ 3-SIGMA-

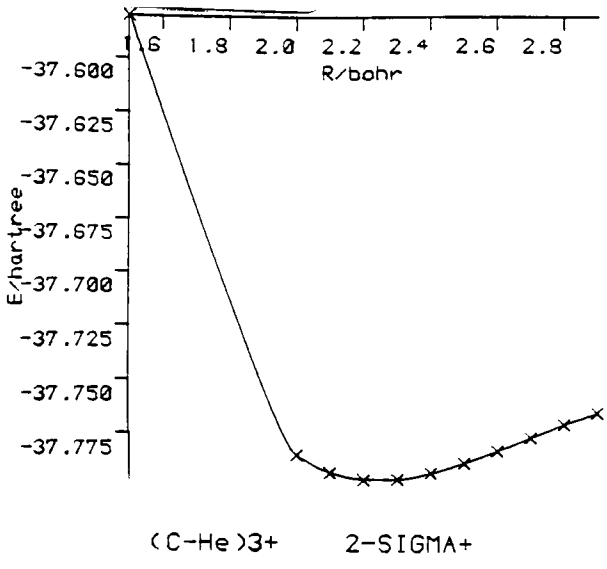

(C-He)3+ 2-SIGMA+

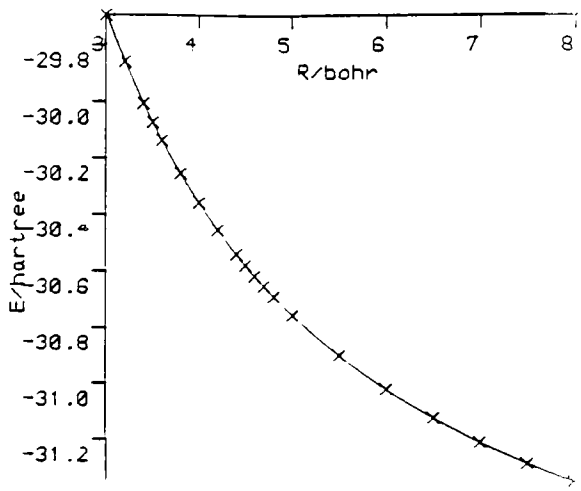

(C-He)6+ 1-SIGMA+

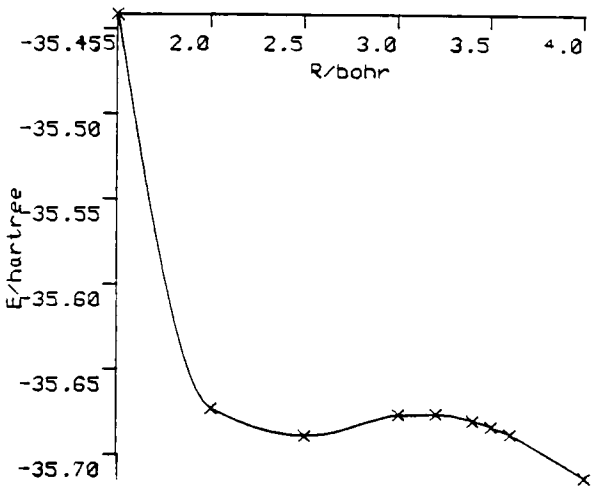

(C-He)4+ 1-SIGMA+

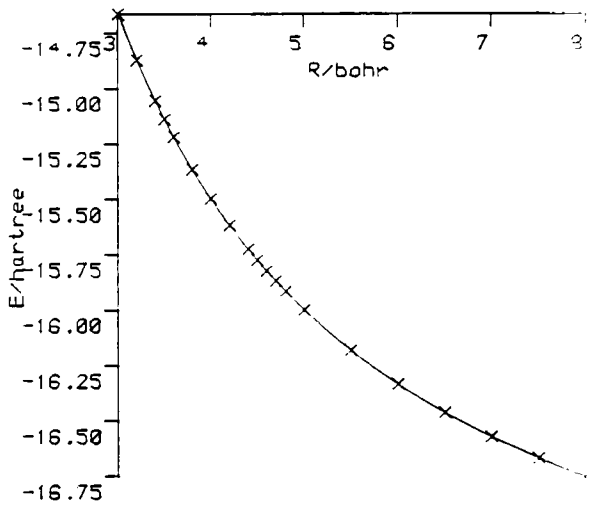

(C-He)7+ 2-SIGMA+

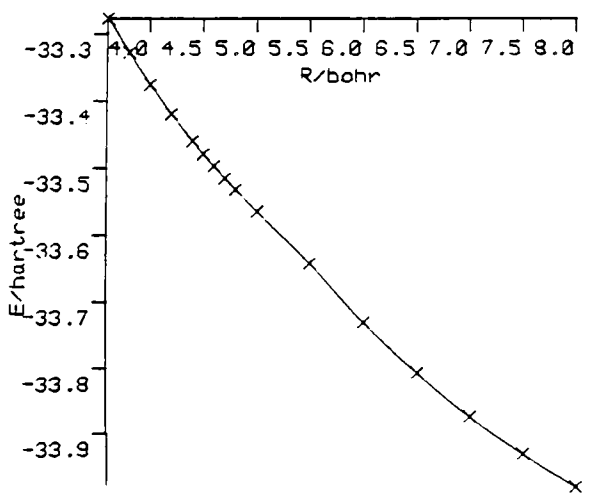

(C-He)5+ 2-SIGMA+

Figure 1

Potential energy curves for diatomic ions of He.

Table III Population analyses and approximate well depths for molecular ions of He.

System	Population analysis A	He	Geometry (in bohr)	Approximate well depth (in cm^{-1}).
CHe^{+} $^2\Pi$	5.027	1.973	4.3	200
CHe^{2+} $^1\Sigma^+$	4.207	1.793	3.0	5000
CHe^{3+} $^2\Sigma^+$	3.580	1.420	2.2	>7000
CHe^{4+} $^1\Sigma^+$	2.853	1.147	2.5	>3000
CHe^{5+} $^2\Sigma^+$	2.250	0.750	2.5	unbound
CHe^{6+} $^1\Sigma^+$	2.000	0.000	2.5	unbound
CHe^{7+} $^2\Sigma^+$	1.000	0.000	2.5	unbound
NHe^{+} $^3\Sigma^-$	6.111	1.889	3.2	600
NHe^{2+} $^2\Pi$	5.423	1.577	2.5	14000
OHe^{+} $^2\Pi$	7.310	1.690	2.5	3000
OHe^{2+} $^3\Sigma^-$	6.736	1.264	2.0	21000

(1973).

The same trends in stability, geometry and electron densities were observed in the corresponding doubly-charged ions. OHe^{2+} ($^3\Sigma^-$) with a well depth of ~21000 cm^{-1} is more strongly bound than NHe^{2+} ($^2\Pi$) with a well depth of ~14000 cm^{-1} which is more strongly bound than CHe^{2+} ($^1\Sigma^+$) with a well depth of ~5000 cm^{-1}. Calculated potentials for the $^4\Sigma^-$ and $^2\Sigma^+$ states of NHe^{2+} were found to have higher energies than the $^2\Pi$ state.

The doubly-charged ions AHe^{2+} are more strongly bound than their singly-charged counterparts. In order to examine further the variation of the stability of the molecular ions with respect to the total charge, a series of calculations was performed on the CHe^{n+} ions for n=3,4,5,6,7. The basis set was not modified as the total charge was increased but this should not seriously affect the results. The stability was found to increase from CHe^+ to CHe^{2+} and again from CHe^{2+} to CHe^{3+} but then to decrease as the charge was further increased.

The various trends in stability are easily understood in terms of the effective charges on the two centres. As electrons are removed from CHe^+, the electron-nucleus screening effects are reduced so that the effective nuclear charges of the component atoms are increased. This leads to an increase in the attraction between the nucleus at one

centre and the electrons on the other centre but also to an increase in the nuclear repulsion energy. The former component of the energy is dominant in the stable ions CHe^{n+} where n=1,2,3,4 but the nuclear repulsion term is dominant for the highly charged unstable ions.

The electrostatic interpretation that has been given for the dependence of stability on total charge should be useful in predicting stable polyatomic species (Cooper and Wilson, 1981). The only systems studied here that have $^2\Pi$ ground states are CHe^+ and NHe^{2+}. It is unlikely that either of these molecular ions will be detected in the interstellar medium via Λ-doubling transitions since CHe^+ is only weakly bound and since no doubly-charged ions are known in the molecular clouds.

7.3 Accidental predissociation.

7.3.1 The photodissociation of Li_2.

Interest in the alkali metal dimers stems from the possible construction of visible lasers based on the $X^1\Sigma_g^+ \leftarrow A^1\Sigma_u^+$ transition and from the study of isotope separation. Clearly, any mechanism which depletes the $A^1\Sigma_u^+$ state will tend to make population inversion rather difficult and so it is important to identify the processes by which Li_2 can dissociate. Potential curves are

illustrated in figure 2.

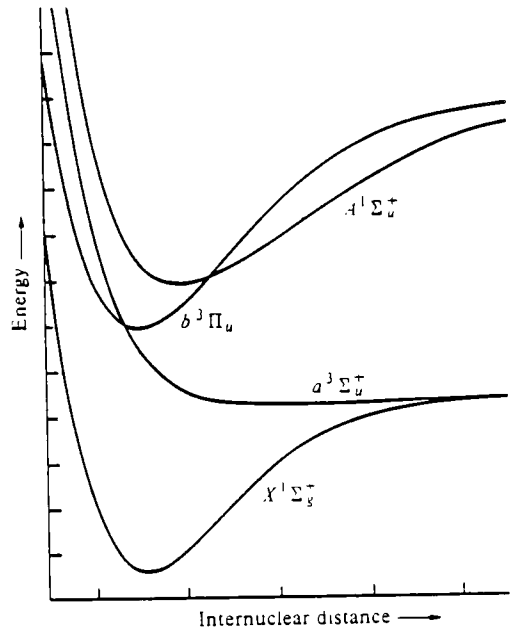

Figure 2

Potential energy curves for Li_2.

Uzer and Dalgarno (1980) have considered three mechanisms by which Li_2 can be dissociated by visible wavelength photons.

(1) Direct photodissocation. From calculated absorption oscillator strengths it is clear that excitation from the v''=0 level of the $X^1\Sigma_g^+$ state to the $A^1\Sigma_u^+$ and $B^1\Pi_u$ electronic states results exclusively in transitions to discrete vibrational levels. Excitations from higher vibrational levels of the $X^1\Sigma_g^+$ state can result in some absorption into the continuum.

(2) Spontaneous radiative dissociation. Excitation from the ground electronic state into discrete vibrational levels of the $A^1\Sigma_u^+$ and $B^1\Pi_u$ states followed by spontaneous radiative decay into the vibrational continuum of the $X^1\Sigma_g^+$ state is

not a likely mechanism. Transitions from the v'=0 levels are exclusively to bound levels; although transitions are possible from higher v' levels to the continuum of the ground state, the probability of populating these levels is very small.

(3) Accidental predissociation. The $A\,^1\Sigma_u^+$ state crosses the $b^3\Pi_u$ state which in turn crosses the $a^3\Sigma_u^+$ state: the $a^3\Sigma_u^+$ state is mostly repulsive and dissociates to ground state atoms.

The rotation of the nuclear framework (H_{rot}) and the spin-orbit coupling (H_{so}) may be treated as a perturbation ($H^{(1)}$) to the vibronic hamiltonian as in section 2.2. The predissociation lifetime τ_i for vibrational level i is given by

$$\frac{1}{\tau_i} = \frac{4\pi^2|T_i|^2}{h}$$

where T_i may be evaluated in the form

$$T_i = \sum_n \frac{\langle A\,^1\Sigma_u^+\ i|H^{(1)}|b^3\Pi_u\ n\rangle\langle b^3\Pi_u\ n|H^{(1)}|a^3\Sigma_u^+\ u\rangle}{E_i - E_n} .$$

Since the $^1\Sigma_0^+$ state has e parity as have $^3\Sigma_1^+$ and $^3\Pi_0^+$ states, the only matrix elements coupling the three states are

$$\langle b^3\Pi_0^+\ n|H^{(1)}|A\,^1\Sigma_0^+\ i\rangle = 2\ \langle b^3\Pi_u\ n|H_{SO}|A\,^1\Sigma_u^+\ i\rangle$$

and $$\langle b^3\Pi_0^+\ n|H^{(1)}|a^3\Sigma_1^+\ u\rangle = -\sqrt{[J(J+1)]}\ \langle b^3\Pi_u\ n|BL^-|a^3\Sigma_u^+\ u\rangle$$

The expression for T_i thus closely resembles that for the

Λ-doubling constant p_v. The continuum state $|a^3\Sigma_u^+\ u\rangle$ lies at the same energy as $|A\,^1\Sigma_u^+\ i\rangle$ and the summation or integral extends over all vibrational levels of the $b^3\Pi_u$ state. This is clearly a problem that could be usefully tackled using the direct summation method described in chapter 4.

Uzer and Dalgarno (1980) took interaction potentials from the model potential calculations of Watson at al. (1977) and estimated values of $1/\tau_i$ using the conventional sum-over-states method. These workers assumed pure precession for the matrix element of L^+ and assumed the matrix element between the $b^3\Pi_u$ and $A\,^1\Sigma_u^+$ states to be independent of internuclear distance and equal to 1 cm^{-1}. These rather severe approximations do not affect the prediction of the specific v'J' levels which predissociate but do affect the estimated lifetimes.

It is clear that near degeneracies will lead to destrucion of specific levels of the $A\,^1\Sigma_u^+$ state and that the dissociation will be sensitive to the isotopic composition of the molecule. It seems worthwhile to calculate ab initio electronic matrix elements so that this problem can be re-examined when accurate potential curves become available.

A basis set for Li_2 was based on that used for LiO in section 3.1. SCF wavefunctions for the $A\,^1\Sigma_u^+$, $a^3\Sigma_u^+$ and $b^3\Pi_u$ states were calculated at a number of internuclear distances and matrix elements of H_{SO} and of L^+ were computed. From the

values given in table IV it can be seen that the spin-orbit coupling matrix elements are quite sensitive to the internuclear distance used. Pure precession is certainly not a valid approximation for the matrix elements of L^+ between the $b^3\Pi_u$ and $a^3\Sigma_u^+$ states. The $2\sigma_u$ molecular orbital in the $a^3\Sigma_u^+$ state is mainly 2s whereas the $1\pi_u$ molecular orbital in the $b^3\Pi_u$ state is mainly 2p and 3p. Note that the figures in table IV have been given to more decimal places than their accuracy warrants - this is to avoid rounding errors in their use.

Geometry (in bohr)	$\langle b^3\Pi_u \lvert H_{so} \rvert A^1\Sigma_u^+ \rangle$ /cm^{-1}	$\langle b^3\Pi_u \lvert L^+ \rvert a^3\Sigma_u^+ \rangle$
2.5	0.98087	0.28156
3.0	0.66449	0.30085
5.0	0.30411	0.37927
6.0	0.27353	0.52390
7.0	0.27407	0.66575
8.0	0.27914	0.78922

Table IV Electronic matrix elements for Li_2.

When accurate potential curves become available, either from experiment or from ab initio calculations, it will be possible to predict which levels are preferentially predissociated and to calculate lifetimes using the matrix elements in table IV and the direct summation method described in chapter 4.

7.3.2 The formation of CH^+.

The abundance of CH^+ in diffuse interstellar clouds is much larger than predictions based on probable formation and destruction mechanisms. This ion is believed to be important in the formation of CH, CO, CN and several other molecules. Spin change scattering of C^+ with H may be an important cooling mechanism in planetary atmospheres and in the interstellar medium. CH^+ is also very important in combustion reactions and in atmospheric chemistry.

One mechanism that has been proposed for the formation of CH^+ is radiative association. This is feasible provided that there exists a bound excited state which dissociates to the same atomic products as the ground state; there must be an appreciable oscillator strength for emission from the excited state. Another suggestion is inverse predissociation from quasibound levels. Cosby et al. (1980) have studied predissociation of CH^+ by the appearance of C^+ photofragments as a function of excitation wavelength. The observation of a very large number of discrete transitions leading to dissociation within 350 cm^{-1} of the dissociation limit was attributed to predissociation of the $A^1\Pi$ and $a^3\Pi$ states. This would greatly increase the number of quasibound levels which could contribute to the radiative association rate.

Potential curves which dissociate to C^+ (^2P) and H (^2S) are shown in figure 3. The atomic limit is split by 64 cm^{-1} due to the spin-orbit coupling in C^+ (^2P); the $A^1\Pi_1$ state correlates with C^+ ($^2P_{3/2}$) while the $a^3\Pi_1$ state correlates with C^+ ($^2P_{1/2}$) so that bound levels of the $A^1\Pi_1$ state which lie above the $^2P_{1/2}$ limit could be predissociated. Note that close to the dissociation limit, the coupling will be intermediate between Hund's cases a and c so that optical transitions from $X^1\Sigma_0^+$ to $a^3\Pi_0^+$, $a^3\Pi_1$ and $A^1\Pi_1$ are all allowed.

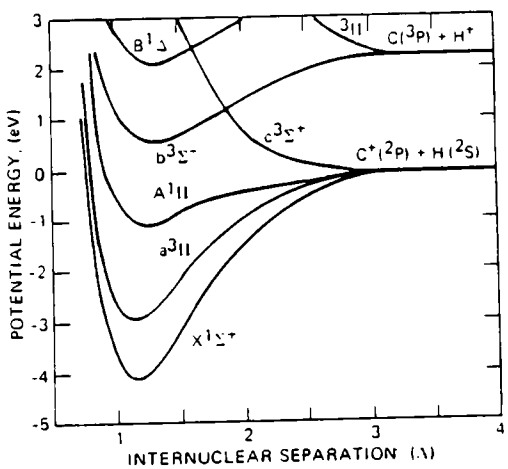

Figure 3

Potential curves for CH^+.

Gerratt and Bocchetta (private communication, 1980) have suggested that study of the predissociation in CH^+ might be amenable to R-matrix scattering calculations. These require off-diagonal matrix elements of the spin-orbit coupling operator. The basis set of Cade and Huo (1967a) has been used to generate potential curves for the various states; these wavefunctions have been used to calculate the

various off-diagonal quantities as a function of internuclear distance and use of these matrix elements is now in progress. Because of the very high density of states in the region of interest, the perturbation theory approach of the previous section cannot be used and extensive scattering calculations are required.

Butler and Dalgarno (1980) have considered the charge transfer process of C^+ with H:

$$C^+ (^2P^0) + H \rightarrow C (^3P) + H^+ \quad -2.33 \text{ eV}$$

At low energy this would proceed via approach along the repulsive $c^3\Sigma^+$ potential curve followed by transition to the attractive $b^3\Sigma^-$ potential. These two states are mixed by matrix elements of the spin-orbit coupling operator which have been estimated to be of the order of 1 cm^{-1} (Lorquet et al., 1971) but the uncertainty is large. Butler and Dalgarno obtained wavefunctions for the nuclear motion by integration of the radial Schrödinger equation and then used these with the distorted wave approximation to calculate rate constants. They concluded that the charge transfer process of C^+ with H is not important in diffuse nebulae. Much of the uncertainty associated with the calculated rate constants was attributed to the lack of reliable spin-orbit coupling matrix elements.

The operator H_{so} has the same symmetry properties as the rotations R_x, R_y and R_z (see McGlynn et al., 1969) so that it is easy to decide which tensor component of the

operator to use from character tables. For $C_{\infty v}$ symmetry (see table V), $\Sigma^+ \times \Sigma^- = \Sigma^-$ so $H_{so}^{\mu=0}$ ("diagonal") rather than $H_{so}^{\mu=\pm1}$ ("off-diagonal") should be used for the matrix element between the $b^3\Sigma^-$ $(1\sigma^2 2\sigma^2 1\pi^2)$ and $c^3\Sigma^+$ $(1\sigma^2 2\sigma^2 3\sigma 4\sigma)$ states:

$$\langle b^3\Sigma^- | H_{so} | c^3\Sigma^+ \rangle = \langle 1\pi^+ \; 1\pi^- | H_{so}^{\mu=0} | 3\sigma \; 4\sigma \rangle - \langle 1\pi^+ \; 1\pi^- | H_{so}^{\mu=0} | 4\sigma \; 3\sigma \rangle$$

$C_{\infty v}$	E	$2C_\infty^\phi$	...	$\infty\sigma_v$	
Σ^+	1	1	...	1	
Σ^-	1	1	...	-1	$H_{so}^{\mu=0}$
Π	2	$2\cos\phi$	...	0	$H_{so}^{\mu=\pm1}$
Δ	2	$2\cos 2\phi$	...	0	

Table V Character table for $C_{\infty v}$.

Note that Slater's rules are not truly applicable (see section 2.5) and that two-centre integrals and higher-order terms are likely to be important in this case. Nonetheless, the one-centre contribution to the spin-orbit coupling was evaluated at 2.5 bohr (close to the minimum of the $b^3\Sigma^-$ state) and at 3.3 bohr (close to the crossing point). The values obtained for $2\langle b^3\Sigma^- | H_{so} | c^3\Sigma^+ \rangle$ were 0.73 cm^{-1} at 2.5 bohr and 0.14 cm^{-1} at 3.3 bohr. The coupling between these states is even weaker than suggested by Lorquet et al. (1971); this gives support to the conclusions of Butler and Dalgarno (1980) that the charge transfer process of C^+ with H is not important in diffuse nebulae.

The formation of CH^+ via inverse predissociation seems a very reasonable mechanism and R-matrix scattering calculations are now being carried out using the spin-orbit matrix elements calculated in this work.

7.4 Conclusions.

It has proved possible to extend the calculation of spin-orbit coupling constants into the realm of small linear molecules and to explain the very different values for CCN and CNC. It is clear that the calculation of off-diagonal quantities for such systems would be intrinsically rather less accurate since the evaluation of the vibrational part of the relevant matrix elements requires detailed knowledge of the potential surfaces. However, it might be a reasonable approximation to neglect bending. This is also a problem for non-linear systems. One approach would be to assume that all the potential surfaces are identical in shape.

The calculation of lifetimes for singlet-triplet crossings for small organic molecules would be very worthwhile. Unfortunately, all of the present methods depend on the cylindrical symmetry of the system since the spin-orbit coupling operator is used in the forms $H_{so}^{m_s=0}$ and $H_{so}^{m_s=\pm 1}$. For formaldehyde, for example, the x and y components of H_{so} transform as different irreducible representations and it is not valid to use $H_{so}^{m_s=\pm 1}$. However, the calculation of one-centre one-electron integrals of the x, y and z components of H_{so} is straightforward and it is possible, by choice of "suitable" effective nuclear charges, to include the two-electron contribution. The approximations required for the calculation of spin-orbit coupling effects in small organic systems are very severe but the results would still

be of considerable value since even an 'order of magnitude' estimate of lifetimes is often sufficient.

A study of noble gas molecular ions has led to a simple electrostatic explanation of the various trends in stability. If open shell systems containg helium can be produced in laboratory experiments then the calculation of spin-orbit coupling constants might be of some assistance in the identification of electronic states. It seems unlikely that the helium analogues of OH and CH will be detected in the interstellar medium via Λ-doubling transitions.

Accidental predissociation via near degeneracies is an important mechanism for the destruction of specific v'J' levels of Li_2. Study of this phenomenon is important for the possible construction of alkali metal dimer lasers and for isotope separation. The matrix elements responsible for the mixing of the relevant states have been calculated; when accurate potential curves become available it will be possible to calculate lifetimes. Matrix elements have also been computed for CH^+ since inverse predissociation may be a favourable process for the formation of this molecule. Further study of this species, whose high abundance in the interstellar medium is something of an enigma, requires extensive scattering calculations. The combination of scattering theory and the ab initio calculation of electronic matrix elements is likely to be a very powerful tool in the study of a number of very interesting problems

of astrophysical importance.

The study of Λ-doubling in molecules such as SeH which contain heavier elements would be very interesting. However, when the elements become sufficiently heavier it will be necessary to replace the present perturbation theory approach to spin-orbit coupling effects by a full relativistic treatment. This would entail a considerable amount of work.

There are number of major areas where the calculation of accurate ab initio spin-orbit coupling matrix elements will be very important in the future. The study of the molecular clouds in the interstellar medium should prove to be particularly interesting. The calculation of approximate spin-orbit coupling matrix elements for small organic systems is also likely to be very useful.

SUMMARY.

Spin-orbit coupling effects are of interest both to experimentalists and to theoreticians. The importance of the related phenomena such as Λ-doubling and spin-splitting is due to the advent of radiofrequency studies of the interstellar medium. Identification of the molecules, and the molecular transitions, in the interstellar dust clouds is necessary for an understanding of the cooling process by which these clouds can contract to form new stars.

For the lightest species, such as CH and OH, rotational transitions lie outside the range studied by radioastronomers. These molecules have been detected via electric-dipole allowed radiofrequency transitions between Λ-doublet components. There are many other species which should be detectable in this way provided accurate frequency predictions are available for a search to be made.

In the denser regions of the interstellar medium, molecules are shielded from ultra-violet radiation by the dust grains so that many polyatomic species can exist. The building blocks in the reaction schemes leading to the polyatomic molecules are small radicals and ions. Many of these are so reactive that their study in laboratory experiments is very difficult. Furthermore, terrestrial experiments are not generally carried out at very low

temperature and very low pressure so that if high resolution spectra can be obtained and analysed then it is necessary to extrapolate to the conditions that prevail in the molecular clouds. This frequently introduces large uncertainties.

Ab initio calculations of Λ-doubling frequencies for CH and for OH have been in remarkable agreement with astrophysical observation. These calculations were extended to the molecule SiH which is of particular interest since silicon is apparently depleted in the molecular clouds relative to its solar abundance. A search for this molecule in interstellar space has been hampered by the difficulty of the relevant terrestrial experiments. Moreover, the choice of different fitting procedures leads to different frequency predictions. The ab initio value of 3000 MHz is closer to the most recent terrestrial value than are many of the earlier experimental values. The results suggest that core polarisation is not a serious problem. This work has stressed the need to obtain continuum wavefunctions by solution of the radial Schrödinger equation rather than pseudo-continuum wavefunctions using box normalisation.

Accurate radiofrequency data for LiO is available from molecular beam studies but only for a fairly limited number of transitions. The large uncertainty in the fitting procedure and the extensive correlation between fitted parameters is rather unfortunate in view of the quality of

the data. The ab initio values for Λ-doublet splittings are in excellent agreement with the observed transitions and this suggests that the experimental radiofrequency spectrum ought to be re-examined. Use of the ab initio value for the spin-orbit coupling constant should help break the extensive correlation of parameters.

Spin-splitting has been considered for CaH since calcium is another element which is heavily depleted in the interstellar medium. The calculated value for the spin-splitting constant, obtained by including the contributions from the two lowest $^2\Pi$ states, is within about 5% of experiment and is only just outside the experimental error limits. Similar methods were used for BH$^+$ for which there are serious problems in the fitting procedure due to unresolved spin-splitting. Study of this system was complicated by physically unreal discontinuities in the SCF wavefunctions.

The theoretical expressions for Λ-doubling and for spin-splitting parameters contain explicit summation over vibrational levels of perturbing states. A method has been described which avoids this explicit sum over vibrational levels and which automatically includes all contributions from the bound levels and from the continuum of a given perturbing state. The method was tested for OH, LiO and for a system with an unbound perturbing state. In the case of

HF^*, the sum over states and the direct summation methods gave different results since the perturbing state is only weakly bound. With the sum over states methods it easy to miss contributions from the top of the ladder of bound levels or from the bottom of the continuum. The direct summation approach automatically includes all such contributions and is computationally cheaper and more convenient. HF^* is of interest since it has been proposed as a possible interstellar maser. The Λ-doubling in NaAr was also examined using this method and good agreement was found with experiment giving some information on the Na + Ar interaction. The spin-orbit coupling in this system is intermediate between molecular and atomic limits; it is not necessarily valid to equate the multiplet splitting with the spin-orbit coupling constant in systems where there is very little interaction between the two atoms. This has also been considered for $HeNe^*$: the variation of spin-orbit coupling energy with distance will be almost entirely due to the recoupling of angular momenta. The inclusion of polarisation functions, which are important for calculating binding energies, had little effect on the ab initio spin-orbit coupling constant.

Extensions to new problems have been discussed and possible systems for future study have been suggested. Spin-orbit coupling in larger systems is one such possibility. Calculations for CCN and for CNC were found to

be very successful. The binding in positive molecular ions containing helium has been studied so as to determine whether the He analogues of molecules such as OH and CH might be detectable in the interstellar medium via Λ-doubling transitions. The conclusion was that this was unlikely but that the ab initio calculation of spin-orbit coupling constants for open-shell noble gas molecular ions might be useful in the identification of electronic states.

Accidental predissociation has been considered in Li_2 and matrix elements have been computed so that, when accurate potential curves are available, it will be possible to identify which levels are preferentially destroyed and to calculate lifetimes. Preliminary work on CH^+ has been reported; this is an important system requiring extensive further study. Evidence has been presented to support the conclusion that the charge transfer process of C^+ with H is not important in diffuse nebulae.

The ab initio calculation of spin-orbit coupling effects in diatomic molecules has been very successful, particularly with reference to the interstellar medium. The combination of these ab initio methods with scattering theory is likely to become very important in the future.

APPENDIX A SOFTY.

A large proportion of the mathematical equations in a monograph by Richards, Trivedi and Cooper (1981) and in this thesis were drawn on the III FR80 film recorder at the Rutherford and Appleton Laboratories (RAL) using specially developed programs which were collectively named SOFTY (Spin-Orbit Fortran TYpesetting). Most of the characters were ultimately processed by the FORTRAN routine SYMBOL which provides access to proportionally spaced software character fonts. SYMBOL is due to N.Wolcott of the U.S. National Bureau of Standards and has been made available at RAL by K.M.Crennell.

SOFTY consists of a number of FORTRAN routines capable of drawing complicated mathematical expressions containing subscripts and superscripts (to several levels), primes, 3j and 6j symbols, bras and kets, centred fractions, numeric fractions and overlined characters. Many of these facilities are available via a routine called PROCS which acts as a preprocessor for SYMBOL and which calls, and is called by, many of the other routines.

A few of the routines which are normally called directly are listed in table I - note that most of these are subroutines with several ENTRY points. The routine PROCS accepts a character string consisting of upper and lower

FRAX	draws centred fractions
GETLEN	obtains the size of the expression
HEADER	produces header and trailer frames
INIT	starts a new page
NL	moves to a new line
NUMB	produces numeric fractions
PUT	resets the current position for PROCS
SIGMA	draws summation signs
SIZE	magnifies or reduces the output
THREEJ	produces 3j and 6j symbols

Table I Some of the routines called directly within SOFTY.

\	next character is a subscript
"	next character is a superscript
@	shift to upper case (rarely used)
#	shift to lower case (rarely used)
&	shift to complex font
^	next character is Greek or mathematical
%	shift to simplex font (default)
?	backspace last character (maximum six)
!	shift to italic font
;	shift to duplex font
:	terminate processing

Table II Control characters.

$B	$\bar{\beta}$	(OVERB)
$C	$\hat{r}$	(CARRET)
$D	subscript mode	(DLCSUB)
$F	$\bar{\pi}$	(OVERN)
$L	prime on superscript	(HPRSUP)
$M	prime on capital letter	(HPRIME)
$N	$\neq$	(NEQ)
$O	$\bar{l}$	(OVERL)
$R	restore previous mode	(DLCRTN)
$S	prime on subscript	(PRSUB)
$U	superscript mode	(DLCSUP)
$0	$\bar{o}$	(OVER0)
$1	$\bar{\pi}$	(OVER1)

Table III Special commands with associated routines.

case alphabetic characters, numerals, the special symbols +-/=()*,.' and several control symbols whose functions are described in table II.

The simplex characters are not very suitable for general purposes; the other characters made available by SYMBOL are drawn in figure 1. The character $ is used to introduce commands which control several special facilities (see table III). A few examples of output from SOFTY are reproduced in figure 2. It is likely that the ideas used in SOFTY will be incorporated into a general text layout program at RAL.

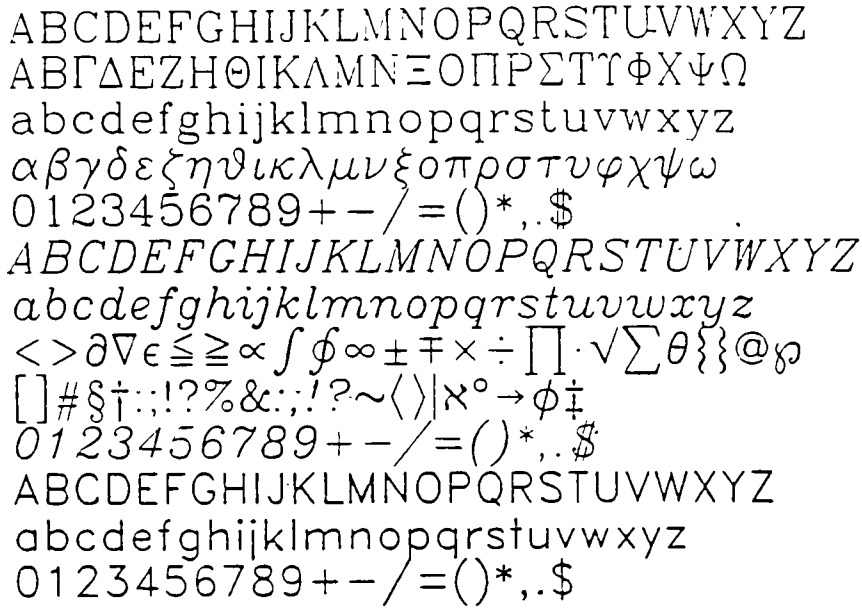

Figure 1

Characters available from SYMBOL.

$$G^{\mu}_{\kappa\beta}(\lambda\, q\, \vec{n}_A, \vec{l}_A) = (-1)^{m_{A'}+m_{A''}+\beta+\kappa+\mu} k(n_{A'}, n_{A'''}; \zeta_{A''}, \zeta_{A'''})$$

$$J^{\mu}_{\kappa\beta}(\lambda, q, \vec{n}_A, \vec{l}_A)[\tfrac{1}{2}(2l_{A''}+1)(2\kappa+1)(2l_{A'''}+1)]^{\frac{1}{2}}$$

$$\begin{pmatrix} l_{A''} & \kappa & l_{A'''} \\ m_A & -q & -m_{A'''} \end{pmatrix} \begin{pmatrix} l_{A''} & \kappa & l_{A'''} \\ 0 & 0 & 0 \end{pmatrix}$$

$$\sum_{v} \frac{\langle v''=0|B|v'\rangle\langle v'|v''=0\rangle}{\nu(^2\Pi\ v', ^2\Sigma^-\ v'')}$$

$$|^2\Pi_{1/2}\rangle \sim |L\ \Lambda=1\rangle\ |S\ -\tfrac{1}{2}\rangle$$

$$\int_0^{\infty} \frac{\langle X^2\Pi\ v|H_{so}|^2\Sigma^-\ E_u\rangle\langle ^2\Sigma^-\ E_u|BL^-|X\ ^2\Pi\ v\rangle dE_u}{\Delta E_v - E_u}$$

SOFTY 2 6X

$$-\frac{1}{\sqrt{2}}\langle 3\sigma 3\bar{\sigma}\, 1\pi^+|L^+|3\sigma 1\bar{\pi}^+ 1\pi^-\rangle$$

Figure 2

Examples of output from SOFTY.

APPENDIX B Publications.

"The accuracy of predicted radioastronomical frequencies and the spectrum of hydroxyl."
David L. Cooper and W. Graham Richards, Nature 278, 624 (1979).

"Spin-doubling in CaH."
David L. Cooper and W. Graham Richards, J. Chem. Phys. 73, 991 (1980).

"Spin-orbit coupling and Λ-doubling in LiO."
David L. Cooper and W. Graham Richards, J. Chem. Phys. 73, 3515 (1980).

"SiH: Λ-doubling and core polarisation."
David L. Cooper and W. Graham Richards, J. Chem. Phys. 74, 96 (1981).

"Spin-splitting in BH^+."
David L. Cooper and W. Graham Richards, J. Phys. B 14, L127 (1981).

"Spin-orbit coupling in CCN and CNC."
David L. Cooper and W. Graham Richards, J. Phys. B 14, L131 (1981).

"Spin-orbit coupling in small molecules."
W. Graham Richards, Harit P. Trivedi and David L. Cooper, Oxford University Press (1981).

"Ab initio calculation of higher order corrections to Λ-doubling and spin-splitting in diatomic molecules."
David L. Cooper and Leif Veseth, J. Chem. Phys. (in press).

"Spin-orbit coupling and Λ-doubling in NaAr."
David L. Cooper, J. Chem. Phys. (in press).

"Direct summation over vibrational levels: Λ-doubling in HF^+."
Jeremy M. Hutson and David L. Cooper, J. Chem. Phys. (in press).

"Noble gas molecular ions."
David L. Cooper and Stephen Wilson, Mol. Phys. (submitted).

"Second-order and third-order Λ-doubling constants in SH."
Kristina Checkland, David L. Cooper and W. Graham Richards, (to be published).

REFERENCES

G.M.Almy and R.B.Horsfall Jr., *Phys. Rev.* **51**, 491 (1937)

S.D.Augustin, W.H.Miller, P.K.Pearson and H.F.Schaefer III, *J. Chem. Phys.* **58**, 2845 (1973)

P.S.Bagus, *in 'Proc. Seminar Selected Topics in Molecular Physics'*, IBM Germany, Ludwigsburg (1969)

P.S.Bagus, B.Lui, A.D.McLean and M.Yoshimine, *'Alchemy studies of small molecules' in 'Selected Topics in Molecular Physics'*, Verlag Chemie, Weinheim/Bergstrasse (1972)

L.-E.Berg and L.Klynning, *Physica Scripta* **10**, 331 (1974)

H.A.Bethe and E.E.Salpeter, *'Quantum mechanics of one- and two-electron atoms'*, Springer, Berlin (1957)

M.Blume and R.E.Watson, *Proc. Roy. Soc. Lond. A* **271**, 565 (1963)

P.Bollmark, L.Klynning and P.Pages, *Physica Scripta* **3**, 219 (1971)

S.E.Butler and A.Dalgarno, *Astron. Astrophys.* **85**, 144 (1980)

P.E.Cade and W.M.Huo, *J. Chem. Phys.* **47**, 614 (1967 a)

P.E.Cade and W.M.Huo, *J. Chem. Phys.* **47**, 649 (1967 b)

J.K.Cashion, *J. Chem. Phys.* **39** 1872 (1963)

E.A.Colbourn and F.D.Wayne, *Mol. Phys.* **37**, 1755 (1979)

J.W.Cooley, *Math. Comput.* **15**, 363 (1961)

D.L.Cooper, *Part II Thesis*, Oxford (1979)

D.L.Cooper and W.G.Richards, *Nature* **278**, 624 (1979)

D.L.Cooper and L.Veseth, *J. Chem. Phys.* (in press, 1981)

D.L.Cooper and S.Wilson, (to be published, 1981)

P.C.Cosby, H.Helm and J T.Moseley, *Astrophys. J.* **235**, 52 (1980)

J.A.Coxon, *J. Mol. Spectrosc.* **58**, 1 (1975)

J.A.Coxon, *Can. J. Phys.* **58**, 933 (1980)

J.Czarny, P.Felenbok and H.Lefèbvre-Brion, *J. Phys. B* **4**, 124 (1971)

I.Dabrowski and G.Herzberg, *J. Mol. Specrtrosc.* **73**, 183 (1978)

A.E.Douglas, *Can. J. Phys.* **35**, 71 (1957)

A.E.Douglas and G.A.Elliott, *Can. J. Phys.* **43**, 496 (1965)

G.C.Dousmanis, T.M.Sanders and C.H.Townes, *Phys Rev.* **100**, 1735 (1955)

J.E.Dyson and D.A.Williams, *The physics of the interstellar medium*
Manchester University Press, (1980)

A.R.Edmonds, *Angular momentum in quantum mechanics*,
Princetown (1957)

R.S.Freedman and A.W.Irwin, *Astron. Astrophys.* **53**, 447 (1976)

S.M.Freund, H.Herbst, R.P.Mariella and W.Klemperer,
J. Chem. Phys. **56**, 1467 (1972)

J.Gerratt and M.Raimondi, *Proc. Roy. Soc. Lond. A* **371**, 525 (1980)

S.Gewurtz, H.Lew and P.Flainek, *Can. J. Phys.* **53**, 1097 (1975)

R.G.Gordon and J.K.Cashion, *J. Chem. Phys.* **44**, 1190 (1966)

S.Green and R.N.Zare, *J. Mol. Spectrosc.* **64**, 217 (1976)

M.F.Guest and V.R.Saunders, *Mol. Phys.* **28**, 819 (1974)

J.A.Hall, *D. Phil. Thesis*, Oxford (1971)

J.A.Hall, J.Schamps, J.M.Robbe and H.Lefèbvre-Brion,
J. Chem. Phys. **59**, 3271 (1973)

R.E.Hammersley, *D. Phil. Thesis.* Oxford (1974)

R.E.Hammersley and W.G.Richards, *Nature* **251**, 597 (1974)

F.E.Harris and H.H.Michels, *Int. J. Quantum Chem.* **52**, 21 (1968)

E.L.Hill and J.H.Van Vleck, *Phys. Rev.* **32**, 250 (1928)

R.K.Hinkley, *D. Phil. Thesis*, Oxford (1971)

R.K.Hinkley, T.E.H.Walker and W.G.Richards,

Proc. Roy. Soc. Lond. A **331**, 553 (1973)

J.A.Horsley and J.A.Hall, *Mol. Phys.* **25**, 483 (1973)

K.P.Huber and G.Herzberg, *'Constants of diatomic molecules'*,

Van Nostrand Reinhold, New York (1979)

J.M.Hutson and B.J.Howard, *Mol. Phys.* **41**, 1113 (1980)

L.Klynning and B.Lindgren, *Ark. Fysik* **33**, 73 (1967)

L.Klynning, B.Lindgren and U.Sassenberg,

Physica Scripta **20**, 617 (1979)

I.Kovács, *'Rotational structure in the spectra of diatomic molecules'*

Adam-Hilger, London (1969)

H.Lefèbvre-Brion and N.Bessis, *Can. J. Phys.* **47**, 2727 (1969)

H.Lefèbvre-Brion, J.Wajsbaum and N.Bessis,

'La structure hyperfine des atomes et des molecules', CNRS (196?

R.J.LeRoy, R.G.Macdonald and G.Burns, *J. Chem. Phys.* **65**, 1485 (1976)

A.J.Lorquet, J.C.Lorquet, H.Wankenne, J.Momigny and

H.Lefèbvre-Brion, *J. Chem. Phys.* **55**, 4053 (1971)

P.O.Löwdin, *Phys. Rev.* **97**, 1474 (1955)

S.P.McGlynn, T.Azumi and M.Kinoshita, *'Molecular spectroscopy of the triplet state'*, Prentice-Hall (1969)

A.J.Merer and D.N.Travis, *Can. J. Phys.* **43**, 1795 (1965)

A.J.Merer and D.N.Travis, *Can. J. Phys.* **44**, 353 (1966)

R.S.Mulliken and A.Christy, *Phys. Rev.* **38**, 87 (1931)

R.S.Mulliken and W.C.Ermler, *'Diatomic molecules - results of ab initio calculations'*, Academic Press (1977)

G.Peach, *Nature* **289**, 349 (1981)

F.Prosser and S.Hagstrom, *Int. J. Quantum Chem.* **2**, 89 (1968)

J.Raftery and W.G.Richards, *J. Chem. Phys.* **62**, 3184 (1975)

G.H.Redman, *D. Phil. Thesis*, Oxford (1970)

W.G.Richards, *Chem. in Britain* **15**, 68 (1979)

W.G.Richards, H.P.Trivedi and D.L.Cooper, *'Spin-orbit coupling in small molecules'*, Oxford University Press (1981)

G.D.Rochester, *Zeit. Physik* **101**, 769 (1936)

C.C.J.Roothaan, *Rev. Mod. Phys.* **23**, 69 (1951)

P.Rosmus and W.Meyer, *J. Chem. Phys.* **66**, 13 (1977)

R.P.Saxon, R.E.Olson and B.Lui, *J. Chem. Phys.* **67**, 2692 (1977)

V.Sidis and H.Lefèbvre-Brion, *J. Phys. B* **4**, 1040 (1971)

R.E.Smalley, D.A.Auerbach, P.S.H.Fitch, D.H.Levy and L.Wharton, *J. Chem. Phys.* **6**, 3778 (1977)

J.Tellinghuisen, A.Ragone, M.S.Kim, D.A.Auerbach, R.E.Smalley, L.Wharton and D.H.Levy, *J. Chem. Phys.* **71**, 1283 (1979)

C.Thomson, *J. Chem. Phys.* **58**, 841 (1973)

H.P Trivedi and W.G.Richards, *J. Chem. Phys.* **72**, 3438 (1980)

T.Uzer and A.Dalgarno, *Chem.Phys.* **51**, 271 (1980)

J.H.Van Vleck, *Phys. Rev.* **33**, 467 (1929)

L.Veseth, *Theoret. Chim. Acta (Berl.)* **18**, 368 (1970)

L.Veseth, *Physica* **56**, 286 (1971)

L.Veseth, *J. Mol. Spectrosc.* **59**, 51 (1976)

T.E.H.Walker, *D. Phil. Thesis*, Oxford (1969)

T.E.H.Walker and W.G.Richards,

Proc. Phys. Soc. London (At. Mol. Phys.) **3**, 271 (1970)

D.K.Watson, *Chem. Phys. Letters* **51**, 513 (1977)

I.D.L.Wilson, *Part II Thesis*, Oxford (1975)

I.D.L.Wilson, *D. Phil. Thesis*, Oxford (1977)

I.D L Wilson, *J. Mol. Spectrosc.* **70**, 394 (1978)

I.D.L.Wilson and W.G.Richards, *Nature* **258**, 133 (1975)

M.Yoshimine, *J. Chem. Phys.* **57**, 1108 (1972)

M Yoshimine, A.D.McLean and B.Lui,

J. Chem. Phys. **58**, 4412 (1973)

R.N.Zare, A.L.Schemeltekopf, W.J.Harrop and D.L.Albritton,

J. Mol. Spectrosc. **46**, 37 (1973)